



**NTNU – Trondheim**  
Norwegian University of  
Science and Technology

# Inflow Forecasting for Nepalese Catchments

**Anup Khanal**

Hydropower Development

Submission date: June 2013

Supervisor: Knut Alfredsen, IVM

Co-supervisor: Netra Prasad Timalina, IVM

Norwegian University of Science and Technology  
Department of Hydraulic and Environmental Engineering



**NTNU  
Norwegian University of  
Science and Technology**

**Faculty of Engineering  
Science and Technology  
Department of Hydraulic and  
Environmental Engineering**



**M.Sc. THESIS IN  
HYDROPOWER DEVELOPMENT**

**Candidate: Anup Khanal**

**Title: Inflow Forecasting for Nepalese Catchments.**

## **1 BACKGROUND**

Inflow forecasting is a commonly used tool in hydrology to predict inflow based on forecasted weather. The method is currently used in for example flood forecasting and inflow forecasting for hydropower reservoirs. The advantages of forecasting systems are evident since responses can be planned for forecasted floods, and efficient water allocation and production planning can be employed by hydropower managers. The method is not commonly used in Nepal and the purpose of this thesis is to demonstrate how to set up a system for inflow forecasting for a couple of catchments in Nepal and show how these could be utilized for practical planning. The work will involve the preparation of the weather forecast, model setup for study catchments and testing/documentation of the system.

## **2 MAIN QUESTIONS FOR THE THESIS**

1. Downscaling of weather forecasts to our study sites. A dataset for input can be found linked here: <http://joewheatley.net/ncep-global-forecast-system/>. There are a number of tools available to do the actual downscaling from global model to ground level. Possible examples to evaluate as a part of the thesis are SDSM or ClimPact. To test the model it is important that collection of NCEP data is started early in the project.
2. Calibration of hydrological model at the study sites. The hydrological model used should be the Excel HBV model with updating and forecasting interfaces. The model calibration should be evaluated and parameters documented.
3. The forecasting system should be established for the study sites. Since real time inflow for updating is unavailable, the setup should be tested on a historical situation where we define an updating period and a forecast period.

4. An example setup should be made for the Kulekhani reservoir and it should be demonstrated how the forecasting system could be employed as a part of a reservoir planning operation.
5. A further example should be made for a flood forecasting site, including carrying out the necessary flood computations to define the warning limits.

### **3 SUPERVISION, DATA AND INFORMATION INPUT**

Professor Knut Alfredsen will be the supervisor of the thesis work, and Netra Prasad Timalsina will co-supervise the work.

Discussion with and input from colleagues and other research or engineering staff at NTNU, SINTEF, power companies or consultants are recommended. Significant inputs from others shall, however, be referenced in a convenient manner.

The research and engineering work carried out by the candidate in connection with this thesis shall remain within an educational context. The candidate and the supervisors are therefore free to introduce assumptions and limitations, which may be considered unrealistic or inappropriate in a contract research or a professional engineering context.

### **4 REPORT FORMAT AND REFERENCE STATEMENT**

The thesis report shall be in the format A4. It shall be typed by a word processor and figures, tables, photos etc. shall be of good report quality. The report shall include a summary, a table of content, lists of figures and tables, a list of literature and other relevant references and a signed statement where the candidate states that the presented work is his own and that significant outside input is identified.

The report shall have a professional structure, assuming professional senior engineers (not in teaching or research) and decision makers as the main target group.

The summary shall not contain more than 450 words it shall be prepared for electronic reporting to SIU. The entire thesis may be published on the Internet as full text publishing through SIU. Reference is made to the full-text-publishing seminar during NORADS winter-seminar. The candidate shall provide a copy of the thesis (as complete as possible) on a CD in addition to the A4 paper report for printing.

The thesis shall be submitted no later than \_\_\_<sup>th</sup> of June 2013.

Trondheim 19<sup>th</sup> of January 2013

---

Knut Alfredsen

Professor

**FOREWORDS**

This report, which is entitled “Inflow Forecasting for Nepalese Catchments”, is submitted to the Department of Hydraulic and Environmental Engineering at the Norwegian University of Science and Technology as a partial fulfillment of the requirements of the Master of Science in Hydropower Development.

This thesis was carried out from January 2013 to June 2013 at Norwegian University of Science and Technology under the supervision of Prof. Knut Alfredsen.

The author hereby declares that the work presented in this report is his own and significant outside input is acknowledged appropriately.

Anup Khanal

June 2013

Trondheim, Norway



## ACKNOWLEDGEMENT

I would like to express my sincere gratitude to my supervisor, Professor Knut Alfredsen, Department of Hydraulic and Environmental Engineering, Norwegian University of Science and Technology, for his continuous guidance from the planning to development of this thesis. His willingness to give his time so generously has been very much appreciated. His advice, suggestion and logic have been a great help in preparing this report.

I would also like to extend my gratitude and sincere thanks to my co-supervisor, Mr. Netra Prasad Timalina, PhD Candidate at NTNU for his continuous help, guidance, support and valuable suggestion.

I am grateful to Mrs. Hilbjørg Sandvik, Course Co-ordinator, for the efficient management and facilitation throughout the thesis period.

I would like to thank Dr. Hari Shankar Shrestha, Ex. PhD candidate at NTNU, for his support in providing valuable information and data.

I am very thankful to Mr. Doug Schuster, Database Engineer with the NCAR Research Data Archive, for his help in retrieving GFS model data and other useful information.

I am grateful to my parents, brothers and sisters who have continuously encouraged me to study and work hard.

Finally, I would like to thank and acknowledge all Nepalese friends, seniors and juniors who have helped me directly or indirectly during my thesis period.



---

## ABSTRACT

Due to the tropical climate, Nepalese rivers experience the large floods during monsoon season. Prediction of flood in advance is very essential not only for the successful hydropower operation but also for establishing effective flood warning system. Though developed country like Norway has been using inflow forecasting as a part of reservoir operation and flood warning system since long ago, so far no study related to inflow forecasting has been carried out in Nepal. This study is the first initiation of work in the field of inflow forecasting for Nepalese catchment. It attempts to establish the inflow forecasting system to the Kulekhani reservoir, employ the forecasted inflow in reservoir operation and present an example of flood warning system.

The outputs of the Global Forecast System (GFS) model which is run in spatial resolution of approximately 50km x 50km and temporal resolution of 3 hrs were selected as meteorological forecasts to carry out the inflow forecast simulation. The spatial resolution of GFS model is on the range of Regional Circulation Model (RCM) so no further downscaling was done but modeled data were subjected to bias correction after comparing it to observed data. Two advanced methods of bias correction viz. empirical adjustment method and statistical bias correction method were applied to the precipitation and temperature forecasts. The empirical adjustment method did not perform very well in bias correction of precipitation forecasts as it requires long series of observational and forecast data. So the statistical method was applied for the bias correction of precipitation forecasts. But in the case of bias correction of temperature forecasts, the empirical adjustment method was found satisfactory.

Due to difficulty in getting real time meteorological data of Kulekhani catchment from Trondheim, a historical period was chosen for the HBV model setup and inflow forecast simulation. The model calibration was done based on the observed hydrometeorological data and the best value of goodness of fit as described by  $R^2$  was found to be 0.76. This low value of  $R^2$  is characterized by the uncertainties in observed inflow since observed inflow was calculated indirectly based on the daily energy production and reservoir level. The model was updated by adjusting values in precipitation and temperature, and model state variables. Then the forecast simulation was run on 8 consecutive days. Large degree of uncertainty was found in inflow forecast due to use of meteorological forecasts produced in coarser spatial resolution and unavailability of measured inflow during HBV model calibration. The inflow forecast was further used in existing reservoir operational model to examine whether Kulekhani project can meet the energy demand or not in relation with forecasted inflow up to 7 days in advance. The forecasted inflow was also analyzed in terms of flood forecast to set up an effective flood warning system.

In conclusion, this study has been successful to carry out inflow forecasting based on meteorological forecasts. However, large degree of uncertainty in inflow forecasting is observed. The reservoir operation and flood warnings are also affected by the uncertainty seen in inflow forecasting. Improvements on this study can be made by using meteorological forecasts with finer spatial resolution and carrying out calibration of the HBV model with measured inflow for sufficiently long period.



---

**TABLE OF CONTENT**

<b>FOREWORDS.....</b>	<b>III</b>
<b>ACKNOWLEDGEMENT .....</b>	<b>IV</b>
<b>ABSTRACT.....</b>	<b>V</b>
<b>TABLE OF CONTENT .....</b>	<b>VI</b>
<b>LIST OF FIGURES .....</b>	<b>IX</b>
<b>LIST OF TABLES .....</b>	<b>XI</b>
<b>LIST OF ABBREVIATIONS .....</b>	<b>XII</b>
<b>1 INTRODUCTION .....</b>	<b>1</b>
1.1 BACKGROUND .....	1
1.2 OBJECTIVE OF THE STUDY .....	1
1.3 SCOPE OF THE STUDY.....	1
1.4 METHODOLOGY .....	2
1.5 STRUCTURE OF THE THESIS.....	2
1.6 LIMITATIONS .....	3
<b>2 DATA ACQUISITION AND QUALITY CONTROL.....</b>	<b>4</b>
2.1 INTRODUCTION TO THE STUDY AREA .....	4
2.1.1 Kulekhani Hydroelectric Project .....	4
2.1.2 Catchment Characteristics .....	5
2.2 COLLECTION OF OBSERVED METEOROLOGICAL DATA .....	6
2.2.1 Precipitation.....	6
2.2.2 Temperature .....	8
2.3 COLLECTION OF METEOROLOGICAL FORECAST DATA.....	9
2.3.1 Precipitation and Temperature .....	9
2.3.2 Application of 'R' In Data Processing .....	10
2.4 QUALITY CONTROL.....	11
2.4.1 Visual Inspection .....	11
2.4.2 Filling of Missing Data .....	12
2.4.3 Accumulation Plot.....	13
2.4.4 Double Mass Curve .....	13
2.5 DISCUSSION AND CONCLUSION .....	14

---

<b>3</b>	<b>GLOBAL FORECAST SYSTEM (GFS)</b> .....	<b>15</b>
3.1	INTRODUCTION .....	15
3.2	BASIC MODEL EQUATIONS .....	15
3.3	GFS MODEL STRUCTURE .....	18
3.4	MODEL PROPERTIES .....	19
3.4.1	Numerical /Computational Properties .....	19
3.4.2	Dynamical/ Physical Properties .....	19
<b>4</b>	<b>COMPARISON BETWEEN GFS MODEL OUTPUT AND OBSERVATIONS</b> .....	<b>21</b>
4.1	INTRODUCTION .....	21
4.2	PURPOSE OF COMPARISON .....	21
4.3	MODEL EVALUATION TECHNIQUES .....	21
4.3.1	Statistical Method .....	21
4.3.2	Graphical Method .....	22
4.4	RESULTS AND DISCUSSION .....	28
4.5	CONCLUSIONS AND RECOMMENDATION .....	28
<b>5</b>	<b>BIAS CORRECTION FOR GFS MODEL OUTPUT</b> .....	<b>29</b>
5.1	INTRODUCTION .....	29
5.2	BIAS CORRECTION METHODS.....	29
5.2.1	Empirical Adjustment Method.....	29
5.2.2	Statistical Bias Correction Method .....	35
5.3	CONCLUSION AND RECOMMENDATION.....	39
<b>6</b>	<b>CALIBRATION OF THE HBV MODEL</b> .....	<b>40</b>
6.1	THE HBV MODEL-AN INTRODUCTION.....	40
6.2	STRUCTURE OF THE HBV MODEL.....	40
6.2.1	The Snow Routine .....	41
6.2.2	The Soil Moisture Routine .....	42
6.2.3	The Runoff Response Routine.....	42
6.3	INPUT DATA PREPARATION.....	43
6.3.1	Air Temperature.....	43
6.3.2	Precipitation.....	44
6.3.3	Potential Evapotranspiration .....	44
6.3.4	Runoff.....	46

6.3.5	Area –Elevation Curve.....	48
6.4	MODEL CALIBRATION.....	49
6.4.1	Confined Parameters .....	50
6.4.2	Model Initial States .....	51
6.4.3	Free Parameters.....	51
6.5	MODEL VALIDATION.....	53
6.6	DISCUSSION AND CONCLUSIONS .....	54
<b>7</b>	<b>SHORT TERM INFLOW FORECASTING AND RESERVOIR OPERATION .....</b>	<b>55</b>
7.1	INTRODUCTION .....	55
7.2	MODEL UPDATING .....	55
7.3	FORCAST SIMULATION .....	58
7.4	RESERVOIR OPERATION .....	59
7.4.1	Introduction .....	59
7.4.2	Reservoir Operation In The Case of Kulekhani Reservoir .....	59
7.4.3	Existing Reservoir Operation Model for Kulekhani Reservoir .....	60
7.4.4	Results.....	62
7.5	DISCUSSION ON UNCERTAINTY IN SHORT TERM INFLOW FORECASTING.....	62
7.6	CONCLUSION AND RECOMMENDATION.....	64
<b>8</b>	<b>FLOOD WARNING SYSTEM.....</b>	<b>65</b>
8.1	INTRODUCTION .....	65
8.2	WARNING TIME AND LEVEL OF ACCURACY .....	66
8.3	WARNING LIMITS .....	67
8.4	OPERATIONAL FLOOD WARNING SYSTEM.....	68
8.5	FLOOD PREPAREDNESS .....	69
8.6	CONCLUSTION .....	71
<b>9</b>	<b>CONCLUSTION AND RECOMMENDATION.....</b>	<b>72</b>
9.1	CONCLUSTION .....	72
9.2	RECOMMENDATION FOR FUTURE RESEARCH .....	73
	<b>REFERENCES .....</b>	<b>74</b>
	<b>APPENDICES .....</b>	<b>76</b>



## LIST OF FIGURES

Figure 1-1: Steps involved in inflow forecasting and its application, a case study of Kulekhani catchment .....	2
Figure 2-1: Satellite image of study site, Kulekhani reservoir .....	4
Figure 2-3: Location of precipitation gauge stations around Kulekhani catchment.....	6
Figure 2-2: Location and Catchment area of Kulekhani project (Sangroula, 2005).....	6
Figure 2-4: Precipitation recorded in Markhu station.....	7
Figure 2-5: Precipitation recorded in Daman station.....	7
Figure 2-6: Precipitation recorded in Thankot station .....	8
Figure 2-7: Temperature timeseries equivalent as recorded in Markhu station .....	9
Figure 2-8: Precipitation forecast time series produced by GFS model .....	10
Figure 2-9: Temperature forecast timeseries produced by GFS model .....	10
Figure 2-10: Temperature forecast value made for the whole globe (Source: NCEP) .....	11
Figure 2-11: Missing data for each station on time scale.....	12
Figure 2-12: Accumulation plot of precipitation timeseries for each station.....	13
Figure 2-13: Double mass curve for Daman and Thankot station .....	14
Figure 3-1: Flow diagram of typical Global Forecast System, GFS (Source: NCEP) .....	18
Figure 4-1: Monthly value of precipitation forecast and observed precipitation for the year 2007 .....	23
Figure 4-2: Monthly value of precipitation forecast and observed precipitation for the year 2008 .....	23
Figure 4-3: Monthly value of precipitation forecast and observed precipitation for the year 2009 .....	24
Figure 4-4: Monthly value of precipitation forecast and observed precipitation for the year 2010 .....	24
Figure 4-5: Monthly value of precipitation forecast and observed precipitation for the year 2011 .....	25
Figure 4-6: Average monthly value of temperature forecast and observed temperature for the year 2007 .....	25
Figure 4-7: Average monthly value of temperature forecast and observed temperature for the year 2008 .....	26
Figure 4-8: Average monthly value of temperature forecast and observed temperature for the year 2009 .....	26
Figure 4-9: Number of days model forecasts 'precipitation' when there is 'no precipitation' in actual and vice versa (Year 2007) .....	27
Figure 4-10: Number of days model forecasts 'precipitation' when there is 'no precipitation' in actual and vice versa (Year 2008) .....	27
Figure 4-11: Number of days model forecasts 'precipitation' when there is 'no precipitation' in actual and vice versa (Year 2009) .....	28
Figure 5-1: Comparison of mean monthly precipitation forecast before and after correction for the year 2009.....	34
Figure 5-2: Comparison of averaged monthly temperature before and after correction (Year 2009).....	34

Figure 5-3: Day to day comparison of temperature forecast before and after correction (Year 2009).....	35
Figure 5-4: Fitted gamma distribution for precipitation forecast in control period.....	36
Figure 5-5: Fitted cumulative distribution for precipitation forecast in control period.....	36
Figure 5-6: Fitted gamma distribution for observed precipitation in control period .....	37
Figure 5-7: Fitted cumulative gamma distribution for observed precipitation in control period.....	37
Figure 5-8: Cumulative gamma distribution including no precipitation days in control period.....	38
Figure 5-9: Transfer function which follows the equation $\text{cdf}_{\text{obs}}(fx)=\text{cdf}_{\text{sim}}(x)$ .....	38
Figure 5-10: Comparison of mean monthly precipitation forecast before and after correction. ....	39
Figure 6-1: Main structure of the HBV model (Killingtveit and Sælthun, 1995) .....	41
Figure 6-2: The snow routine in the HBV-model (Killingtveit and Sælthun, 1995).....	41
Figure 6-3: The soil moisture routine in HBV-model (Killingtveit and Sælthun, 1995) .....	42
Figure 6-4: The runoff response routine in the HBV-model (Killingtveit and Sælthun, 1995) .....	43
Figure 6-5: Precipitation and Temperature inputs in HBV model.....	44
Figure 6-6: Monthly average value of potential evapotranspiration computed by Thornthwaite method .....	45
Figure 6-7: Daily reservoir level and energy generation from Kulekhani I project .....	46
Figure 6-8: Reservoir capacity curve of Kulekhani reservoir (Shrestha, 2012) .....	46
Figure 6-9: Daily inflow to Kulekhani reservoir .....	48
Figure 6-10: Hypsometric curve for Kulekhani catchment.....	49
Figure 6-11: Model calibration process (Killingtveit and Sælthun, 1995) .....	49
Figure 6-12: Soil moisture storage for Kulekhani catchment .....	53
Figure 6-13: Observed and simulated runoff for Kulekhani catchment 2007-2011 .....	53
Figure 6-14: Inflow to the Kulekhani reservoir for January month .....	54
Figure 7-1: Model update results for first two consecutive model run.....	57
Figure 7-2: Model update results for the past 7 days from 01 August, 2009.....	57
Figure 7-3: Working principle of Kulekhani reservoir operation model (Shrestha, 2012) ..	60
Figure 7-4: Daily load demand to Kulekhani plant .....	61
Figure 7-5: Uncertainty in short term inflow forecasting .....	63
Figure 7-6: Uncertainty in reservoir level forecast and error variability .....	64
Figure 8-1: Type of water-related natural disasters, 1990-2001 (Source: UNESCO).....	65
Figure 8-2: The trade-off between warning time and warning accuracy for flash flood situations (Wright, 2001).....	66
Figure 8-3: Inflow forecast made on 01 August, 2009 and flood warning limits.....	68
Figure 8-4: Components of operational flood warning system (Australian Government, 2009).....	69

---

**LIST OF TABLES**

Table 2-1:	Salient features of the Kulekhani hydroelectric project (Sangroula, 2005).....	5
Table 2-2:	Description of meteorological stations around the Kulekhani catchment (Source: DHM).....	8
Table 5-1:	Main parameters of empirical adjustment method applied for GFS model output .....	31
Table 5-2:	Elevation used in GFS model for each cell (Source: NCEP).....	32
Table 6-1:	Computation of potential evapotranspiration by Thornthwaite method .....	45
Table 6-2:	Surface area and reservoir volume (Shrestha, 2012) .....	47
Table 6-3:	Area-Elevation curve for Kulekhani catchment .....	48
Table 6-4:	Main parameters for the Kulekhani catchment.....	50
Table 6-5:	Elevation for Markhu station .....	50
Table 6-6:	Model states at start .....	51
Table 6-7:	Free parameters in the HBV model (Killingtveit and Sælthun, 1995) and calibrated value.....	52
Table 7-1:	Correction in model input and state variables for each consecutive model run	56
Table 7-2:	Precipitation forecasts made on different date .....	58
Table 7-3:	Temperature forecasts made on different date.....	58
Table 7-4:	Inflow forecasts made on different date.....	59
Table 7-5:	Loadshedding forecast made on different date .....	62
Table 7-6:	Reservoir level forecast made on different date .....	62
Table 8-1:	Maximum flood in the Kulekhani river (NIPPON KOEI Co. Ltd., 1983) .....	67



---

**LIST OF ABBREVIATIONS**

BC	Bias Correction
cdf	cumulative distribution function
CISL	Computational and Information System Laboratory
DEM	Digital Elevation Model
DHM	Department of Hydrology and Meteorology
GCM	General Circulation model
GFS	Global Forecast System
GRIBB	GRIdded binary
Gwh	Giga watt hour
HBV	Hydrologiska Byråns Vattenbalansavdelning
HIRLAM	High Resolution Limited Area Model
hrs	hours
INPS	Integrated Nepalese Power System
km <sup>2</sup>	Kilometer square
m	meter
m <sup>3</sup> /s	cubic meter per second
masl	meter above sea level
mm	millimeter
Mm <sup>3</sup>	Million cubic meters
Mw	Mega watt
Mwh	Mega watt hour
NCAR	National Center for Atmospheric Research
NCEP	National Centers for Environmental Prediction
NEA	Nepal Electricity Authority
nve	norges vassdrags- og energidirektorat

NWS	National Weather Service
P	Precipitation
pdf	probability density function
$R^2$	Nash-Sutcliffe coefficient
RCM	Regional Circulation model
RDA	Research Data Archive
SRTM	Shuttle Radar Topography Mission
T	Temperature
UNESCO	United Nations Educational, Scientific and Cultural Organization
USA	United States of America
USGS	United States Geological Survey
US\$	US dollar
WMO	World Meteorological Organization
WWAP	World Water Assessment Program

---

## 1 INTRODUCTION

### 1.1 BACKGROUND

Nepal is the second richest country in the world in water resources. The tremendous number of large rivers following steep gradient has made the country an ideal place for the hydropower development. Nepal can get large economical benefits through an effective water resources planning.

On the other hand, Southern parts of the country are at risk of flooding during the monsoon season. Every year hundreds of people lose their lives and properties in large floods which emphasize the immediate need of an effective early warning system to be established in the flood prone zones.

Runoff forecasting is a very useful tool in water resource planning, development and flood mitigations. However, accurate forecasting of the runoff is the challenging job in hydrology. The accuracy of the runoff forecast depends on the quality of meteorological forecasts (precipitation and temperature) and ability of the calibrated hydrological model to represent the actual response of the catchment. There are several hydrological models which can be run on the forecast mode when the meteorological forecasts are available. In this study, excel based HBV model with updating and forecasting interfaces is used to carry out the runoff forecasting based on the forecasted precipitation and temperature. The forecasted runoff will be further linked to reservoir operation and flood warnings.

### 1.2 OBJECTIVE OF THE STUDY

Inflow forecasting is the topic which receives considerable attention in water resources planning and flood warning but it is still a new topic in the context of Nepal. On this background, the intention of this study will be to establish inflow forecasting system for the Kulekhani reservoir in Nepal based on the meteorological forecasts and to link the forecasting system to the reservoir operation and flood warning system.

### 1.3 SCOPE OF THE STUDY

The following systematic tasks will be carried out to meet the proposed objectives:

- Literature review on methods of inflow forecasting and its application in reservoir operation and flood warnings
- Reviewing existing documents related to the study area
- Collection of measured meteorological data, quality check and data processing
- Acquisition of meteorological forecasts (precipitation, temperature), downscaling if necessary and carrying out bias correction
- Calibration of the HBV model at the study area
- Model validation and forecast simulation based on forecasted temperature and precipitation data.
- Application of the inflow forecasting in the reservoir operation and flood warning

## 1.4 METHODOLOGY

Successful inflow forecasting system involves many steps to be carried out in sequential order. However, the approach varies according to the study site, selection of the hydrological model and meteorological forecast model. This report presents all the necessary tasks that were carried out to perform inflow forecasting for Kulekhani reservoir and to use it in reservoir operation and flood warning system. Figure 1-1 shows all the steps that were carried out in preparing the report.

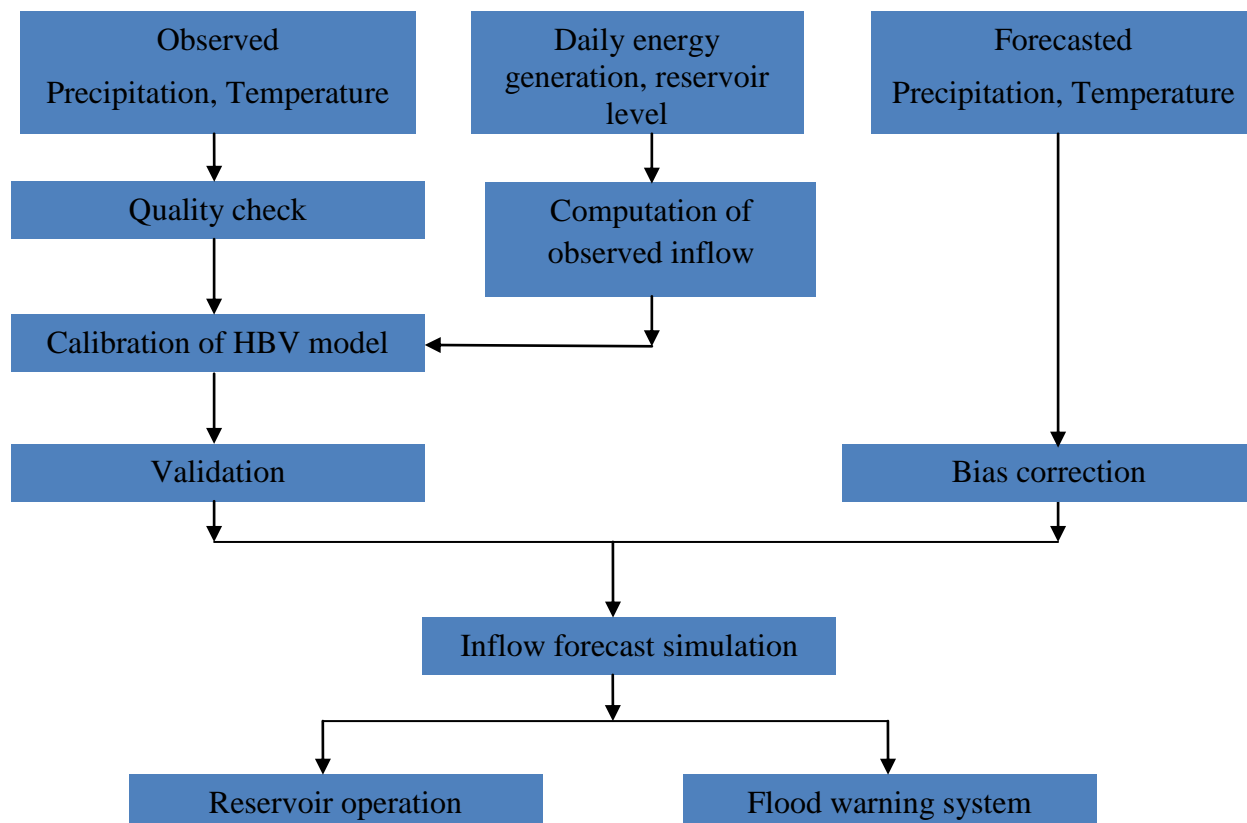


Figure 1-1: Steps involved in inflow forecasting and its application, a case study of Kulekhani catchment

## 1.5 STRUCTURE OF THE THESIS

This report tries to cover all the necessary tasks which are required in inflow forecasting and discusses its use in reservoir operation and flood warning system. Different chapters are made to describe the different sub tasks. Each chapter describes the working procedures for the respective sub task in sequential order and presents the conclusion. The work flow within each chapter and in between the different chapters is well maintained with necessary discussions and conclusions. The relevant theory for each subtask is included in the respective chapter.

Chapter 1 gives a brief introduction to the need of inflow forecasting in water resources planning and flood warnings, objectives and scopes of the study, methodology and structure of the thesis.

Chapter 2 describes the data acquisition and quality checking procedures in systematic order.

Chapter 3 gives a general idea to the Global Forecast System (GFS) and its structure.

Chapter 4 presents the result from comparison between GFS model outputs and observed data and highlights the need of bias correction to the model outputs.

Chapter 5 describes two types of bias correction techniques and explains all the steps carried out in bias correction.

Chapter 6 explains the HBV model parameterization procedures, observed inflow calculation method and computation of potential evapotranspiration.

Chapter 7 describes the model validation and forecast simulation processes and use of inflow forecasting in reservoir operation.

Chapter 8 deals with flood warning system.

Chapter 9 presents the main conclusion of the study and recommendation for the future research as an extension of the current study.

## **1.6 LIMITATIONS**

Very limited data are used in the calculations due to unavailability of long historical meteorological forecast data and recorded reservoir level data to calculate the inflow to the reservoir. This study is carried out for the demonstration purpose. Therefore, there is a sufficient room for more work to improve this study and can be made as a useful operational model of the national interest.



## 2 DATA ACQUISITION AND QUALITY CONTROL

### 2.1 INTRODUCTION TO THE STUDY AREA

The aim of this thesis is to establish an inflow forecasting system and apply the inflow forecasts in reservoir operation and flood warnings. For that purpose to be fulfilled, Kulekhani reservoir is chosen. A satellite image of Kulekhani reservoir is presented in the Figure 2-1.

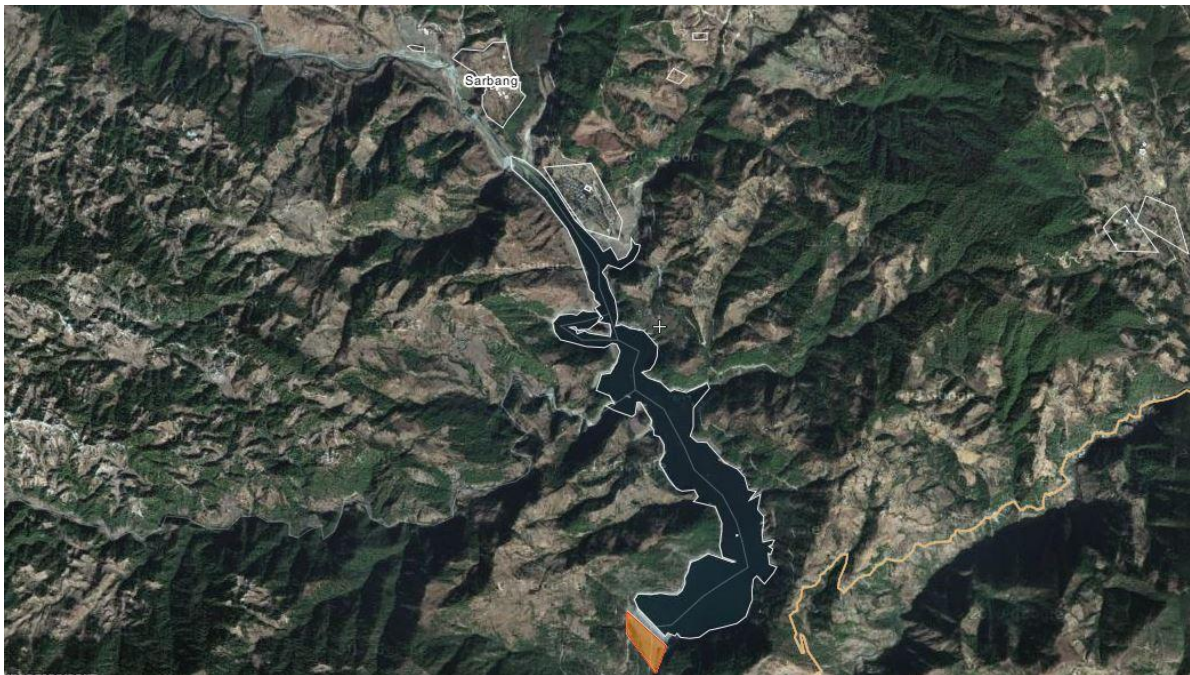


Figure 2-1: Satellite image of study site, Kulekhani reservoir

All the data relevant to the Kulekhani catchment are collected and processed which is discussed in subsequent sections.

#### 2.1.1 Kulekhani Hydroelectric Project

Kulekhani I (hereafter called as only 'Kulekhani') is the only one reservoir type hydroelectric project in Nepal. Its installed capacity is 60 MW having two units each of 30 MW. The annual expected energy generation capacity as primary energy is 165 GWH and 46 GWH as secondary energy. The salient features of the Kulekhani project is presented in Table 2-1 below:

The main purpose for the construction of this power station was to take the peak load only but the unavailability of the sufficient power with respect to demand, the power station is forced to operate as and when required.

Table 2-1: Salient features of the Kulekhani hydroelectric project (Sangroula, 2005)

Topographical and hydrological features	Watershed	Watershed area	Average annual flow	Annual total runoff
		Km <sup>2</sup>	m <sup>3</sup> /s	Mm <sup>3</sup>
	Kulekhani	126	3.9	123
	Chankhel	23	0.7	24.5
	Sim	7	0.4	11.8
	Total	156	5	157.3
Dam	Dam height			114 m
	Crest elevation			1534.0 masl
	Crest length			397.0 m
Reservoir	Highest regulated water level (HRWL)			1530.0 masl
	Lowest regulated water level (LRWL)			1476.0 masl
	Drawdown			54.0 m
	Water surface area at HRWL			2.2 Km <sup>2</sup>
	Gross storage capacity (design)			85.3 Mm <sup>3</sup>
	Effective storage capacity (design)			73.3 Mm <sup>3</sup>
Hydrology	Maximum intake storage			13.1 m <sup>3</sup> /s
	Net head available			550m
Turbine	Turbine types and numbers			Pelton, 2 sets
	Installed capacity			2 X 30 Mw
Waterways	Intake type			Bell mouth type
	Intake size			14m wide x 6m high
	Length of headrace tunnel			6.2 km
	Diameter of headrace tunnel			2.5 m
	Length of penstock			1356 m
	Diameter of penstock			2m - 1.5 m

### 2.1.2 Catchment Characteristics

The Kulekhani catchment is located at the northeast part of Makwanpur district which lies at 21 km southwest of Kathmandu, Nepal. The catchment area is approximately 126 km<sup>2</sup>. The area is basically composed of rugged terrain and is surrounding by numerous mountains and valleys. Palung Khola is the main river to drain the catchment and other two streams Tistung and Chitlang contribute water to the Palung along its waterway. The land use pattern of the catchment is shown in Figure 2-2.

The elevation of the catchment area ranges from 1,534 masl at the dam site to 2621 masl at the peak of Simbhanjyang of the Mahabharat Range. The catchment area comprises wide and relatively flat land throughout the middle part of watershed. These areas are well cultivated and densely populated (Shrestha, 2012).

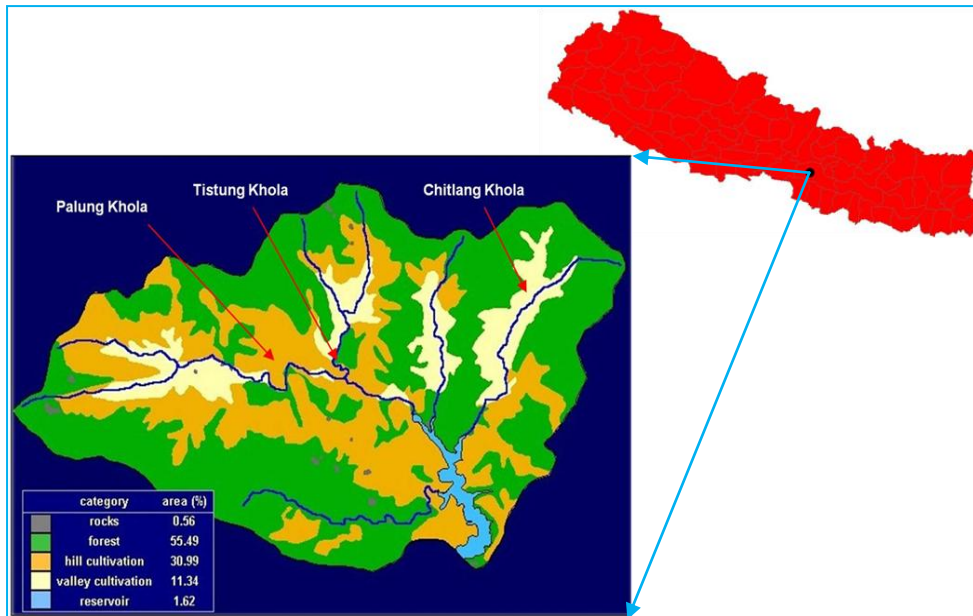


Figure 2-2: Location and Catchment area of Kulekhani project (Sangroula, 2005).

Most of the area of catchment is covered by forest. The catchment is characterized by no snow zone.

## 2.2 COLLECTION OF OBSERVED METEOROLOGICAL DATA

### 2.2.1 Precipitation

All the precipitation data are collected from the Department of Hydrology and Meteorology (DHM), Ministry of science, technology and environment. Six meteorological stations are found at the vicinity of Kulekhani catchment which is shown in Figure 2-3.

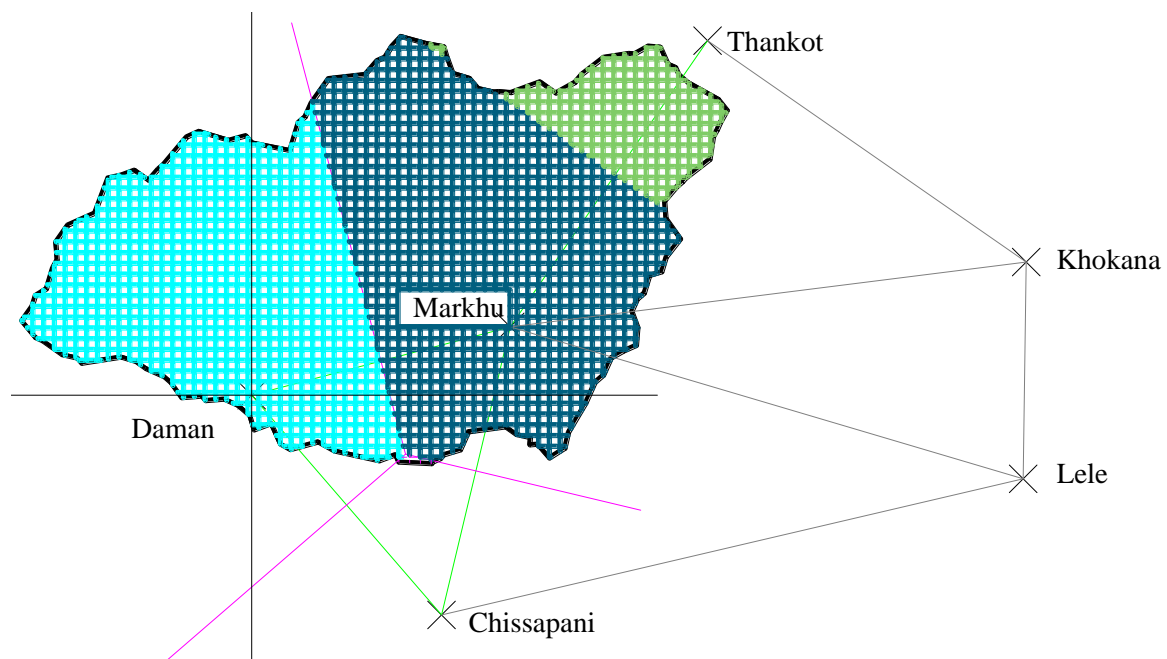


Figure 2-3: Location of precipitation gauge stations around Kulekhani catchment

Only three main precipitation gauge stations viz. Markhu, Thankot and Daman are applicable for Thiessen polygon method of calculating areal precipitation. Therefore, Precipitation data are only collected from three gauge stations only.

The precipitation data for the period of five years (2007-2011) are only used in calculation due to unavailability of long historical meteorological forecast data which are going to be compared with observed ones. Figure 2-4, Figure 2-5 and Figure 2-6 show the precipitation time series recorded in three different gauge stations.

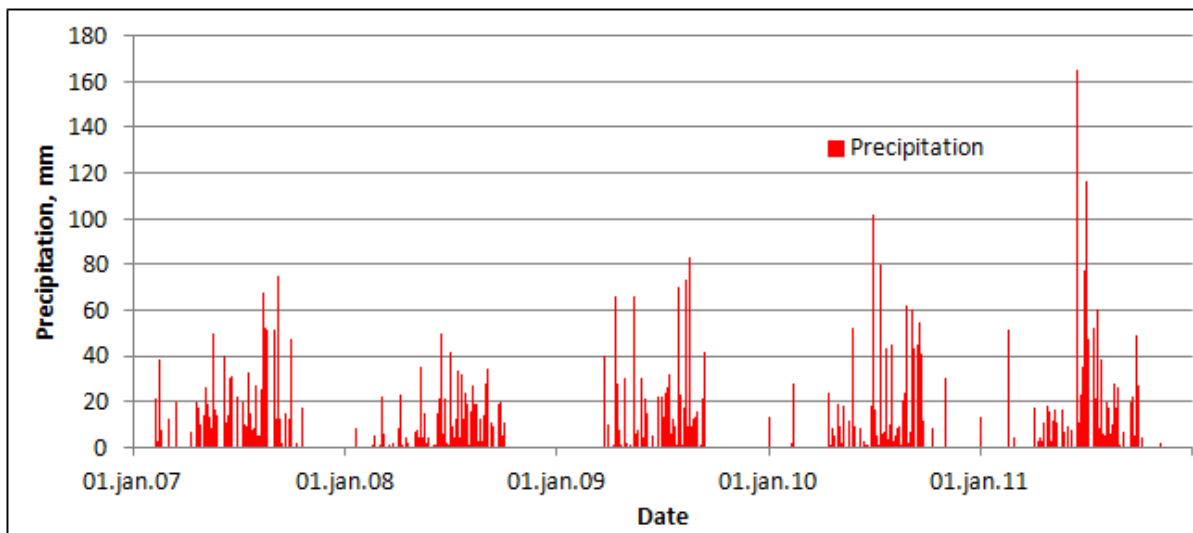


Figure 2-4: Precipitation recorded in Markhu station

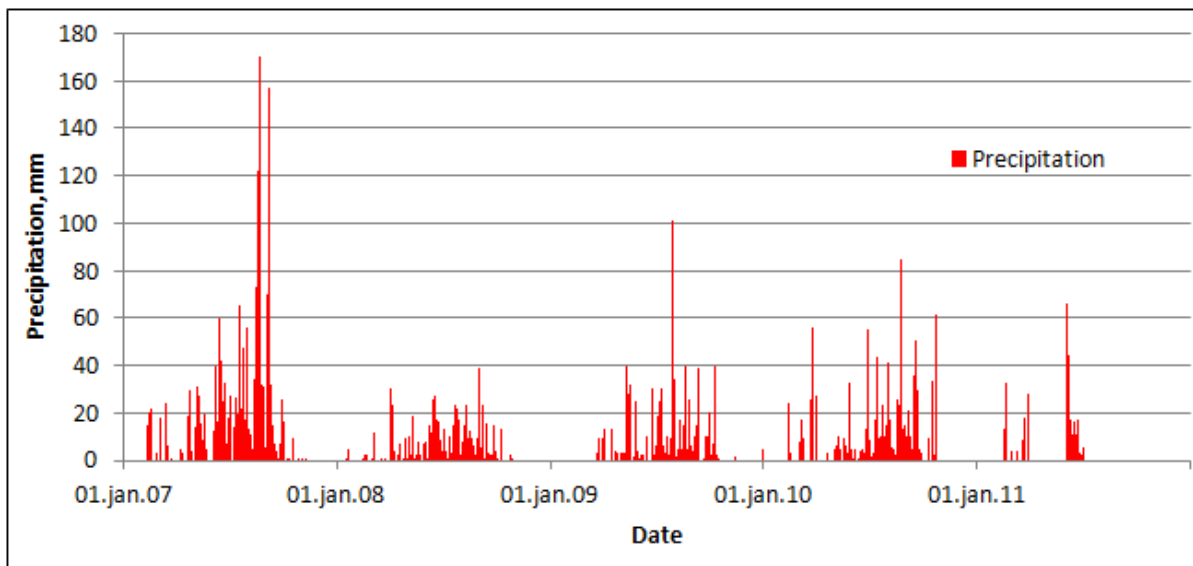


Figure 2-5: Precipitation recorded in Daman station

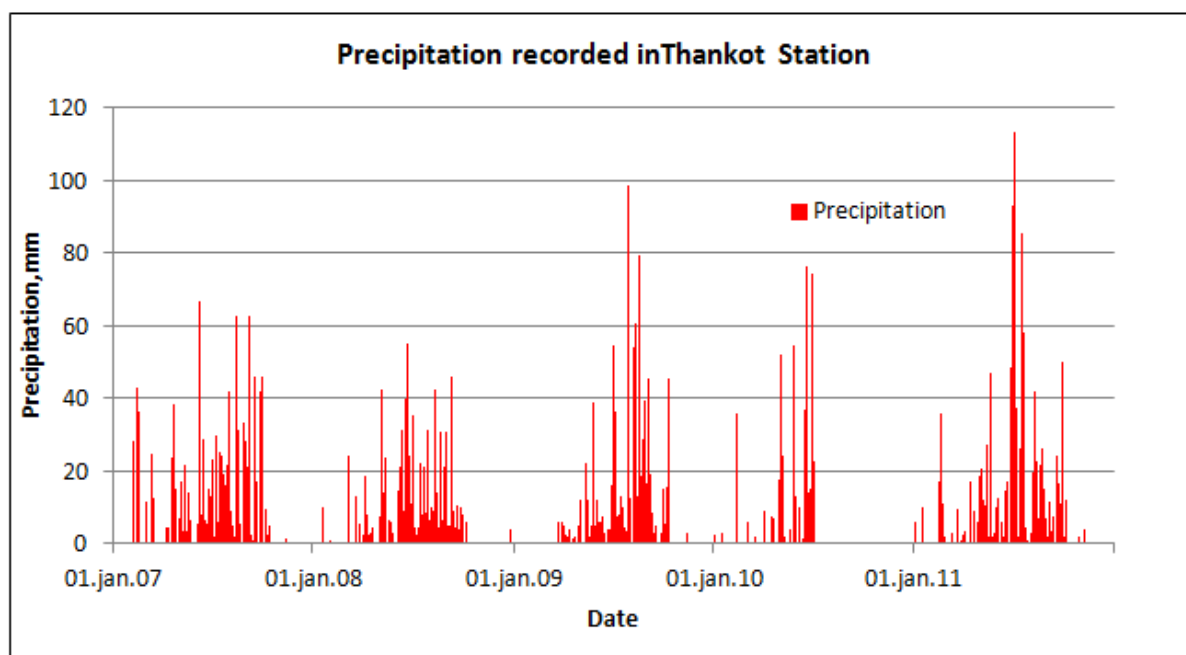


Figure 2-6: Precipitation recorded in Thankot station

Some data are missing in the precipitation time series. The filling procedure is discussed in section 2.4.2.

### 2.2.2 Temperature

There are only two meteorological gauge stations i.e. Khokana and Hetaunda stations to record the air temperature. Neither of them has the complete recordings of temperatures for the whole five years. So first 3 years of complete data are taken from Khokana station and last 2 years of data are taken from Hetaunda gauge station, however Hetaunda gauge station is very far from the Kulekhani catchment. Table 2-2 shows the location and elevation of meteorological gauge stations which are applicable for Kulekhani catchment.

Table 2-2: Description of meteorological stations around the Kulekhani catchment (Source: DHM)

Station Name	Index no.	Type of Station	District	Latitude	Longitude	Elevation
Markhu	0915	Precipitation	Makwanpur	27° 37'	85° 09'	1530 m
Daman	0905	Climatology	Makwanpur	27° 36'	85° 05'	2314 m
Thankot	1015	Precipitation	Kathmandu	27° 41'	85° 12'	1630 m
Khokana	1073	Climatology	Lalitpur	27° 38'	85° 17'	1212 m
Hetaunda	0906	Climatology	Makwanpur	27° 25'	85° 03'	474 m
Chisapani	0904	Precipitation	Makwanpur	27° 33'	85° 08'	1706 m

Thus the temperature recorded in Khokana and Hetaunda stations are transferred to the Markhu station which weights the major part in Thiessen polygon, by using temperature lapse rate. The following formula is used to transfer the temperature from one station to another:

$$T_n = T_r + 0.65 \times \frac{H_r - H_n}{100}$$

Where,  $T_n$  = Temperature at new station

$T_r$  = Temperature at recorded station

$H_r$  = Elevation of recorded station

$H_n$  = Elevation of new station

The new transferred temperature timeseries is shown in the Figure 2-7:

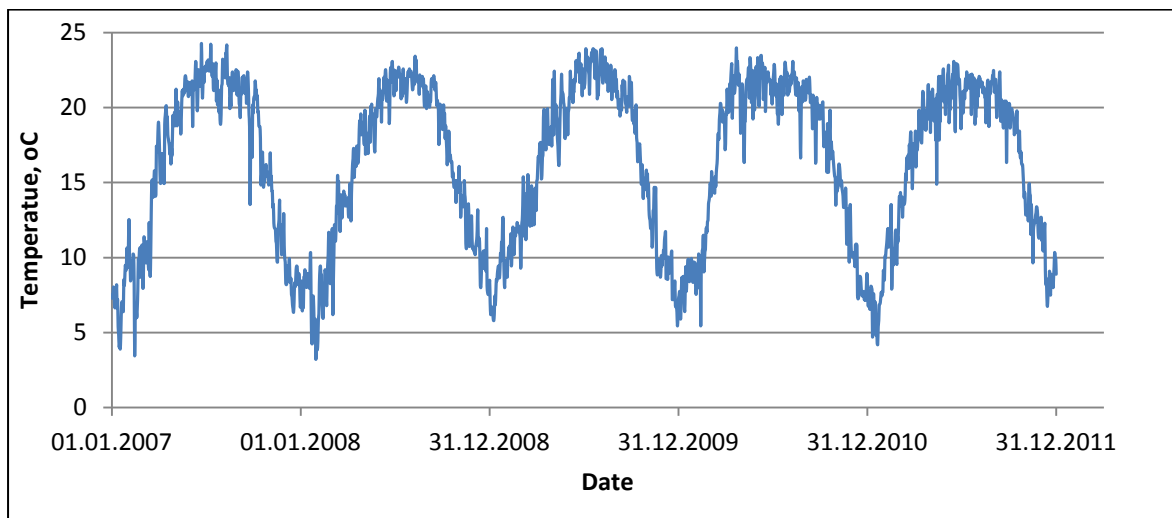


Figure 2-7: Temperature timeseries equivalent as recorded in Markhu station

## 2.3 COLLECTION OF METEOROLOGICAL FORECAST DATA

### 2.3.1 Precipitation and Temperature

The precipitation and temperature data for this study are obtained from the Research Data Archive (RDA) which is maintained by the Computational and Information Systems Laboratory (CISL) at the National Center for Atmospheric Research (NCAR). NCAR is sponsored by the National Science Foundation (NSF). The original data are available from the RDA (<http://rda.ucar.edu/datasets/ds335.0/#description>) in dataset number ds335.0. These data are the output of the Global Forecast System (GFS) model which is run with  $0.5^\circ \times 0.5^\circ$  spatial resolution approximately equivalent to 50km x 50km and temporal resolution of 3 hrs. More information about the GFS model is given in chapter 3. The precipitation and temperature forecast timeseries for the years 2007 to 2011 are shown in Figure 2-8 and Figure 2-9.

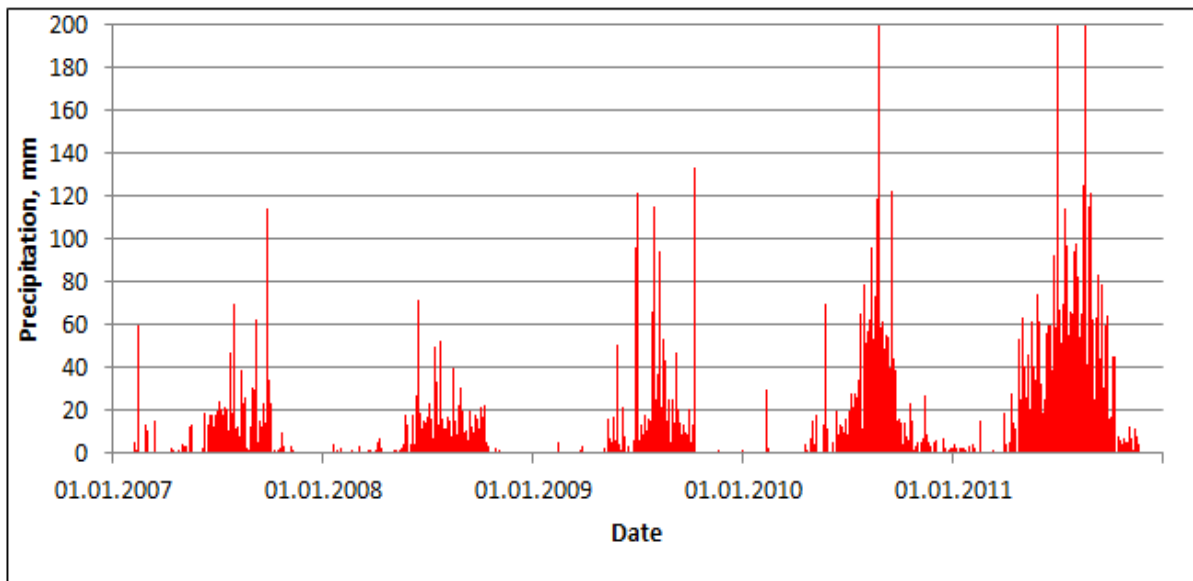


Figure 2-8: Precipitation forecast time series produced by GFS model

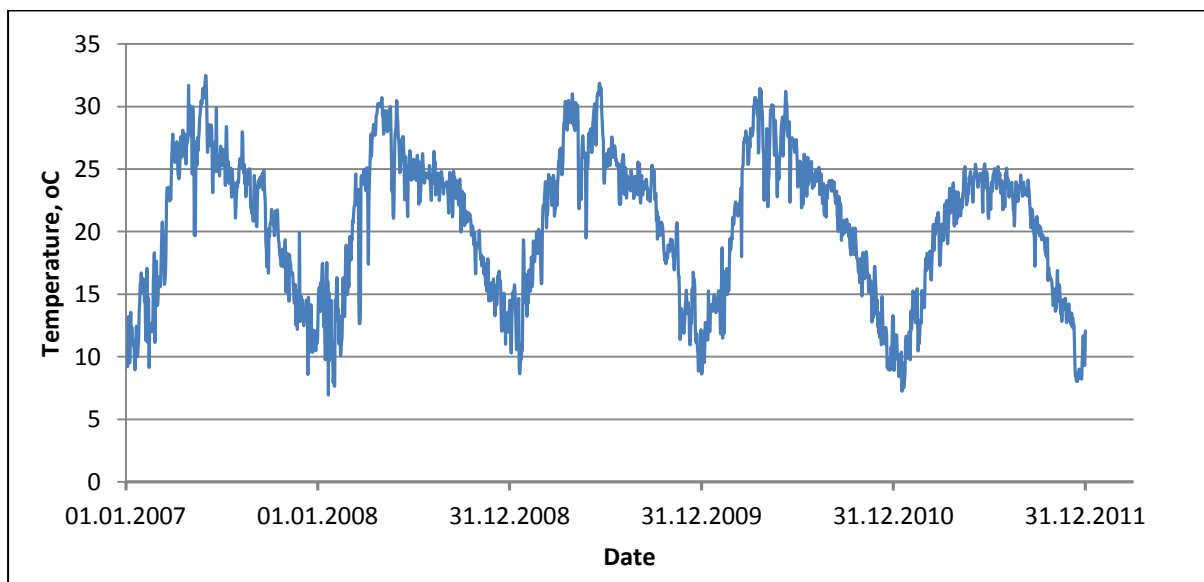


Figure 2-9: Temperature forecast timeseries produced by GFS model.

Meteorological forecast data are stored in GRIB (GRIdded Binary or General Regularly-distributed Information in Binary form) which can be only opened with some special software packages. 'R' programming language for statistical computing and graphics, is used to read the GRIB files which contain meteorological forecasts.

### 2.3.2 Application of 'R' In Data Processing

The GFS model produces the temperature and precipitation forecast for all over the world and their values are stored in raster format. For an example, originally the temperature forecasts made on 000 hrs for 006hrs, 01 January, 2012 looks like as shown in Figure 2-10.

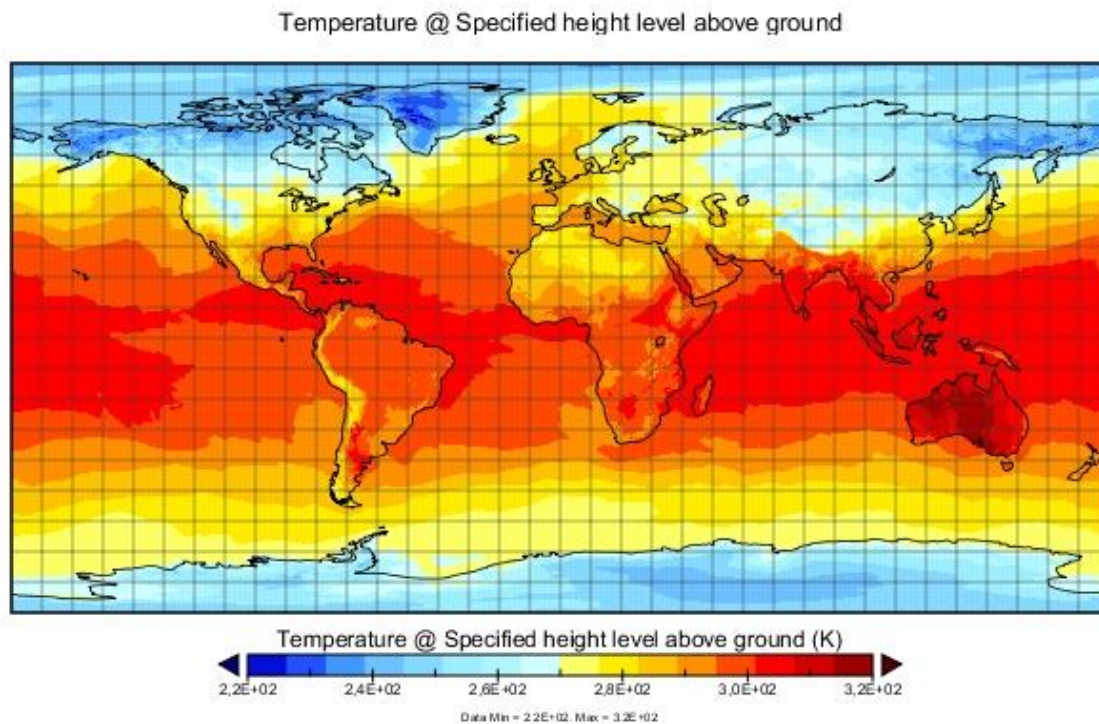


Figure 2-10: Temperature forecast value made for the whole globe (Source: NCEP)

'R' program is used for spatial subsetting to extract the forecast value recorded for the cell where Kulekhani catchment lies at. 'R' can be used for further data processing such as to compute average daily temperature from the temperature files recorded for every 3 hrs and to create timeseries. 'R' can also return the values in excel format so further data analysis can be done in excel. As an example, an 'R' script prepared to read the temperature files created for every 3 hrs, to compute the average daily temperature and finally to create the timeseries, is shown in Appendix A.

## 2.4 QUALITY CONTROL

Before the data are used for further analysis, it is very important to check the quality of the available data. The quality of the output from any kind of hydrological model is always affected by the quality of input hydro-meteorological data. There are some standard procedures to check and improve the quality of data which are discussed sequentially as below:

### 2.4.1 Visual Inspection

Available meteorological data are visually examined to check if the date and record is incomplete and contains any unphysical values. It is noticed that Daman and Thankot stations do not have complete record of precipitation data. Figure 2-11 shows the extent of missing data for each station on time scale.

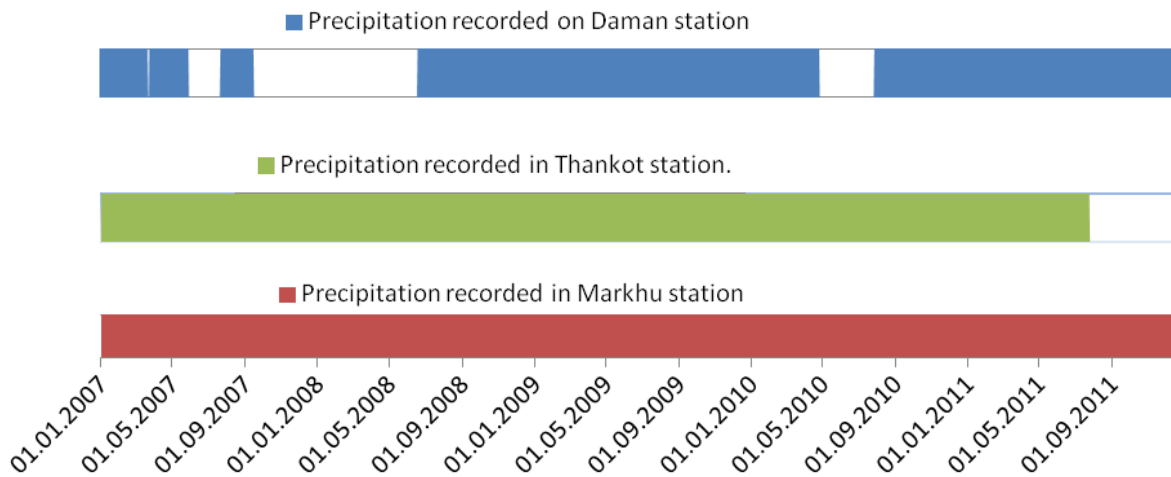


Figure 2-11: Missing data for each station on time scale

So, the next step is to estimate the missing data and make the timeseries complete and check the consistency of the available precipitation data.

#### 2.4.2 Filling of Missing Data

It is obvious that the continuity of the record may be broken with missing data due to many reasons such as sensor malfunctioning, errors in data storage/transfer/ converting and other operational difficulties. So, the missing data must be filled with correct scaling before it is sent for subsequent application.

There are many methods to estimate the missing data with the help of neighboring station data. If the annual precipitation value at each of the neighboring gauge stations differs by less than 10% from that for the gauge with missing data, station average method can be applied (Dingman, 1994).

$$p_o = \frac{1}{G} \times \sum_{g=1}^G p_g$$

If the difference in annual precipitation value exceeds by 10%, Normal ratio method is used.

$$p_o = \frac{1}{G} \times \sum_{g=1}^G \frac{P_o}{P_g} \times p_g$$

Where,

$p_o$  = Missing data estimate

$p_g$  = Observed values for corresponding day at  $g = 1, 2, 3, \dots, G$  nearby gauges

$P_o$  = Annual average precipitation at the gauge with missing values

$P_g$  = Annual average precipitation at the nearby gauge stations

Due to unavailability of annual average precipitation for each station, an inverse distance weighing method is applied in this study. The precipitation recorded in one more station i.e.

Chisapani, is also used in filling missing data. It is assumed that the weight is inversely proportional to distance squared ( $b=2$ ) and  $D$  is calculated as:

$$D = \sum_{g=1}^G d_g^{-b}$$

Then the missing value is estimated as:

$$p_o = \frac{1}{D} \times \sum_{g=1}^G d_g^{-b} \times p_g$$

Where, symbols carry the same meaning as above.

### 2.4.3 Accumulation Plot

Once the missing data are filled, it is important to check if the data are estimated with correct scaling. If the scaling is correct, the accumulation plot should continue with same gradient over the long period. Figure 2-12 shows the accumulation plot of precipitation timeseries recorded on different gauge stations.

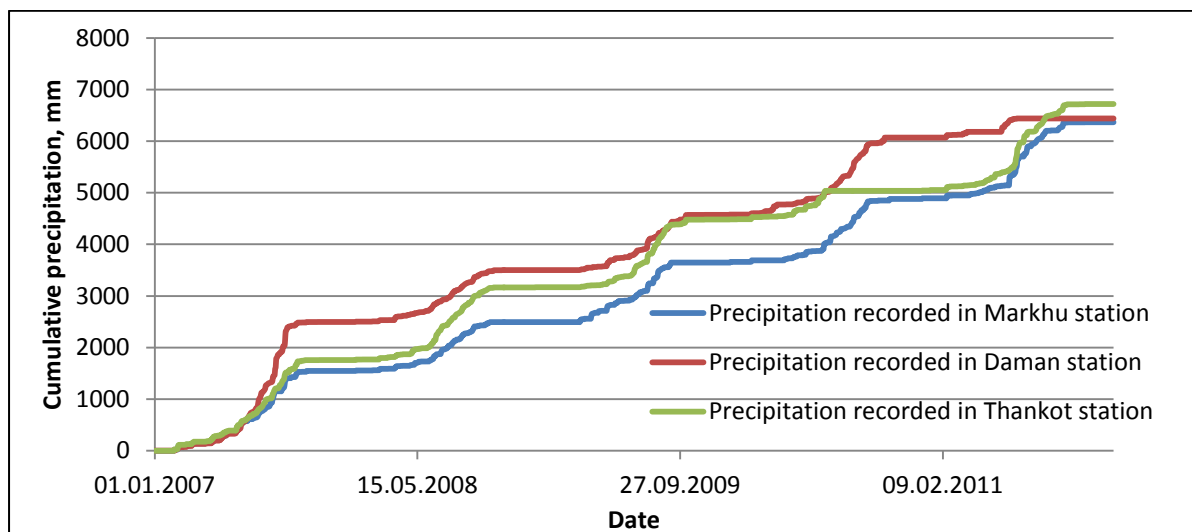


Figure 2-12: Accumulation plot of precipitation timeseries for each station

The accumulation plot shows almost the same gradient throughout the whole period for each station. Now, these cumulative precipitations are plotted against each other to check the consistency of the data.

### 2.4.4 Double Mass Curve

Double mass curve is the very useful technique to detect the consistency of data recorded in one station with respect to other station. Markhu station has complete set of precipitation data so it is considered as a reference station and the cumulative precipitation recorded in other two stations: Daman and Thankot are plotted against the cumulative precipitation recorded in Markhu station.

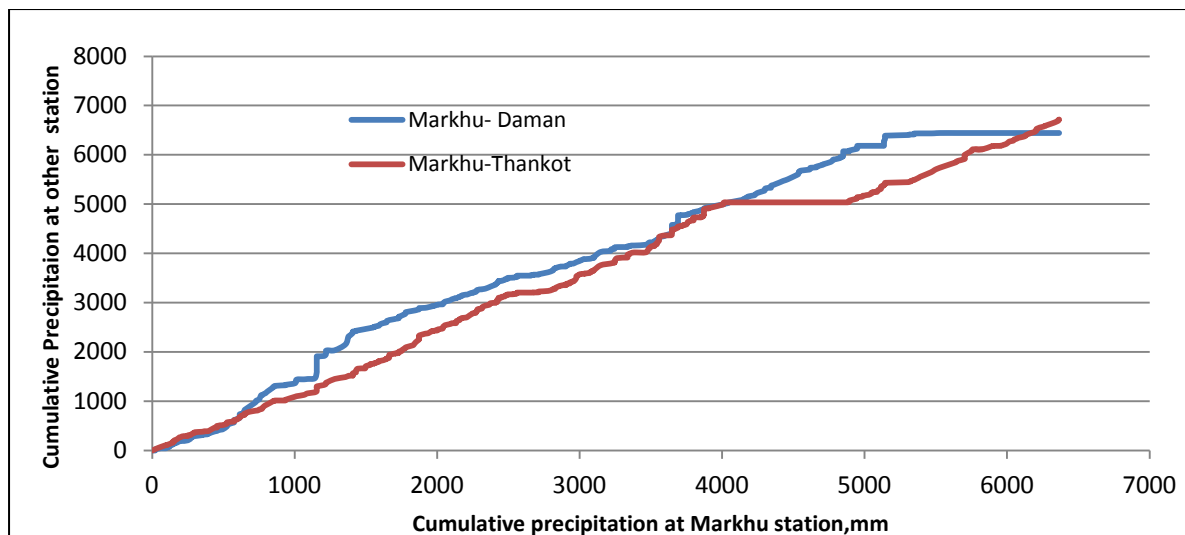


Figure 2-13: Double mass curve for Daman and Thankot station

Figure 2-13 shows that there is a break in the slope in each double mass plot about the last part which implies that the recordings in both stations are not consistent with Markhu station. Figure 2-5 and Figure 2-6 also show that the precipitation variability over the monsoon season for the year 2011 and 2010 are not well maintained for Daman and Thankot stations respectively. After having closer look to the precipitation records for Daman and Thankot station, it is found that both stations record zero precipitation almost for whole monsoon season for the year 2011 and 2010 respectively when there should be precipitation in actual. By examining the data in various aspects, now it is confirmed that there is a serious error in precipitation records made at Daman and Thankot stations so they are not used in further analysis.

## 2.5 DISCUSSION AND CONCLUSION

The quality of precipitation timeseries recorded in three gauge stations: Markhu, Daman and Thankot are examined in various aspects. Double mass curve has given very useful information about the consistency of recorded data and showed that there is a serious error in precipitation records at Daman and Thankot stations. So these data are not used in further calculations.

The areal precipitation for the Kulekhani catchment is assumed to be equal to precipitation recorded in Markhu station due to lack of consistent data recorded in nearby stations which form the Thiessen polygon. So no further computation for areal precipitation is made in this study.



### 3 GLOBAL FORECAST SYSTEM (GFS)

#### 3.1 INTRODUCTION

The Global Forecast System (GFS) is a global numerical weather forecast containing a global computer model and variational analysis run by the National Weather Service (NWS), U.S.A. This is the only one global model whose outputs are available for free in public domain. This mathematical model is run four times a day in every 6 hrs and produces forecasts up to 16 days in advance, but with decreasing spatial and temporal resolution over time. It is widely accepted that beyond 7 days the forecast is very general and not very accurate, and most nongovernmental agencies rarely use any of the model's results beyond 10 days.

The model runs in two steps: In the first step model produces forecasts up to 192 hours (8days) in advance with higher resolution and in the second step model is run with lower resolution and produces forecasts from 192 to 384 hours (16 days). The resolution of the model varies in each step of the model: horizontally, it divides the surface of the earth into 35 or 70 kilometer grid squares; vertically, it divides the atmosphere into 64 layers. The model produces a forecast for every 3rd hour for the first 192 hours, after that they are produced for every 12th hour.

The GFS model is a coupled model, composed of four separate models (an atmosphere model, an ocean model, a land/soil model, and a sea ice model), which work together to provide an accurate picture of weather conditions. Changes are regularly made to the GFS model to improve its performance and forecast accuracy. It is a constantly evolving and improving weather model.

The GFS model outputs in Gridded format are available for free download through number of different websites, some of them are:

[http://nomads.ncdc.noaa.gov/data.php?name=access#hires\\_weather\\_datasets](http://nomads.ncdc.noaa.gov/data.php?name=access#hires_weather_datasets)

<http://dss.ucar.edu>

*(Note: This chapter is written with the help of document posted in NCEP website (<http://www.emc.ncep.noaa.gov/GFS/doc.php>) in conjunction with Wikipedia so no referencing is made, unless otherwise stated).*

#### 3.2 BASIC MODEL EQUATIONS

The model is based on the usual expressions of conservation of mass, momentum, energy and moisture. Conservation of mass states that matter cannot be created nor be destroyed. Conservation of energy ensures that internal energy can be altered only by work done or by adding or removing heat to/from the system. The law of motion states that the momentum can be changed only by a force. These principles, expressed in quantitative form, provide the framework for the study of atmospheric dynamics. The physical principles may be expressed mathematically in terms of differential equations(Lynch, 2006). Some fundamental model

equations are discussed here; detail explanation is not presented in this report since it involves so many complex differential equations.

## 1. Momentum Equation

The momentum equation used in model is (Eq1)

$$\begin{aligned} \frac{\partial \vec{v}_k}{\partial t} = & -\nabla \left( \frac{\vec{v}_k \cdot \vec{v}_k}{2} \right) - \xi_k \vec{k} \times \vec{v}_k - \frac{1}{2\Delta_k} [\hat{O}_{k+1}(\vec{v}_{k+1} - \vec{v}_k) + \hat{O}_k(\vec{v}_k - \vec{v}_{k-1})] \\ & - \nabla \phi_k - RT_k \nabla \ln \eta_* - f \vec{k} \times \vec{v}_k + \vec{F}_k \end{aligned} \quad (1)$$

Where,  $v$  = meridional velocity

$R$  = gas constant

$T$  = temperature

$\phi$  = latitude

$K$  = total number of layers

$\vec{k}$  = vertical unit vector

$\eta$  = pressure

$\eta_*$  = surface pressure

$\vec{F}$  represents dissipative processes in the model

## 2. Thermodynamic Equation

The thermodynamic equation is (Eq 2)

$$\begin{aligned} \frac{\partial T_k}{\partial t} = & -\vec{v}_k \cdot \nabla T_k + KT_k \left( \frac{\partial}{\partial t} + \vec{v}_k \cdot \nabla \right) \ln \eta_* + \frac{H_k}{C_p} \\ & - \frac{1}{2\Delta_k} \left[ \hat{O}_{k+1} \left( \frac{\pi_k}{\pi_{k+1}} T_{k+1} - T_k \right) + \hat{O}_k \left( T_k - \frac{\pi_k}{\pi_{k-1}} T_{k-1} \right) \right] \end{aligned} \quad (2)$$

Where,

$$T_k = p_k \theta_k$$

$$\pi_k = (p_k / p_0)^K$$

and

$$K = R / C_p$$

### 3. Surface Pressure Equation

This equation is obtained from the continuity equation by integration over the full sigma domain (Eq 3.1):

$$\int_{\sigma}^1 \left( \frac{\partial \ln p_*}{\partial t} + \vec{V} \cdot \nabla \ln p_* + \nabla \cdot \vec{V} \frac{\partial \sigma}{\partial \sigma} \right) d\sigma = 0 \quad (3.1)$$

Since

$$\hat{\sigma}(0) = \hat{\sigma}(1) = 0,$$

Now the final equation becomes (Eq 3.2)

$$\frac{\partial \ln \eta_*}{\partial t} = - \sum_{k=1}^K \left( \nabla \cdot \vec{V}_k + \vec{V}_k \cdot \nabla \ln \eta_* \right) \Delta_k \quad (3.2)$$

The symbols carry the same meaning as in Eq.1

### 4. Moisture Equation

We assume that the mixing ratio  $q$  is conserved subject to sources and sinks represented by  $S$ . Then

$$\frac{dq}{dt} = S \quad (4.1)$$

Transforming Eq. (4.1) into flux form and performing the vertical derivative approximation yields (Eq 4.2)

$$\frac{\partial q_k}{\partial t} = - \vec{V}_k \cdot \nabla q_k - \frac{1}{2\Delta_k} \left[ \hat{\sigma}_{k+1} (q_{k+1} - q_k) + \hat{\sigma}_k (q_k - q_{k-1}) \right] + S_k \quad (4.2)$$

### 5. Divergence Equation

The divergence equation is (Eq 5)

$$\frac{\partial D_k}{\partial t} = \frac{1}{\alpha \cos^2 \varphi} \left( \frac{\partial B_k}{\partial \lambda} - \cos \varphi \frac{\partial A_k}{\partial \varphi} \right) - \nabla^2 (E_k + \Phi_k + RT_{0k} \ln \eta_*) \quad (5)$$

### 6. Vorticity Equation

The vorticity equation is (Eq 6)

$$\frac{\partial \eta_k}{\partial t} = - \frac{1}{\alpha} \cos^2 \varphi \left( \frac{\partial A_k}{\partial \lambda} + \cos \varphi \frac{\partial B_k}{\partial \varphi} \right) \quad (6)$$

### 7. Hydrostatic Equation

The governing hydrostatic equation is (Eq 7)

$$\Phi_{k-1} - \Phi_k = \frac{C_p}{2} \left[ T_{k-1} \left( \frac{\pi_k}{\pi_{k-1}} - 1 \right) + T_k \left( 1 - \frac{\pi_{k-1}}{\pi_k} \right) \right] \quad (7)$$

for  $k = 2, \dots, K$ , and

$$\sum_{i=1}^K \hat{\phi}_i \Delta_i = \hat{\phi}_1 + R \sum_{i=1}^K T_i \Delta_i$$

where  $\hat{\phi}_1$  is the surface geo-potential.

### 8. Vertical Velocity

The vertical velocity is approximated by following equation (Eq 8)

$$\hat{\sigma}_{k+1} = \hat{\sigma}_k + \Delta_k \left[ \sum_{k=1}^K (\vec{V}_k \cdot \nabla \ln p + \nabla \cdot \vec{V}_k) \Delta_k - \vec{V}_k \cdot \nabla \ln p - \nabla \cdot \vec{V}_k \right] \tag{8}$$

This recursive relation starts from  $\hat{\sigma}$  (surface) = 0 and satisfies  $\hat{\sigma}$  (top) = 0.

### 3.3 GFS MODEL STRUCTURE

There exists only one document on NCEP website to show how the system works. As per document posted in NCEP, the system utilizes a collection of job scripts that perform the tasks for each step. A job script runs each step and initiates the next job in the sequence. Example: When the “preparation” job finishes it submits the “analysis job”. When the “analysis” job finishes it submits the “forecast job”. It converts resulting analysis and forecast fields to WMO grib for use by other models and external users “post”. Additional steps run in experimental mode are verification and archive jobs.

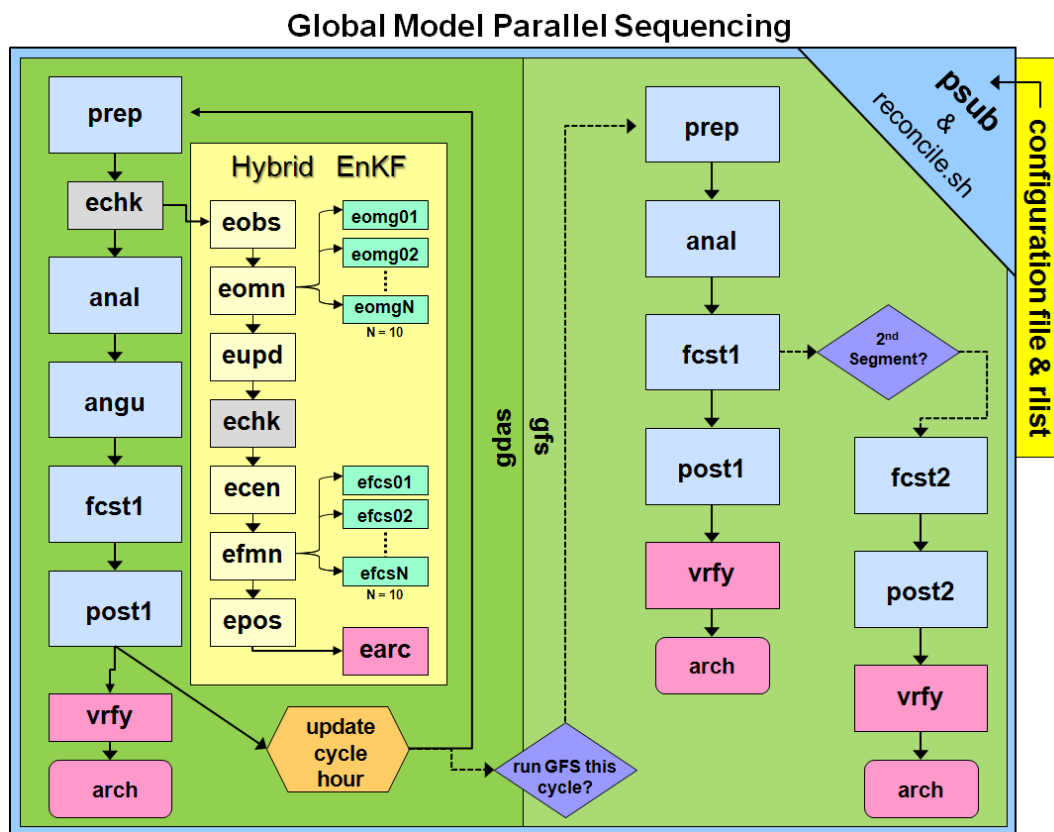


Figure 3-1: Flow diagram of typical Global Forecast System, GFS (Source: NCEP)

### 3.4 MODEL PROPERTIES

Different model properties of the current version of the atmospheric model of NCEP's Global Forecast System (GFS) are briefly explained in this section. The aim is to give the short overview of model properties; detail explanation is not presented here as it is not great concern for the proposed aim of thesis.

#### 3.4.1 Numerical /Computational Properties

1. Horizontal Resolution

Spectral triangular 254 (T254); Gaussian grid of 768X384, roughly equivalent to 0.5 X 0.5 degree latitude/longitude.

2. Vertical Domain

The vertical domain is from the earth's surface ( $\sigma=1$ ) to the top of the atmosphere ( $\sigma=0$ ). This domain is divided into 64 layers with enhanced resolution near the bottom and the top. For a surface pressure of 1000 hPa, the lowest atmospheric level is at a pressure of about 997.3 hPa and the top level is at about 0.27 hPa.

3. Vertical Resolution

64 unequally-spaced sigma levels. For a surface pressure of 1000 hPa, 15 levels are below 800 hPa, and 24 levels are above 100 hPa.

#### 3.4.2 Dynamical/ Physical Properties

1. Atmospheric Dynamics

Primitive equations with vorticity, divergence, logarithm of surface pressure, specific humidity virtual temperature, and cloud condensate are used as dependent variables.

2. Radiation

For the shortwave (SW) computation, the parameterization uses a correlated-k distribution method for water vapor and transmission function look-up tables for carbon dioxide and oxygen absorptions. The model contains eight broad spectral bands covering ultraviolet (UV) and visible region ( $< 0.7 \mu\text{m}$ ), and choices of one or three spectral bands in the near infrared (NIR) region ( $> 0.7 \mu\text{m}$ ).

For the longwave (LW), the parameterization scheme uses a correlated-k distribution method and a linear-in-tau transmittance table look-up to achieve high accuracy and efficiency. The algorithm contains 140 unevenly distributed intervals (g-point) in 16 broad spectral bands. In addition to the major atmospheric absorbing gases of ozone, water vapor, and carbon dioxide, the algorithm also includes various minor absorbing species such as methane, nitrous oxide, oxygen, and up to four types of halocarbons (CFCs).

3. Orography

New orography data sets are constructed based on a United States Geological Survey (USGS) global digital elevation model (DEM) with a horizontal grid spacing of 30 arc

---

seconds (approximately 1 km). Orography statistics including average height, mountain variance, maximum orography, land-sea-lake masks are directly derived from a 30-arc second DEM for a given resolution.

4. Sea ice

Sea-ice is obtained from the analysis by the marine Modeling Branch, available daily. The sea ice is assumed to have a constant thickness of 3 meters, and the ocean temperature below the ice is specified to be 271.2 K. The surface temperature of sea ice is determined from an energy balance that includes the surface heat fluxes and the heat capacity of the ice. Snow accumulation does not affect the albedo or the heat capacity of the ice.

5. Snow cover

Snow cover is obtained from an analysis by NESDIS (the IMS system) and the Air Force, updated daily. When the snow cover analysis is not available, the predicted snow in the data assimilation is used. Precipitation falls as snow if the temperature at  $\sigma=0.85$  is below 0 C. Snow mass is determined prognostically from a budget equation that accounts for accumulation and melting. Snow melt contributes to soil moisture, and sublimation of snow to surface evaporation. Snow cover affects the surface albedo and heat transfer/capacity of the soil, but not of sea ice. See also Sea Ice, Surface Characteristics, Surface Fluxes, and Land Surface Processes.

6. Land surface processes

Soil temperature and soil volumetric water content are computed in two layers at depths 0.1 and 1.0 meters by a fully implicit time integration scheme (Pan and Mahrt, 1987). For sea ice, the layer depths were specified as 1.5 and 3 meters. Heat capacity, thermal and hydraulic diffusivity and hydraulic conductivity coefficients are strong functions of the soil moisture content. A climatological deep-soil temperature is specified at the third layer of 4 meters for soil and a constant value of 272 K is specified as the ice-water interface temperature for sea ice. The vegetation canopy is allowed to intercept precipitation and re-evaporation. Runoff from the surface and drainage from the bottom layer are also calculated.

## 4 COMPARISON BETWEEN GFS MODEL OUTPUT AND OBSERVATIONS

### 4.1 INTRODUCTION

Weather forecasting is the process of predicting the state of the atmosphere with the help of current state of atmosphere, sky condition and many other atmospheric factors. The reliability and robustness of the weather models to represent the actual atmospheric process can be assessed in terms of how close model simulations are with observational values. If there are significant differences between model output and measured data, it means model developers have more work to do and must go back, check their data, check their algorithms, and see if they are missing any critical components of the system. Validation of GFS model is not of our prime interest and beyond the scope of the thesis but to see how model output corresponds to observational data, where they are similar and where they diverge could be of great interest to us. It is also equally important to check how model works in catchment scale.

### 4.2 PURPOSE OF COMPARISON

The meteorological forecasts used in this study are the output of Global Forecast System (GFS) model which is run in approximately 50km x 50km spatial resolution. The meteorological forecasts made in larger scale do not match the observations made in catchment scale because the model cannot resolve the local terrain effects. Thus, the comparison chapter is made to examine at what degree the meteorological forecasts correspond to the observations and to check whether any bias correction method is needed further.

### 4.3 MODEL EVALUATION TECHNIQUES

Numerous model evaluation techniques can be found in published literatures. Various model evaluation techniques as suggested by Moriasi et al. (2007) viz. Pearson's correlation coefficient ( $r$ ) and coefficient of determination ( $R^2$ ), Index of agreement ( $d$ ), Nash-Sutcliffe efficiency (NSE), RMSE-observations standard deviation ratio (RSR), Daily root-mean square (DRMS), are equally capable to assess the model soundness and reliability. They can be distinctly divided into two broad class i.e. statistical method and graphical comparison. Some commonly used statistical methods viz. Pearson's correlation coefficient ( $r$ ) and Nash-Sutcliffe efficiency (NSE), and graphical comparison of model output with observational data is presented in this report.

#### 4.3.1 Statistical Method

##### 4.3.1.1 Pearson's correlation coefficient ( $r$ )

Pearson's correlation coefficient ( $r$ ) measures the linear dependence between two variables (Eq.1)

$$r = \frac{\sum_{i=1}^n (X_i - \bar{X})(Y_i - \bar{Y})}{\sqrt{\sum_{i=1}^n (X_i - \bar{X})^2} \sqrt{\sum_{i=1}^n (Y_i - \bar{Y})^2}} \quad (1)$$

Its value ranges from -1 to 1. A perfect positive linear relationship exists when  $r = 1$ , no linear relationship exists when  $r = 0$  and negative linear relationship exists when  $r = -1$ .

The Pearson's correlation coefficient is calculated by using excel formula (Eq.2)

$$r = \text{PEARSON} (A1:A10; B1:B10) \quad (2)$$

Where, A1:A10 is observed precipitation time series

B1:B10 is precipitation forecasts time series

Similarly, correlation between temperature forecast and measured temperature is also calculated. The Pearson's correlation coefficient ( $r$ ) is found to be 0.31 i.e 31% with precipitation time series and 0.86 i.e 86 % for temperature time series.

#### 4.3.1.2 Nash-Sutcliffe efficiency (NSE)

The Nash-Sutcliffe efficiency (NSE) is a normalized statistic that determines the relative magnitude of the residual variance compared to the measured data variance (Moriassi et al., 2007).NSE indicates how well the plot of observed versus simulated data fits the 1:1 line and is calculated with the equation (Eq.1).

$$\text{NSE} = 1 - \frac{\sum_{i=1}^n (Y_i^{\text{obs}} - Y_i^{\text{sim}})^2}{\sum_{i=1}^n (Y_i^{\text{obs}} - Y^{\text{mean}})^2} \quad (1)$$

Where,  $Y_i^{\text{obs}}$  is the  $i$ th observation for the constituent being evaluated,  $Y_i^{\text{sim}}$  is the  $i$ th simulated value for the constituent being evaluated,  $Y^{\text{mean}}$  is the mean of observed data for the constituent being evaluated, and  $n$  is the total number of observations.

Nash-Sutcliffe efficiencies can range from  $-\infty$  to 1. An efficiency of 1 ( $E = 1$ ) corresponds to a perfect match of modeled discharge to the observed data. An efficiency of 0 ( $E = 0$ ) indicates that the model predictions are as accurate as the mean of the observed data, whereas an efficiency less than zero ( $E < 0$ ) occurs when the observed mean is a better predictor than the model.

The Nash-Sutcliffe efficiencies are calculated for precipitation and temperature with the model data and measured data using excel formula as below (Eq.2).

$$\text{NSE} = 1 - \text{sumproduct} ((A1:A12 - B1:B12)^2) / \text{sumproduct} ((A1:A12 - C1)^2) \quad (2)$$

Where, C1 =average(A1:A12) ,and A1:A12 contains the observed data and B1:B12 contains the modeled data.

An efficiency of -1.12 is computed for precipitation and -0.19 is calculated for temperature using model output and measured data in daily timestep.

#### 4.3.2 Graphical Method

Graphical techniques provide visual comparison between simulated and observed data for qualitative analysis. Statistical method was applied to examine the reliability of GFS model with the daily time step data in the previous section. Now, the model output is compared to

corresponding measured data in large timestep i.e. month especially in two aspects viz. Comparison in monthly value, and precipitation frequency.

### 4.3.2.1 Comparison in monthly value

#### a. For precipitation

It is clearly noticed that the GFS model has overestimated the amount of precipitation when their monthly values are compared to observed data. Figure 4-1, Figure 4-2 and Figure 4-3 shows that the disagreement of monthly value between precipitation forecast and measured precipitation is getting higher as we move forward from year 2007 to 2009. Negative sign is used to make clear distinction between two graphs and does not carry any specific meaning.

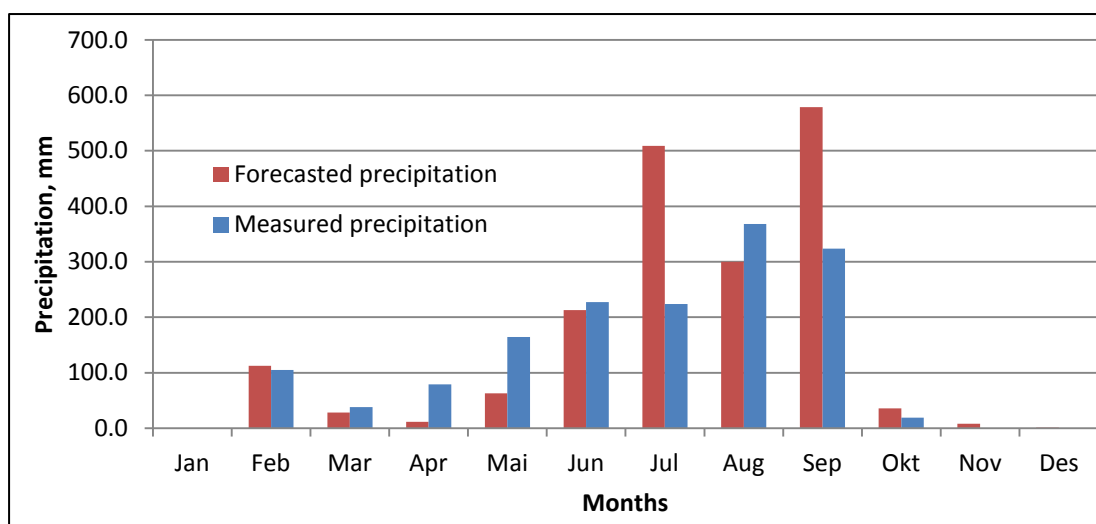


Figure 4-1: Monthly value of precipitation forecast and observed precipitation for the year 2007

It is also noticed that the GFS model has underestimated the precipitation for dry season but overestimated the precipitation for monsoon than that of observed ones.

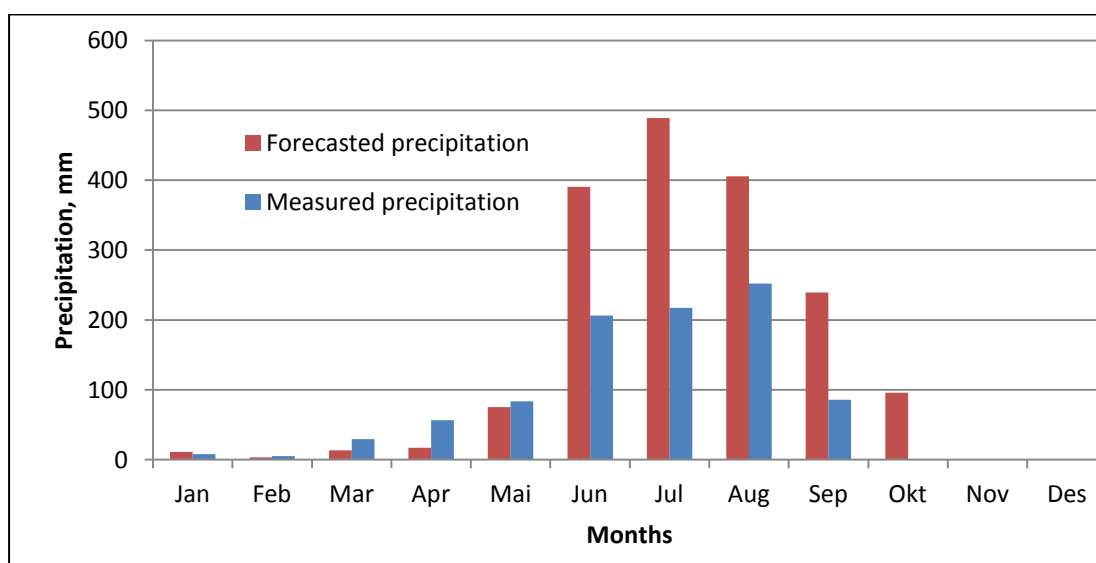


Figure 4-2: Monthly value of precipitation forecast and observed precipitation for the year 2008

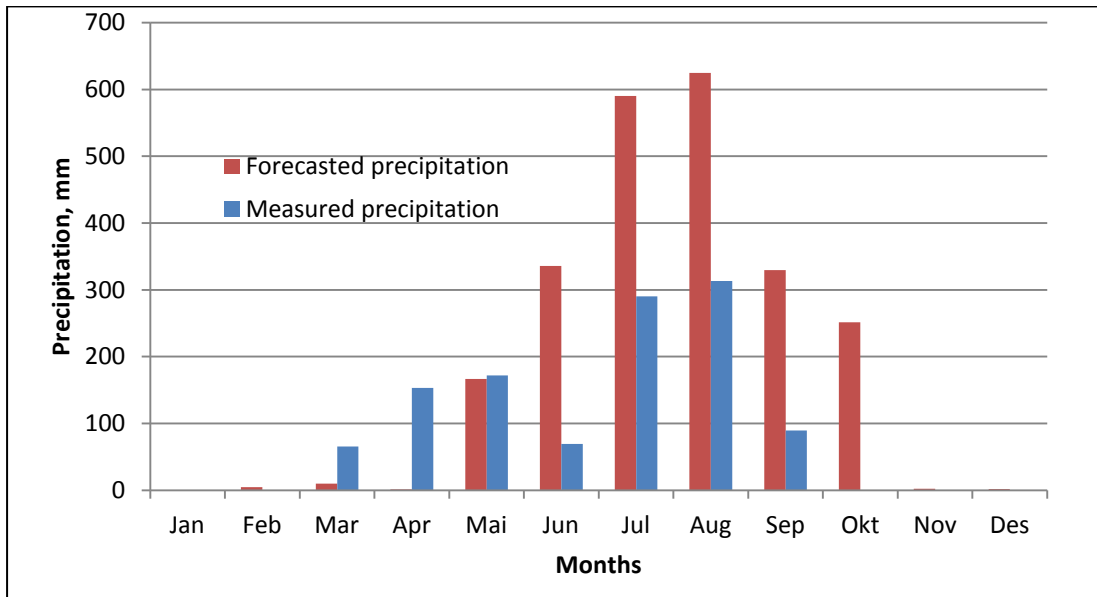


Figure 4-3: Monthly value of precipitation forecast and observed precipitation for the year 2009

There is a big difference between precipitation forecast and measured precipitation particularly for the years 2010 and 2011 as shown in Figure 4-4 and Figure 4-5 so the precipitation forecast for these period are not being used in further analysis since it may greatly affect the degree of correspondence between observed value and forecast in its subsequent application.

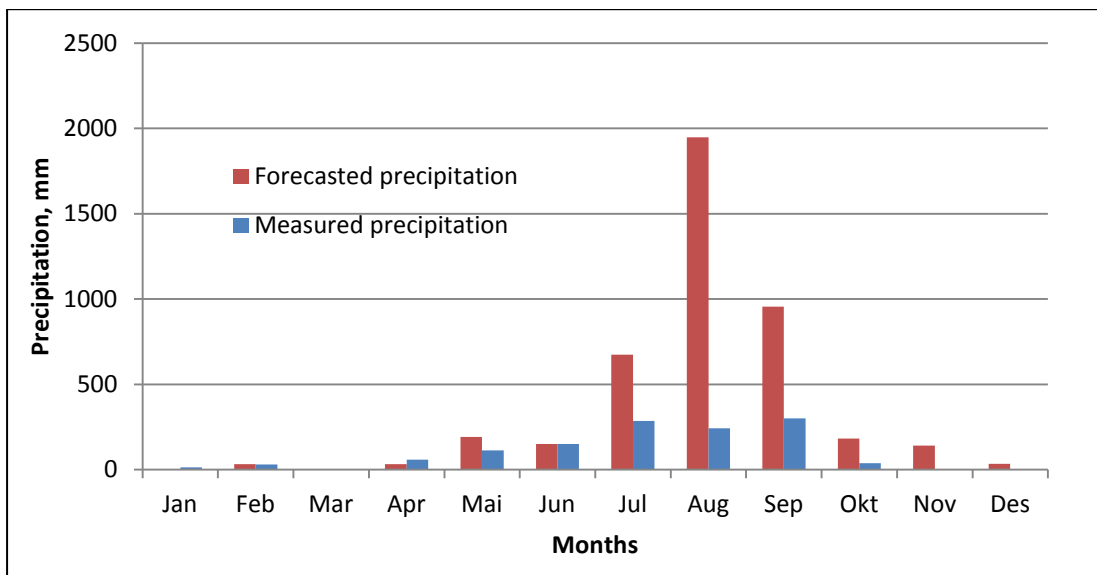


Figure 4-4: Monthly value of precipitation forecast and observed precipitation for the year 2010

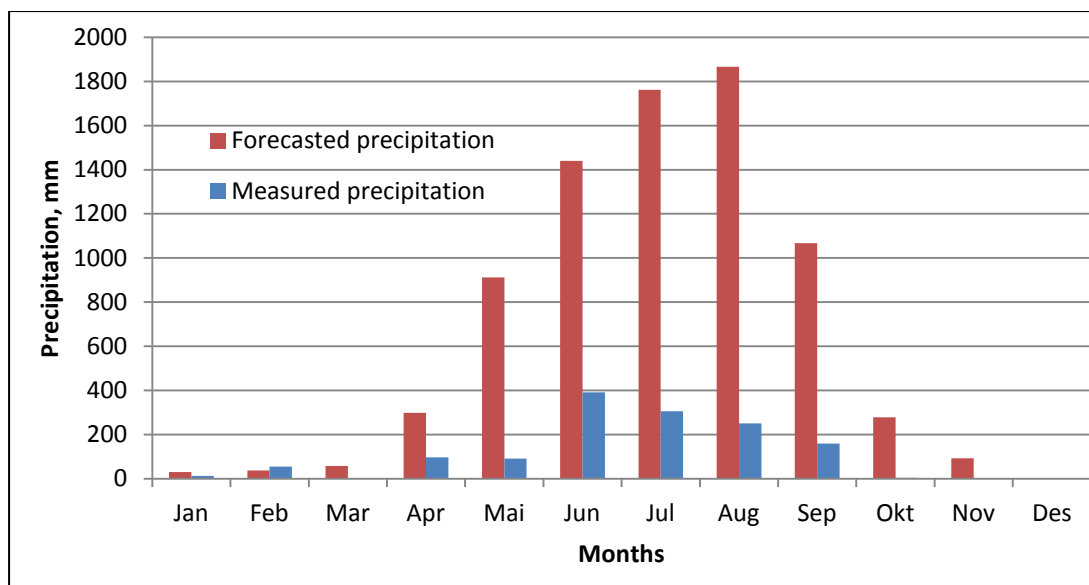


Figure 4-5: Monthly value of precipitation forecast and observed precipitation for the year 2011

The reason for the GFS model to forecast the much higher precipitation could be that the model has problems in resolving the monsoon season over the study area thus produces way too much rain.

**b. For temperature**

The similar pattern has appeared in temperature forecast as well. The GFS model has overestimated the temperature for all months when their averaged monthly values are compared to observed values.

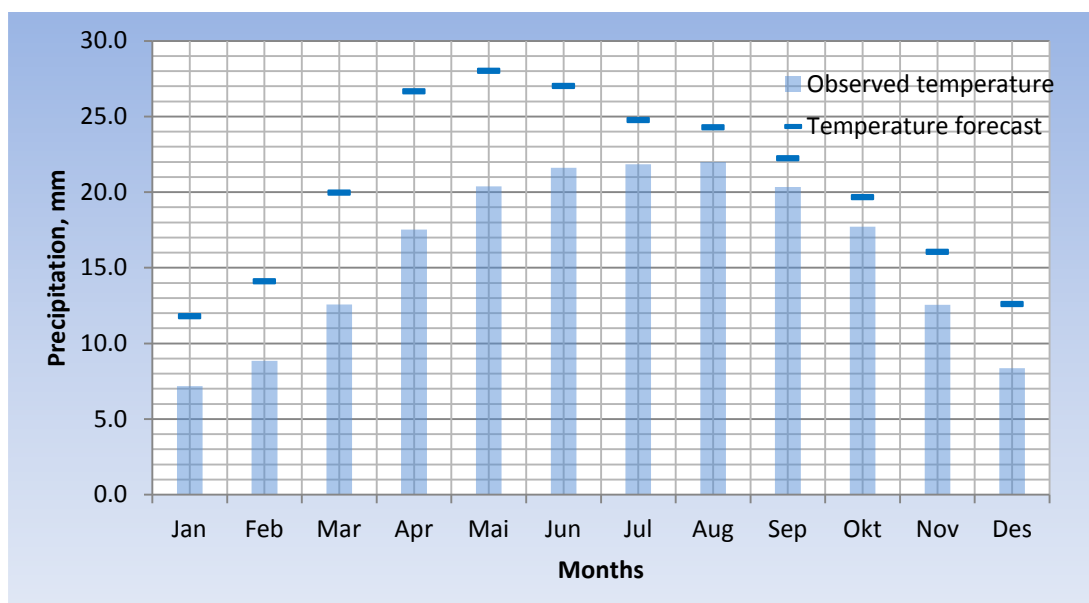


Figure 4-6: Average monthly value of temperature forecast and observed temperature for the year 2007

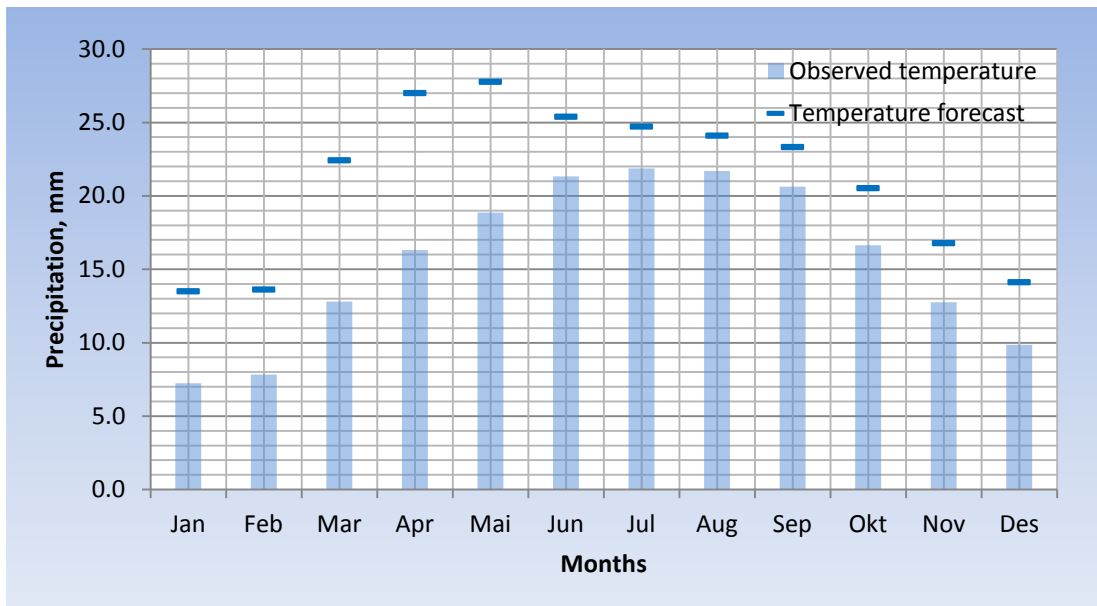


Figure 4-7: Average monthly value of temperature forecast and observed temperature for the year 2008

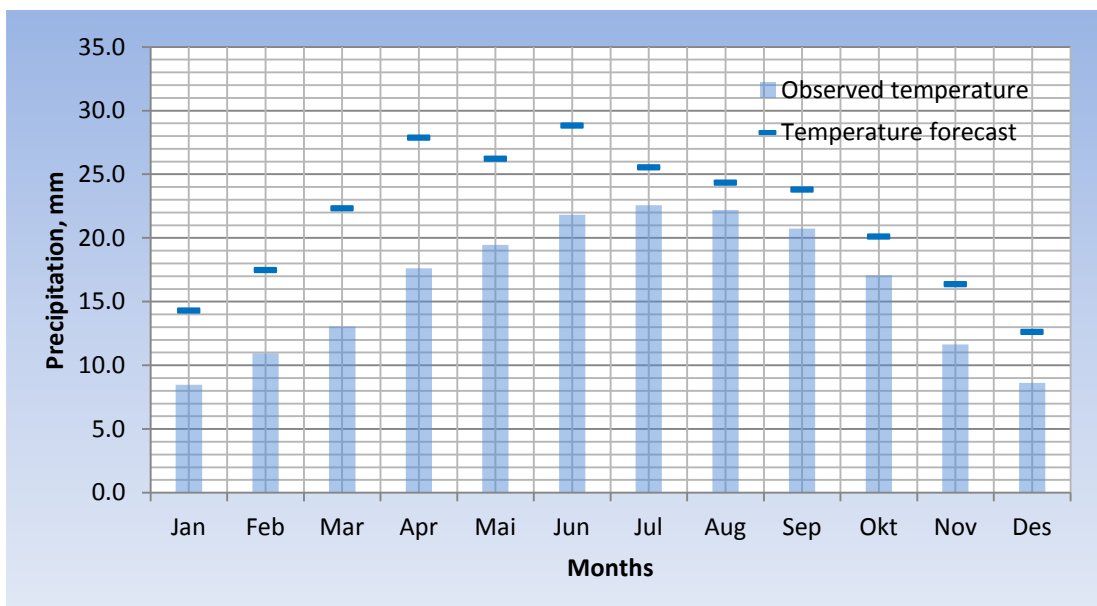


Figure 4-8: Average monthly value of temperature forecast and observed temperature for the year 2009

One reason for the temperature forecast to be higher than observed one is that GFS model has used lower elevation level as a vertical co-ordinate of the grid than the actual elevation of the site. The result can be improved by adjusting it with lapse rate, which is discussed in following chapter.

#### 4.3.2.2 Comparison in precipitation frequency

A very useful and self describing comparison technique is applied to compare the modeled precipitation to measured precipitation. In Figure 4-9, Red bars show the number of days GFS model forecasts 'precipitation' when there is 'no precipitation' in actual and blue bars show the number of days model forecasts 'no precipitation' when there is 'precipitation' in actual in each month.

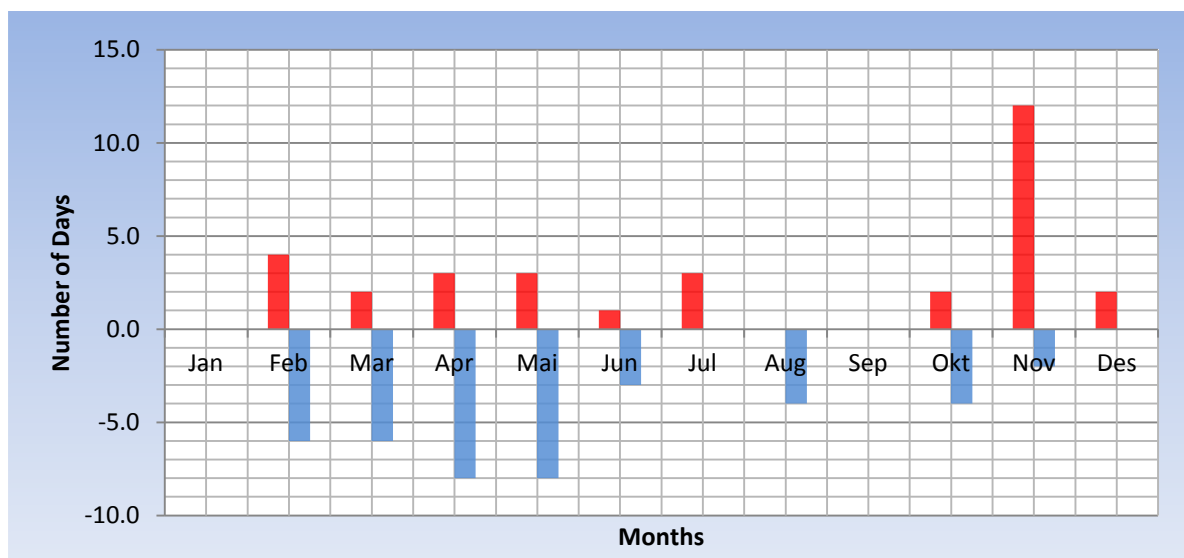


Figure 4-9: Number of days model forecasts 'precipitation' when there is 'no precipitation' in actual and vice versa (Year 2007)

Figure 4-10 shows that the GFS model has overestimated the number of days with precipitation when there is no precipitation in actual. The model has unexpectedly forecasted precipitation for too many days in February month when the days with precipitation are supposed to be too small.

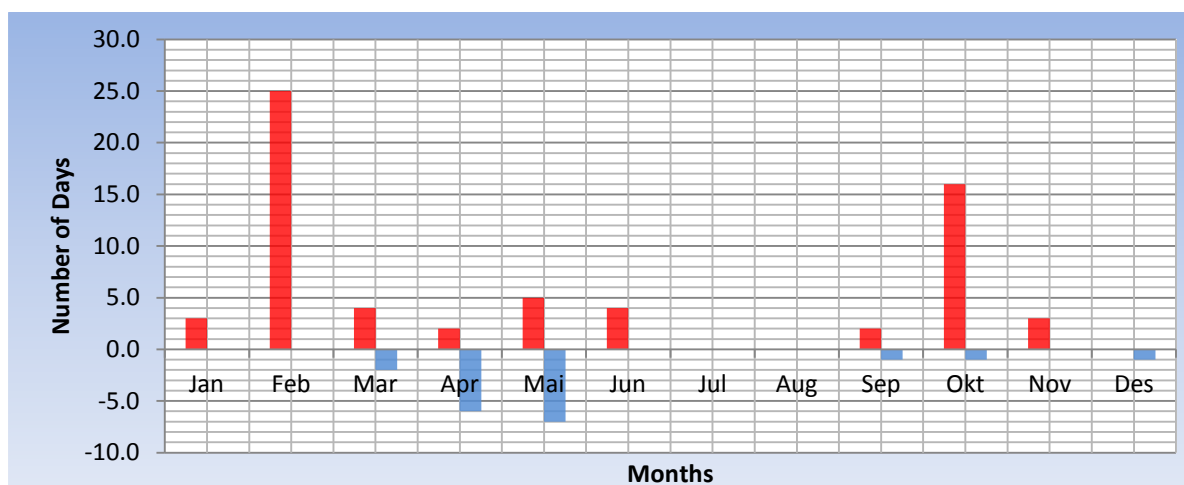


Figure 4-10: Number of days model forecasts 'precipitation' when there is 'no precipitation' in actual and vice versa (Year 2008)

In most of the months, Figure 4-11, the GFS model has overestimated the number of days with precipitation than the days with precipitation reported from the gauge stations. In

contrast to this general statement, there exists one month (April) when forecast shows high number of days with no precipitation when there is precipitation in actual.

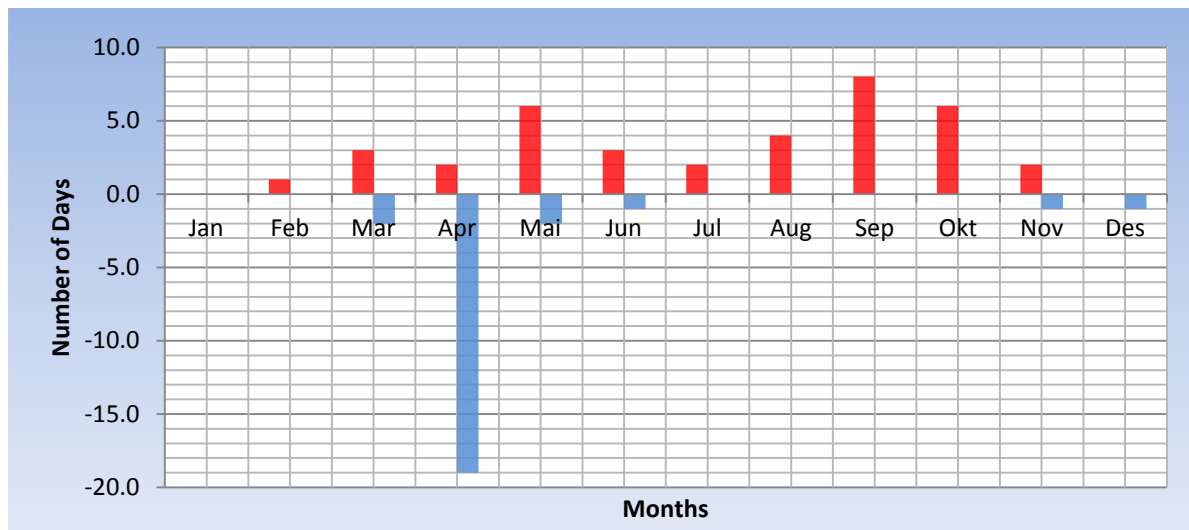


Figure 4-11: Number of days model forecasts 'precipitation' when there is 'no precipitation' in actual and vice versa (Year 2009)

Analyzing above figures it is noticed that the frequency of precipitation which is forecasted by GFS model is more than that of actual one, however opposite case exists for few months.

#### 4.4 RESULTS AND DISCUSSION

Low Pearson's correlation coefficient (0.31) is achieved for the precipitation time series when the forecast is compared to measured data. A better result (0.86) is achieved in temperature field. Nash-Sutcliffe efficiency -1.12 tells that GFS model is not capable to forecast the precipitation with daily time step that fits with observed value.

A graphical comparison in larger time step i.e. monthly shows that in most of the cases, the forecasted values are higher than the corresponding measured value both for precipitation and temperature. Not only forecasted precipitation amount is higher than observed value but also frequency of precipitation is higher in forecast than the corresponding measurement. It is also noticed that temperature forecasts are more reliable than precipitation forecasts.

#### 4.5 CONCLUSIONS AND RECOMMENDATION

Since the study is carried out for mountainous area, the coarse resolution global forecast model will generally do a poor job at depicting precipitation and temperature at catchment scale because it won't be able to resolve local terrain impacts. It would be best to use data from a high resolution mesoscale model that is run over the study area (such as the US, NAM-12km model which is run over the US), but there is no mesoscale model that is operationally run over Nepal till this moment.

The further data processing is followed by bias correction which is discussed in next chapter.

---

## 5 BIAS CORRECTION FOR GFS MODEL OUTPUT

### 5.1 INTRODUCTION

In general sense, bias refers to any deviation of interest (e.g. with respect to the mean, variance, covariance, length of dry spells, etc.) of the model from the corresponding “true” value (Ehret et al., 2012). The model output deviates significantly from actual value and the reason for that biased model output are imperfect model representation of the atmospheric physics, also the local modeled response to external forcing, i.e., the local climate sensitivity is biased in general (Maraun, 2012).

Thus the output from general circulation model (GCM) cannot be used directly in its subsequent application e.g. in hydrological or other impact models without some form of prior bias correction if realistic output is sought (Piani et al., 2010).

Generally, output from the both Global and Regional Circulation Models are affected with significant degree of biases which prevents its direct use, especially in climate change impact studies. The standard way to overcome this problem is the bias correction (BC), i.e. the correction of model output towards observations in a post processing step for its subsequent application (Ehret et al., 2012). Some methods which can be found in literatures are discussed below:

### 5.2 BIAS CORRECTION METHODS

So far little has been reported in literature on investigation of adjustment methods of daily output from climate model. Engen-Skaugen (2007) has mentioned some bias correction methods on her technical paper. Some traditional techniques such as delta change method is used in different ways to omit the problem with local representativity by concentrating on the changes rather than the absolute values. The delta change method modifies the time series obtained by the RCM or the output from global forecast model by altering the variability and important values as extremes, drought etc. And the method is not applicable for scenarios transient in time. The spline method smoothens out the mean monthly temperature values to daily values, neglecting the day-to-day variability. Other two advanced techniques viz. empirical adjustment method and statistical bias correction method are applied and checked their effectiveness in each case for our study purpose.

#### 5.2.1 Empirical Adjustment Method

##### 5.2.1.1 Introduction

This method was applied by Engen-Skaugen (2007) for one precipitation and temperature scenario dynamically downscaled with HIRLAM from the Atmospheric-Ocean General Circulation Model at the Max-Planck Institute in Hamburg, ECHAM4/OPYC4 GSDIO with emission scenario IS92a. This method reproduces mean monthly values and standard deviations based on daily observations. This method was successfully employed and the trend obtained in the regional climate model both for temperature and precipitation was maintained, and the frequency of modeled and observed rainy days showed better agreement. It is assumed that this method also works for bias correction of GFS model output for our

case. Though the forecasts used in this study is weather forecasts not climate forecasts, it is possible to use the bias correction method used in climate forecasts since we are working with historical period.

### 5.2.1.2 Methodology

#### a. For precipitation adjustment

As real time observed precipitation data are not available, the study is carried out using historical data from 2007 to 2009, as discussed in section 4.3.2.1. The year 2007 and 2008 are chosen as the control period and rest year 2009 is considered as analysis period. The bias correction factor is derived using daily precipitation data within control period and applied to daily precipitation forecast in analysis period. The method suggested by Engen-Skaugen (2007) is followed step by step as below:

Daily precipitation values are both normalized and standardized for the analysis period (2009) to obtain a residual containing the variability of the daily precipitation data series, (Eq. 1).

$$\varepsilon P_{anls,ijk} = \frac{P_{fcst,anls,ijk} - mP_{fcst,anls,j}}{\sigma P_{fcst,anls,j}} \quad (1)$$

Where,  $\varepsilon P_{anls,ijk}$  is the residual at day  $i$  of month  $j$  in year  $k$  in the analysis period.  $P_{fcst,anls,ijk}$  is daily forecasted precipitation at day  $i$  of month  $j$  in the year  $k$  in the analysis period.  $mP_{fcst,anls,j}$  is the mean monthly forecasted precipitation value in the month  $j$  in the analysis period.  $\sigma P_{fcst,anls,j}$  is the standard deviation based on forecasted daily values for month  $j$  in the analysis period.

The method assumes that the monthly GFS model output error of variability in the analysis period is the same as for the control period, (Eqs. 2a and 2b).

$$\gamma P_j = \frac{\sigma P_{obs,ctrl,j}}{\sigma P_{fcst,ctrl,j}} \quad (2a)$$

$$\sigma P'_{anls,j} = \gamma P_j \times \sigma P_{fcst,anls,j} \quad (2b)$$

Where,  $\sigma P_{obs,ctrl,j}$  is monthly ( $j$ ) standard deviation ( $\sigma$ ) based on observed daily values (obs) within the control period.  $\sigma P_{fcst,ctrl,j}$  is monthly ( $j$ ) standard deviation ( $\sigma$ ) based on forecasted daily values (fcst) within the control period. Some main parameters that are derived during calculations are shown in Table 5-1 below:

Table 5-1: Main parameters of empirical adjustment method applied for GFS model output

Month	$\gamma P_j$	$\sigma P_{obs,ctrl,j}$	$\sigma P_{fcst,ctrl,j}$	$\sigma P_{fcst,anls,j}$	$\sigma P'_{anls,j}$	$\beta P_j$
Jan	1.46	1.02	0.69	0.00	0.00	0.00
Feb	0.87	7.46	8.55	0.93	0.81	0.08
Mar	1.67	4.06	2.43	0.73	1.22	0.48
Apr	4.22	5.40	1.28	0.10	0.44	0.08
Mai	2.29	9.03	3.94	9.99	22.89	2.42
Jun	1.12	11.87	10.60	27.75	31.08	1.11
Jul	0.69	8.94	12.90	23.63	16.38	1.18
Aug	1.50	15.22	10.14	18.04	27.08	1.77
Sep	0.78	13.74	17.64	8.25	6.43	0.81
Okt	0.53	2.17	4.07	25.68	13.68	3.82
Nov	0.00	0.00	0.54	0.30	0.00	0.52
Des	0.00	0.00	0.10	0.29	0.00	4.00

$\beta P_j$  is the ratio between the analysis mean monthly (j) sums  $mP_{fcst,anls,j}$  and control mean monthly (j) sums  $mP_{fcst,ctrl,j}$  based on forecasted daily values, (Eq.3)

$$\beta P_j = \frac{mP_{fcst,anls,j}}{mP_{fcst,ctrl,j}} \quad (3)$$

Adjusted daily precipitation is obtained by multiplying daily residuals (Eq. 1) with the adjusted standard deviation for the analysis period (Eq. 2b). Mean monthly values of daily precipitation based on observations within the control period multiplied with  $\beta P_j$  is added.

The mean differences between mean monthly values in a analysis period and a control period are maintained:

$$P'_{fcst,anls,ijk} = \varepsilon P_{anls,ijk} \times \sigma P'_{anls,j} + mP_{obs,ctrl,j} \times \beta P_j \quad (4a)$$

$$P'_{fcst,anls,ijk} = (P_{fcst,anls,ijk} - mP_{fcst,anls,j}) \times \gamma P_j + mP_{obs,ctrl,j} \times \beta P_j \quad (4b)$$

Where,  $P'_{fcst,anls,ijk}$  is the adjusted precipitation for day i in month j for the analysis period.

If  $mP_{fcst,anls,j} > mP_{obs,ctrl,j}$  values of daily precipitation in analysis period  $P'_{fcst,anls,ijk}$  will be negative. Negative values are set equal to 0.0 mm, thus, the mean monthly precipitation sum and standard deviation based on daily precipitation will be too large compared to the statistical moments based on observations. The Eqs. 1–4a and 4b are therefore performed all over again on the new dataset  $P'_{fcst,anls,ijk}$ . The iteration is repeated until the mean value and the standard deviation is satisfactorily reproduced.

**b. For temperature adjustment**

The forecasted temperature cannot be compared directly with local temperature of the study site because the GFS model uses flat elevation value as a vertical coordinates for each cell. Thus the spatial variability of the temperature within a cell cannot be achieved. So before carrying out empirical adjustment, correction to the daily temperatures for altitude biases must be done. The temperature lapse rate ( $-0.65^{\circ}\text{C}/100\text{ m}$ ) as suggested by Houghton (1985) is used to transfer the simulated temperature in to as recorded by the gauge stations (Eq.1).

$$T_{fcst,ijk} = T_{ofcst,ijk} - 0.65 \times \frac{\Delta h}{100} \tag{1}$$

Where,  $T_{ofcst,ijk}$  is the simulated temperature from the GFS Model,  $T_{fcst,ijk}$  is the height corrected temperature values and  $\Delta h$  is the height difference. Table 5-2 shows that 984 m is used in GFS model as vertical level for the study site with latitude/longitude (27.5/85.0). This table is created with the help of ‘panoply’ software using data retrieved from NCEP website upon request.

Table 5-2: Elevation used in GFS model for each cell (Source: NCEP)

		X-Axis: longitude (°E)									
		83,000	83,500	84,000	84,500	85,000	85,500	86,000	86,500	87,000	
Y-Axis: latitude (°N)	30,500	5366	5526	5594	5284	5225	5008	5066	5164	5139	
	30,000	5023	4757	5002	5449	5635	5566	5433	5332	5315	
	29,500	4876	5179	4890	4832	4903	5105	5148	5108	5042	
	29,000	4397	5158	4887	5286	5015	4929	4982	5010	4967	
	28,500	3035	3063	3716	4124	4338	5043	5247	4899	4634	
	28,000	1045	1139	761	786	1592	2664	3602	5167	5607	
	27,500	55	94	283	376	984	1238	1415	2393	2572	
	27,000	100	108	88	74	35	83	347	723	951	
	26,500	77	68	59	44	68	71	52	64	2	
	26,000	72	53	54	65	56	42	44	50	64	
	25,500	69	55	63	63	46	47	41	50	36	
	25,000	159	170	109	79	82	70	80	112	54	
	24,500	280	308	222	206	198	294	300	267	199	
	24,000	342	351	260	366	498	491	325	238	151	
	23,500	515	648	725	676	608	473	301	184	114	
	23,000	603	778	794	664	575	458	244	226	100	
	22,500	457	483	382	374	316	418	256	190	74	
22,000	241	300	247	329	357	542	432	395	13		

The empirical method which is used for adjusting forecasted precipitation can also work for temperature adjustment. Daily height corrected temperatures modeled with GFS is first normalized and standardized (Eq.2)

$$\varepsilon T_{anls,ijk} = \frac{T_{fcst,anls,ijk} - mT_{fcst,anls,j}}{\sigma T_{fcst,anls,j}} \tag{2}$$

Where,  $\varepsilon T_{anls,ijk}$  is the residual at day i of month j in year k in the analysis period.  $T_{fcst,anls,ijk}$  is daily forecasted temperature at day i of month j in the year k in the analysis period.  $mT_{fcst,anls,j}$  is the mean monthly forecasted temperature value in the month j in the analysis period.  $\sigma T_{fcst,anls,j}$  is the standard deviation based on forecasted daily values for month j in the analysis period.

The method, as for precipitation, assumes that the monthly GFS model output error of variability in the analysis period is the same as for the control period, (Eqs. 3a and 3b).

$$\gamma T_j = \frac{\sigma T_{obs,ctrl,j}}{\sigma T_{fcst,ctrl,j}} \quad (3a)$$

$$\sigma T'_{anls,j} = \gamma T_j \times \sigma T_{fcst,anls,j} \quad (3b)$$

Where,  $\sigma T_{obs,ctrl,j}$  is monthly (j) standard deviation ( $\sigma$ ) based on observed daily values (obs) within the control period.  $\sigma T_{fcst,ctrl,j}$  is monthly (j) standard deviation ( $\sigma$ ) based on forecasted daily values (fcst) within the control period.

The method force the modeled data to satisfactorily reproduce mean monthly values in the control period obtained by GFS by using the absolute change ( $\beta P_j$ ) between the analysis mean monthly values  $mT_{fcst,anls,j}$  and control mean monthly values  $mT_{fcst,ctrl,j}$  (Eq.4).

$$\beta P_j = mT_{fcst,anls,j} - mT_{fcst,ctrl,j} \quad (4)$$

Adjusted daily temperatures are obtained by multiplying daily residuals (Eq. 2) with adjusted standard deviation for the scenario period (Eq. 3b) and add the observed mean value and  $\beta P_j$  (Eq.5).

$$T'_{fcst,anls,ijk} = \varepsilon T_{anls,ijk} \times \sigma T'_{anls,j} + mT_{obs,ctrl,j} + \beta T_j \quad (4a)$$

$$T'_{fcst,anls,ijk} = (T_{fcst,anls,ijk} - mT_{fcst,anls,j}) \times \gamma T_j + mT_{obs,ctrl,j} + \beta T_j \quad (4b)$$

Mean value and variability for the control period is then reliably estimated and the mean differences in mean value and standard deviation as obtained by GFS model output is maintained.

### 5.2.1.3 Results and discussion

There is a marked disagreement between observed mean monthly values and standard deviation in observed and simulated precipitation even after correction with empirical adjustment method. The trend of the temporal variability of precipitation is also destroyed.

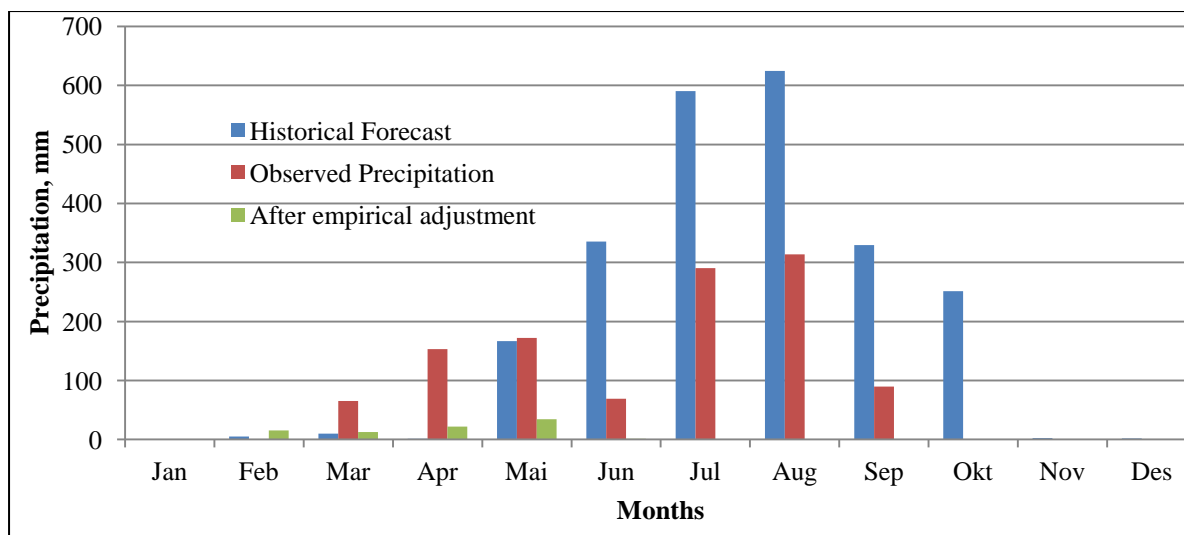


Figure 5-1: Comparison of mean monthly precipitation forecast before and after correction for the year 2009

The Figure 5-1 clearly shows that there is a big reduction in precipitation amount for monsoon season. The reason why empirical adjustment method has given poor result is that this method requires long timeseries of historical observed and forecasted data to work in satisfactory level. Therefore the bias correction for precipitation forecast is further carried out with statistical method.

But, the empirical adjustment method has given unexpectedly good result when applied to temperature forecast. The average monthly temperature forecast is well reproduced to be comparable with observed temperature as shown in Figure 5-2.

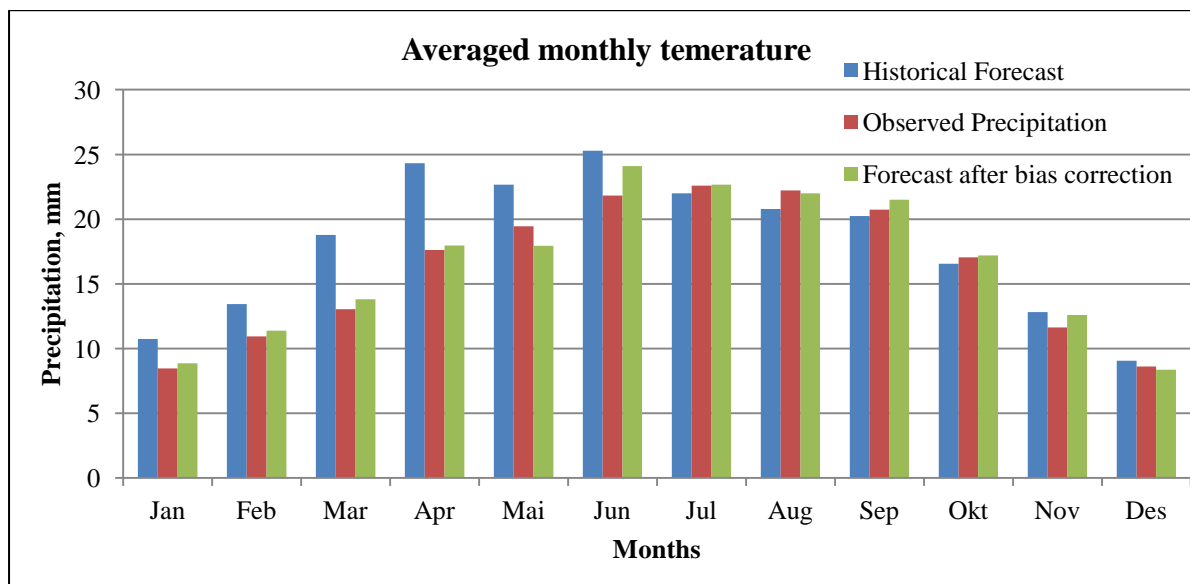


Figure 5-2: Comparison of averaged monthly temperature before and after correction (Year 2009)

A good correspondence between observed and forecasted temperature is also maintained in day to day level as well which is shown in Figure 5-3.

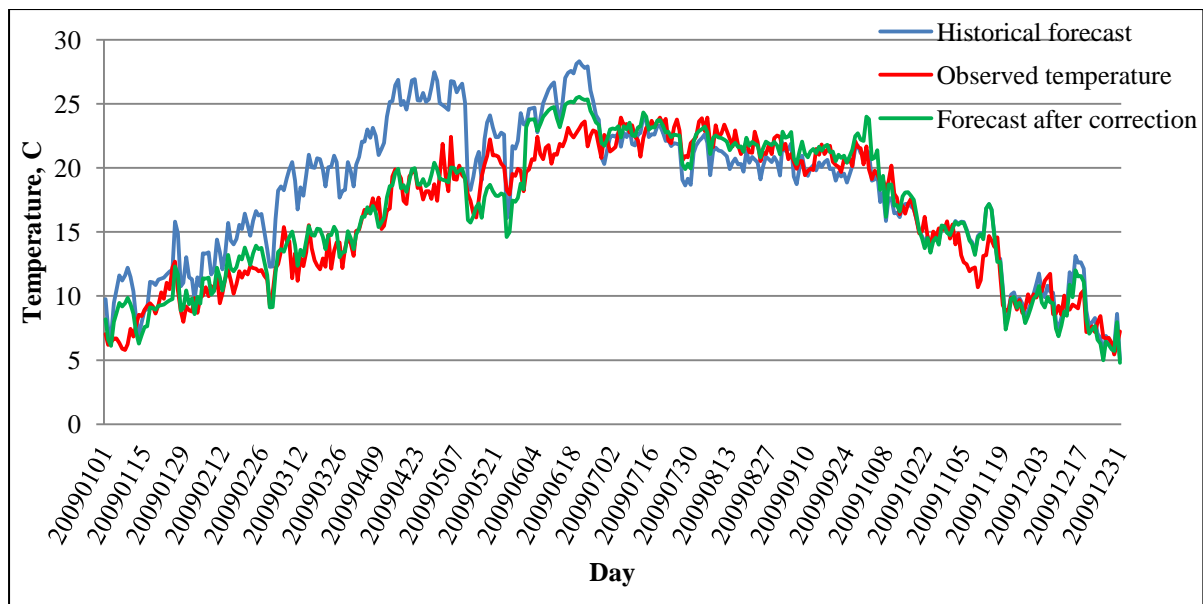


Figure 5-3: Day to day comparison of temperature forecast before and after correction (Year 2009)

The empirical adjustment method has performed very well when applied for bias correction of temperature forecast so other method of bias correction for temperature is not applied further.

## 5.2.2 Statistical Bias Correction Method

### 5.2.2.1 Introduction

Unlike empirical adjustment method which requires long observational data, statistical method can be applied when limited observational data are available. The statistical bias correction method is used for correcting climate model output to produce internally consistent fields that have the same statistical intensity distribution as the observations. This method is considered to be robust and practical statistical bias correction method, which was applied and validated by Piani et al. (2010) using regional model output over Europe from the ENSEMBLES project. It derives some form of transfer function using daily observed and simulated data from the control period and maintains the statistical distribution of the daily precipitation in analysis period.

### 5.2.2.2 Methodology

It is based on the initial assumption that both observed and simulated probability distribution can be well approximated by gamma distribution (Eq.1).

$$\text{Pdf}(x) = \frac{e^{(-\frac{x}{\theta})} \cdot x^{(k-1)}}{\tau(k) \cdot \theta^k} \quad (1)$$

Where,  $x$  is daily precipitation.  $k$  and  $\theta$  are the shape and scaling parameter, respectively.  $\tau(k)$  is gamma function evaluated at  $k$ .

Like as in previously discussed empirical adjustment method, the years 2007 and 2008 are considered as control period and the year 2009 is used as analysis period. The transfer

function derived using daily precipitation data from control period is applied to the daily precipitation forecast in analysis period to correct biases.

Two histograms are plotted using GFS model data and the observed daily precipitation within control period. No subdivision in seasons is done at this point. The bin size is set to be 2mm/day, while the lower limit of the lowest bin was set at 0.01 mm/day. This is done to remove dry days from the statistics. The histograms of both observed and simulated daily precipitation are fitted with the two-parameter ( $k$ ,  $\theta$ ) gamma distribution defined in Eq. 1. The fitting is done by plotting the histograms in excel with different set of  $k$  and  $\theta$  values and best value of  $k$  and  $\theta$  are selected by looking at graph which shows better fit. The model output is well fitted in to the gamma distribution with  $k = 0.71$  and  $\theta = 17.5$ , while as observed precipitation received  $k = 0.48$  and  $\theta = 23.0$  to be fitted in to the gamma distribution.

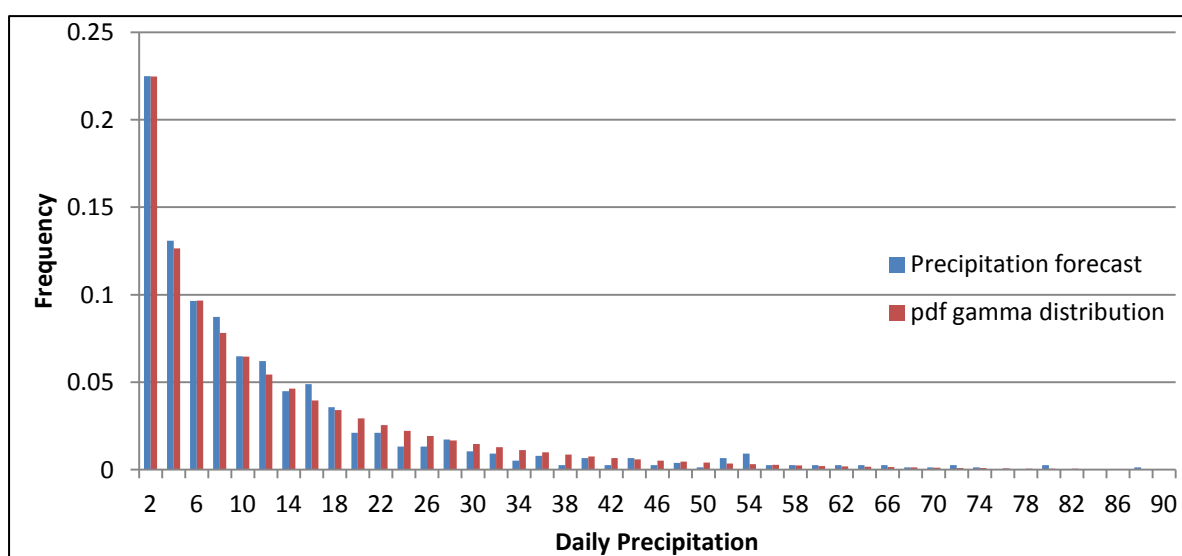


Figure 5-4: Fitted gamma distribution for precipitation forecast in control period

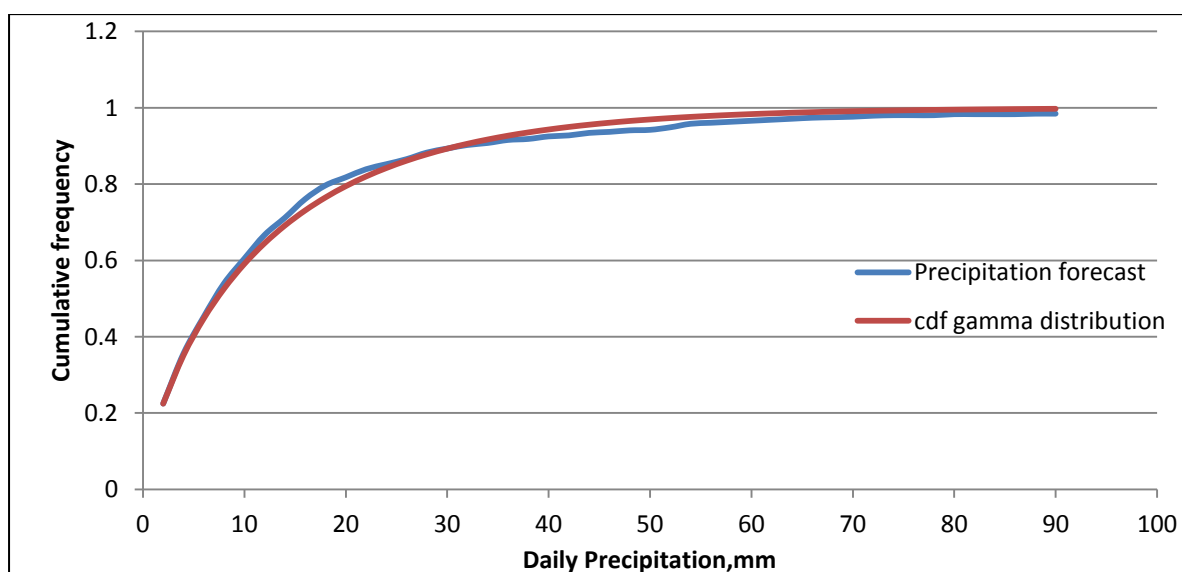


Figure 5-5: Fitted cumulative distribution for precipitation forecast in control period

Figures show that the daily precipitation forecast for the control period (2007 and 2008) is well fitted into gamma distribution and so is daily observed precipitation.

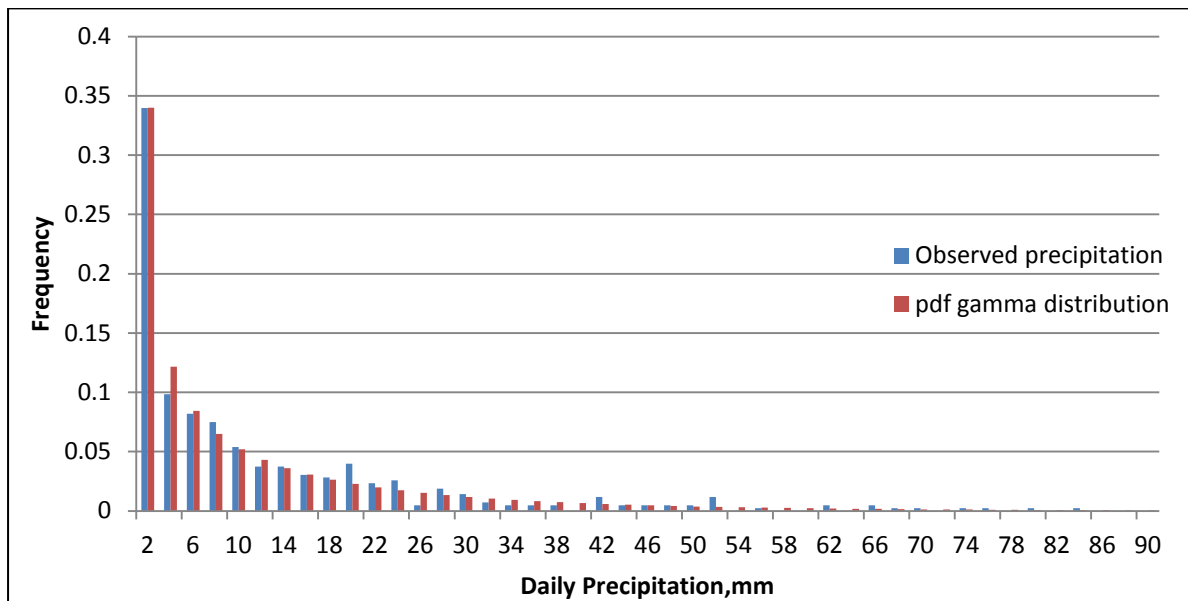


Figure 5-6: Fitted gamma distribution for observed precipitation in control period

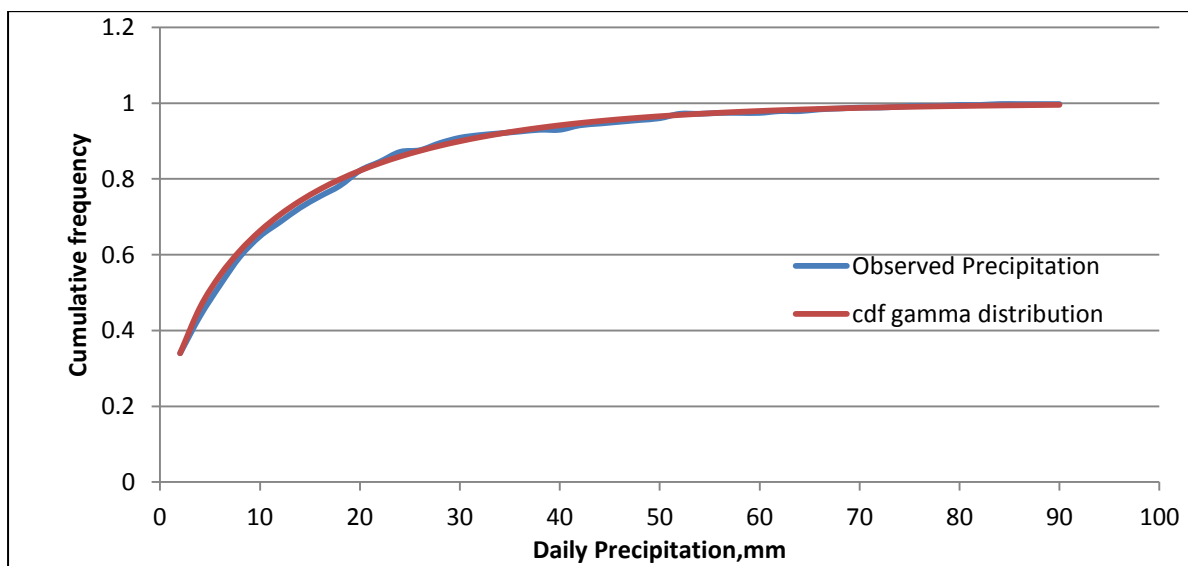


Figure 5-7: Fitted cumulative gamma distribution for observed precipitation in control period

To derive the transfer function the cumulative distribution (cdf) is plotted with the simulated and observed daily precipitation value. The cdf is calculated as (Eq.2).

$$cdf(x) = \int_0^x \frac{e^{(-\frac{x}{\theta})}.x^{(k-1)}}{\tau(k).\theta^k} dx + cdf(0) \tag{2}$$

Where, x, k, θ and τ(k) hold the same meaning as in Eq.1 and cdf(0) is the fraction of the days with no precipitation.

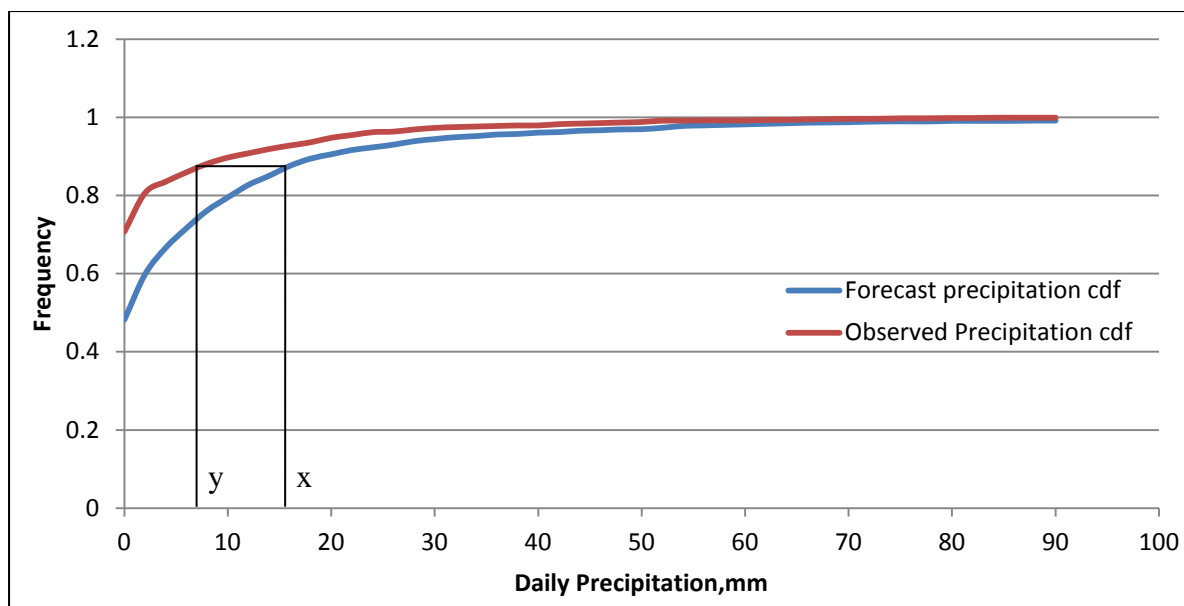


Figure 5-8: Cumulative gamma distribution including no precipitation days in control period

The desired transfer function  $y=f(x)$  obeys the relationship:  $cdf_{obs}(f(x))=cdf_{sim}(x)$  , where  $x$  and  $y$  are the simulated and corrected values of daily precipitation, respectively and can be derived graphically from Figure 5-8. The Autocad 2D is used to generate the transfer function. The transfer function  $y=f(x)$  thus derived from Autocad is shown in Figure 5-9.

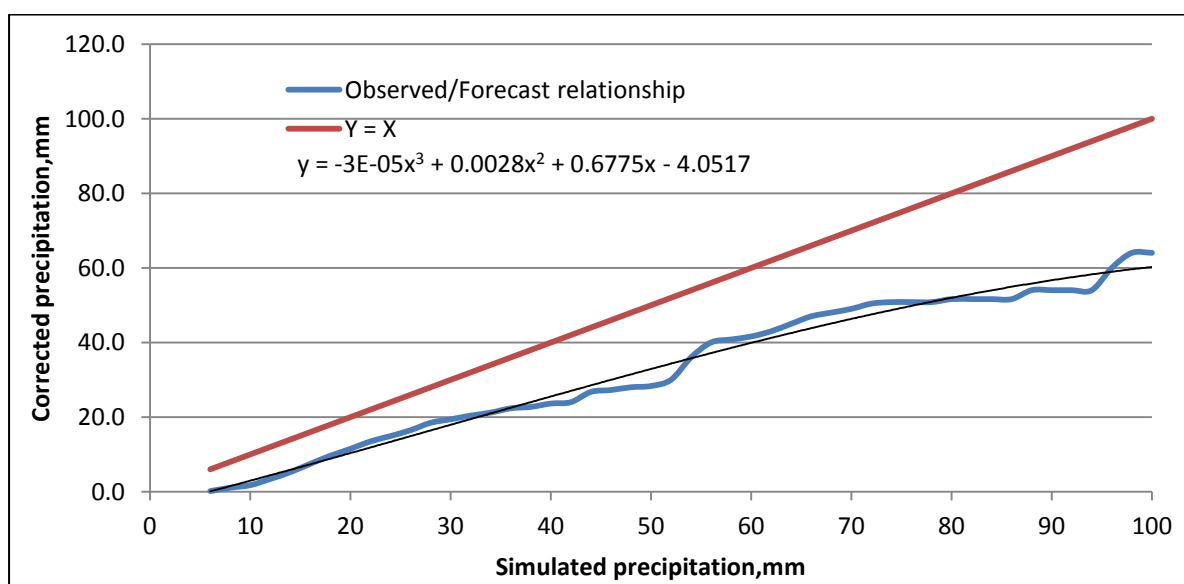


Figure 5-9: Transfer function which follows the equation  $cdf_{obs}(f(x))=cdf_{sim}(x)$

The degree to which  $f(x)$  deviates from the  $y=x$  line as shown in Figure 5-9 is a measure of the difference between the observed and simulated pdfs. Thus derived transfer function ( $y = -3E-05x^3 + 0.0028x^2 + 0.6775x - 4.0517$ ) is used to correct the simulated daily precipitation in analysis period.

### 5.2.2.3 Results and discussions

As expected statistical bias correction method has given better result than empirical adjustment method. Having worked with historical data, it has been possible to compare the precipitation forecast with the observed one even in analysis period otherwise it will not be the case if the analysis is done for future period. A graph is presented to show the mean monthly precipitation before and after statistical bias correction in comparison with observed precipitation for analysis period in Figure 5-10.

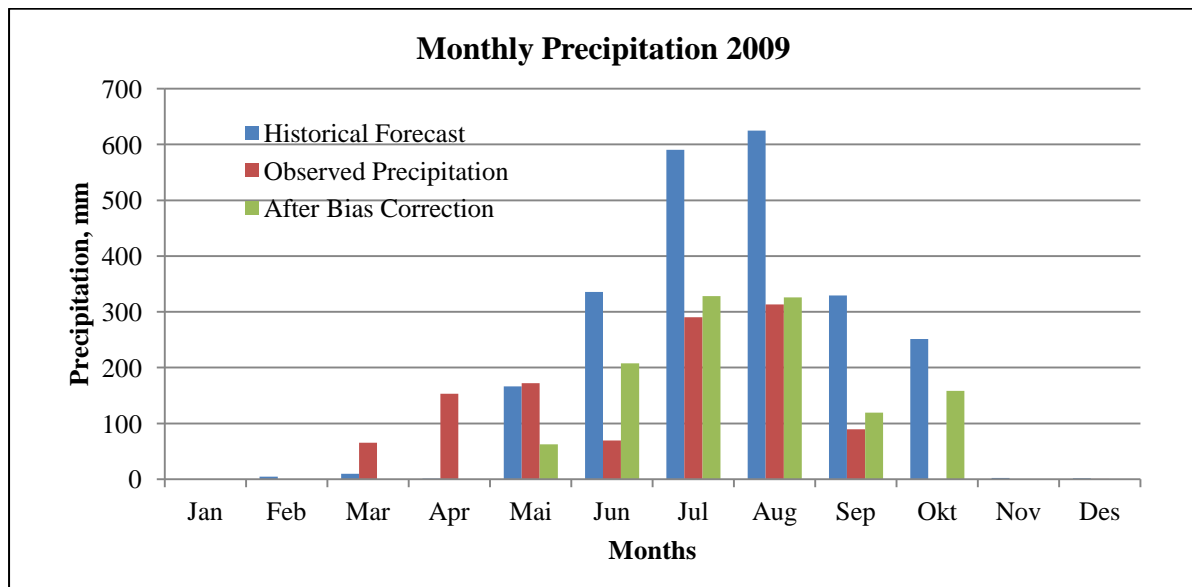


Figure 5-10: Comparison of mean monthly precipitation forecast before and after correction

A comparison of day to day precipitation is also made and result shows that statistical method has done moderate job in reproducing the daily precipitation as of observed precipitation. Nash-Sutcliffe efficiency ( $R^2$ ) is improved to  $R^2 = -0.28$  after bias correction from  $R^2 = -2.55$  when it is not corrected.

## 5.3 CONCLUSION AND RECOMMENDATION

Two advanced methods of bias correction i.e. empirical adjustment method and Statistical bias correction method, have been applied for bias correction of GFS model output. The empirical adjustment method has given unexpectedly good result for temperature forecast but not given satisfactory result when applied to precipitation forecast. Thus the bias correction for precipitation is further carried out with statistical method which expectedly has given better result. The statistical method is moderate to reproduce the day to day precipitation as of observed one but their mean monthly values are reproduced in satisfactory level. The result can be improved by using finer histogram bin size and fitting algorithm but with expenses of time and effort applied in analysis.

The temperature forecast after correction with empirical adjustment method and precipitation forecast corrected with statistical method are carried to next steps i.e. to use as HBV model input, which will be discussed in following chapter.



## 6 CALIBRATION OF THE HBV MODEL

### 6.1 THE HBV MODEL-AN INTRODUCTION

The HBV or Hydrologiska Byråns Vattenbalansavdelning model is a conceptual rainfall-runoff model which is used for runoff simulation, inflow and flood forecasting. Inputs data are observations of precipitation, temperature and potential evapotranspiration. Based on these inputs, the model calculates snow accumulation, snow melt, actual evapotranspiration, storage in soil moisture and groundwater and runoff from the catchment (Killingtveit and Sælthun, 1995). The model is generally run with precipitation and temperature time series on daily time step, but it is possible to use shorter time step too.

The HBV model includes conceptual numerical descriptions of hydrological processes at the catchment scale. The general water balance (Bergstrom, 1976) can be described as:

$$P - E - Q = \frac{d}{dt} [SP + SM + UZ + LZ + lakes]$$

Where,

- P: precipitation
- E: evapotranspiration
- Q: runoff
- SP: snow pack
- SM: soil moisture
- UZ: upper groundwater zone
- LZ: lower groundwater zone
- lakes: lake volume

As the HBV model considers the catchment as a single unit without any considerations of the spatial distribution within the catchment, it can be considered as lumped model. However, the snow routine is distributed. The model is extensively used in runoff forecasting, flood simulation in spillway design, water resources evaluation, and evaluation of climate change effects.

### 6.2 STRUCTURE OF THE HBV MODEL

The main structure of the HBV model includes the four main storage components: snow, soil moisture, upper zone and lower zone as shown in Figure 6-1. These all four components together represent the main components in the land phase of the hydrological cycle. The model calculates storage in each component based on hydro-meteorological inputs such as precipitation, temperature and potential evapotranspiration in relation with catchment parameters assigned in calibration. The final output from the model is the runoff from the catchment.

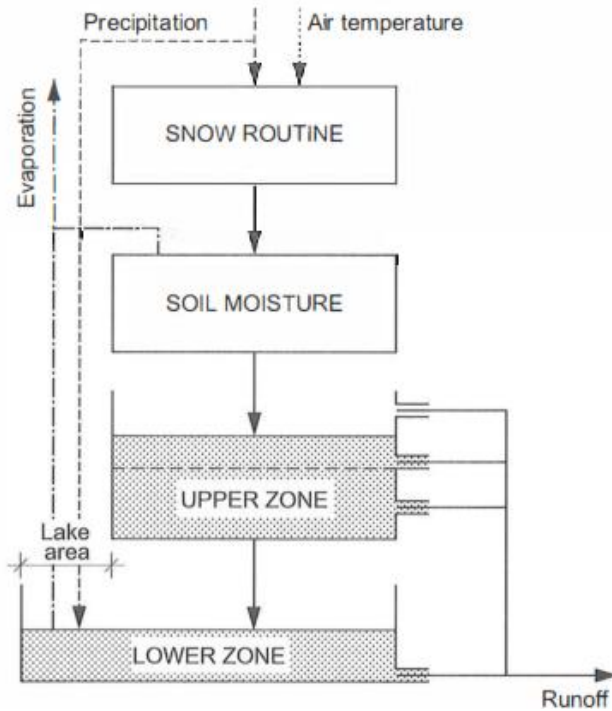


Figure 6-1: Main structure of the HBV model (Killingtveit and Sælthun, 1995)

### 6.2.1 The Snow Routine

The standard snowmelt routine of the HBV model is a degree-day approach, based on air temperature, with a water holding capacity of snow which delays runoff. The snowpack is assumed to retain melt water as long as the amount does not exceed a certain fraction of the snow. When temperature decreases below the threshold temperature, this water refreezes gradually. The structure for the snow routine is shown in Figure 6-2 as below:

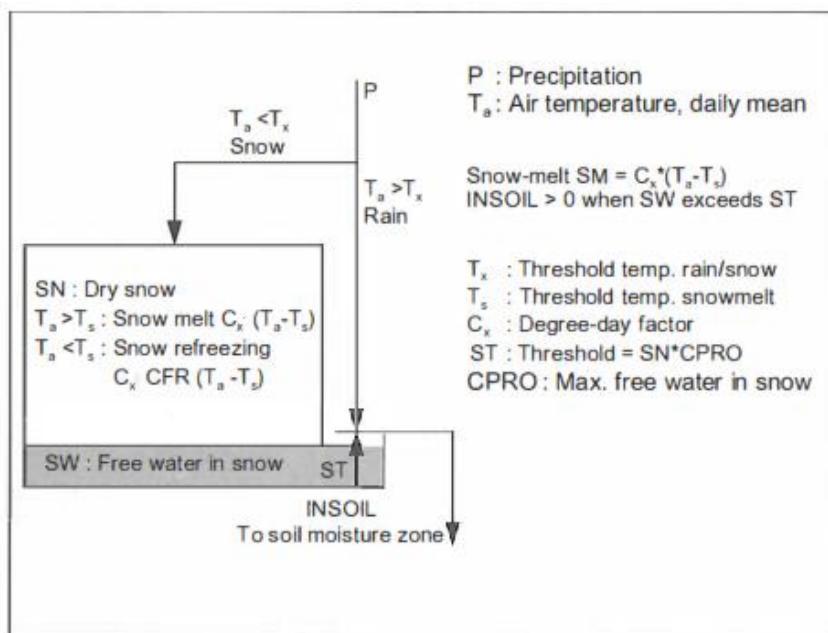


Figure 6-2: The snow routine in the HBV-model (Killingtveit and Sælthun, 1995)

The catchment is divided into 10 elevation levels (zones) according to the area elevation curve. At each zone the model computes air temperature, amount of precipitation, precipitation type, snow melt or refreezing based on air temperature and temperature lapse rate. So the structure for the snow routine in HBV model is distributed.

### 6.2.2 The Soil Moisture Routine

The rainfall or snowmelt from the snow routine (INSOIL) is the input for the soil moisture routine. It computes the storage of water in soil moisture, actual evapotranspiration and produces net runoff generating precipitation as output to the runoff response routine.

This part is the main part controlling runoff formation. This routine is based on the three parameters, BETA, LP and FC, as shown in the Figure 6-3:

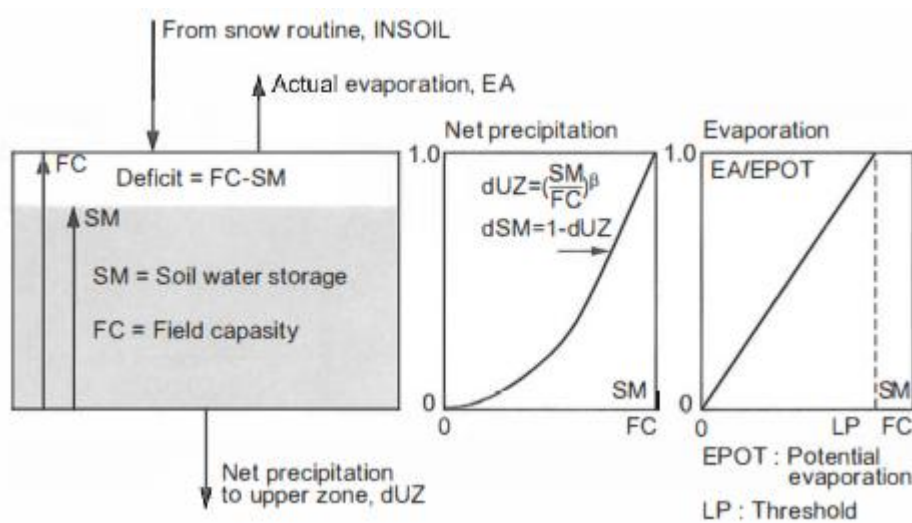
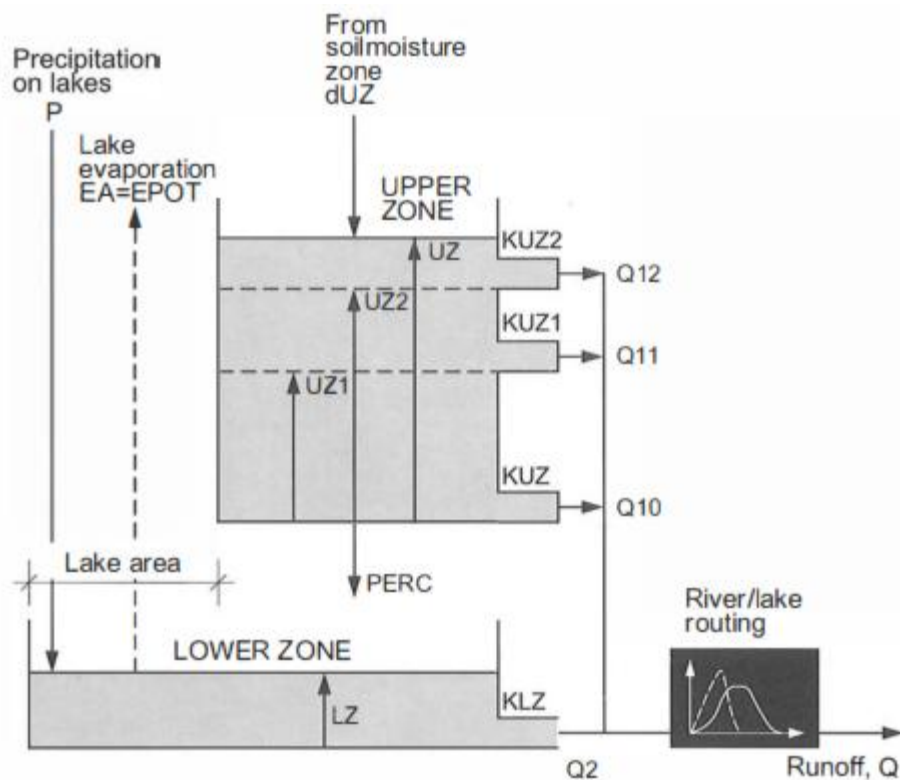


Figure 6-3: The soil moisture routine in HBV-model (Killingtveit and Sælthun, 1995)

The parameter  $\beta$  controls the contribution to the runoff response routine. LP is a soil moisture value above which evapotranspiration reaches its potential value, and FC is the maximum soil moisture storage in the model. The parameter LP is given as a fraction of FC. All these three parameters are free parameters and so must be determined by model calibration. If the intensity of rainfall or snow melt exceeds infiltration capacity the excess water is transferred directly to the run-off response function.

### 6.2.3 The Runoff Response Routine

The runoff response routine receives net precipitation produced from the soil moisture routine as input, computes the storage in upper zone and produces runoff. The runoff response is described by two linear reservoirs: upper zone and lower zone, arranged as shown in Figure 6-4. The effect of direct precipitation on and evaporation from rivers and lakes in the catchment are well incorporated in this routine.



PARAMETERS IN THE RESPONSE FUNCTION :

KLZ : Time constant, lower zone, 1/t  
 KUZ : Time constant, upper zone, 1/t  
 KUZ1 : Time constant, upper zone, 1/t  
 KUZ2 : Time constant, upper zone, 1/t  
 UZ1 : Threshold for quick flow, mm  
 UZ2 : Threshold for very quick flow, mm  
 PERC : Percolation to lower zone, mm/day

RUNOFF COMPONENTS :

$Q = Q10 + Q11 + Q12 + Q2$   
 $Q10 = \text{MIN}(UZ, UZ1) * KUZ$   
 $Q11 = \text{MAX}(0, ((\text{MIN}(UZ, UZ2) - UZ1) * KUZ1))$   
 $Q12 = \text{MAX}(0, (UZ - UZ2)) * KUZ2$   
 $Q2 = KLZ * LZ$

Figure 6-4: The runoff response routine in the HBV-model (Killingtveit and Sælthun, 1995)

The upper zone describes storage in active groundwater, and runoff delay and timing. Upper zone computes fast runoff (Storm runoff) while as lower zone describes storage in deep groundwater and lakes, and runoff delay and timing. Lower zone computes slow runoff (Base flow) from groundwater reservoir and lakes.

### 6.3 INPUT DATA PREPARATION

The HBV model computes the runoff from the catchment based on observed timeseries of climatic data as input. Usually, these data are observed at standard meteorological stations. The quality of these data must be checked and processed in various ways before they are used in HBV model.

#### 6.3.1 Air Temperature

The temperature timeseries prepared on section 2.2.2 is used as a temperature input in HBV model. This air temperature is used in the HBV model for computation of snow melt, type of precipitation (snow or rain).

### 6.3.2 Precipitation

As described in the section 2.2.1 the precipitation recorded in Markhu station is used in HBV model as a precipitation input. The quality of such data was already checked and gaps were filled if any. The precipitation and temperature inputs for HBV model are shown in Figure 6-5.

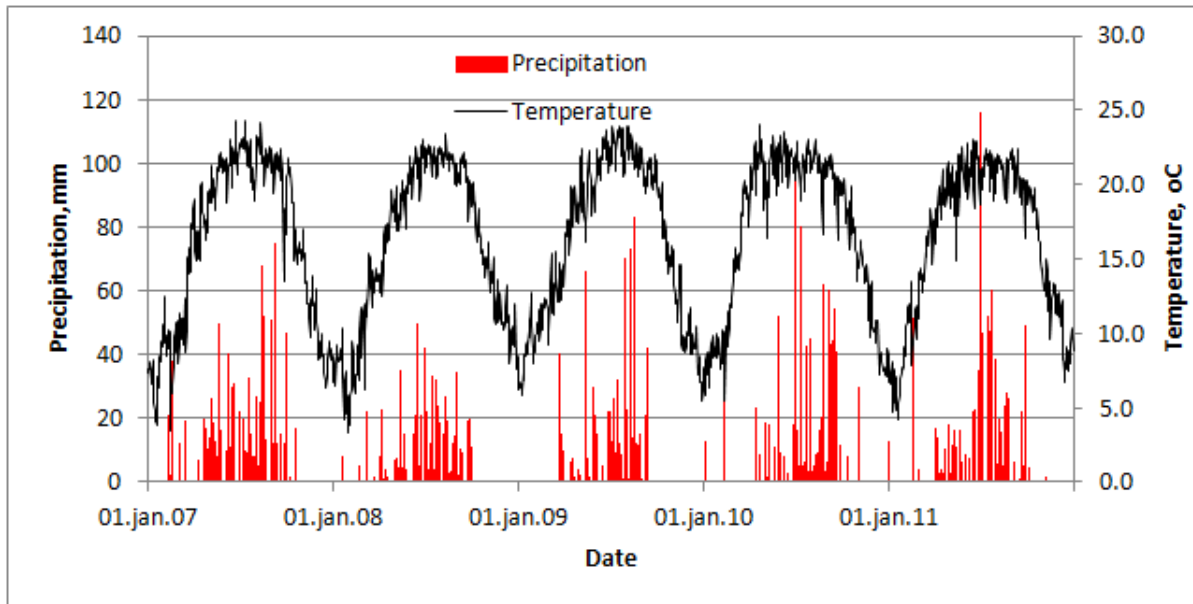


Figure 6-5: Precipitation and Temperature inputs in HBV model

### 6.3.3 Potential Evapotranspiration

The Thornthwaite method (temperature based model) is used to compute the average monthly values of potential evapotranspiration (Ponce, 1989). The method is based on an annual temperature efficiency index (J), defined as the sum of 12 monthly values of heat index (I) and average monthly values of daylight hours (d). I is the function of mean monthly temperature (T), in degrees Celsius as shown below:

$$I = \left(\frac{T}{5}\right)^{1.514}$$

Unadjusted evapotranspiration is calculated by

$$PET(0) = 1.6 \times \left(\frac{10T}{J}\right)^c$$

Where, PET(0) is potential evapotranspiration at 0° latitude in centimeters per month and c is an exponent evaluated as

$$c = 67.5 \times 10^{-8} J^3 - 77.1 \times 10^{-6} J^2 + 0.01792J + 0.49239$$

The unadjusted monthly evapotranspiration values PET(0) are adjusted depending on the number of days N in a month (1-31) and the duration of average monthly day light d (in hours), which is a function of season and latitude (Xu and Singh, 2001).

$$PET = PET(0) \times \left(\frac{d}{12} \left(\frac{N}{30}\right)\right)$$

in which PET is the adjusted monthly potential evapotranspiration (mm), d is the duration of average monthly daylight (hr); and N is the number of days in a given month, 1–31 (days).

The 'R'-programming language for statistical computing and graphics, is used to calculate the monthly value of potential evapotranspiration by Thornthwaite method by using contributed packages for example SPEI. 'R' calculates the monthly value of potential evapotranspiration based on mean monthly temperature and latitude of the catchment. The script for the 'R' program to calculate monthly potential evapotranspiration by Thornthwaite method is shown in Appendix B and the result is presented below.

Table 6-1: Computation of potential evapotranspiration by Thornthwaite method

Month	Monthly mean Temperature °C	Monthly PET_thorn mm/month	Monthly average daily PET mm/day
Jan	7.6	15.7	0.5
Feb	9.2	20.4	0.7
Mar	12.8	41.5	1.3
Apr	17.2	69.9	2.3
May	19.6	94.2	3.0
Jun	21.6	109.4	3.6
Jul	22.1	116.2	3.7
Aug	22.0	110.7	3.6
Sep	20.6	90.3	3.0
Oct	17.1	64.0	2.1
Nov	12.3	34.0	1.1
Dec	8.9	20.1	0.6

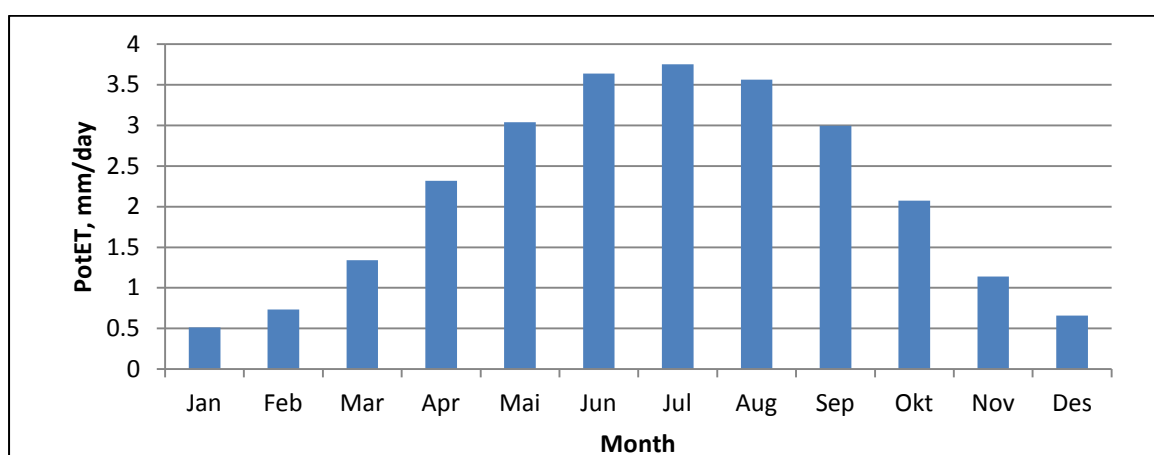


Figure 6-6: Monthly average value of potential evapotranspiration computed by Thornthwaite method

The monthly values are divided by number of days in corresponding month to get the monthly average daily values of potential evapotranspiration to use in HBV model.

### 6.3.4 Runoff

Since there exists no gauge station to record the runoff from the Kulekhani catchment for the study period of 2007-2009, the daily inflow to the Kulekhani reservoir is computed by indirect method based on the daily reservoir level and the energy generation from Kulekhani I project. The daily reservoir level and energy generation data as shown in Figure 6-7 are obtained from the Nepal Electricity Authority (NEA).

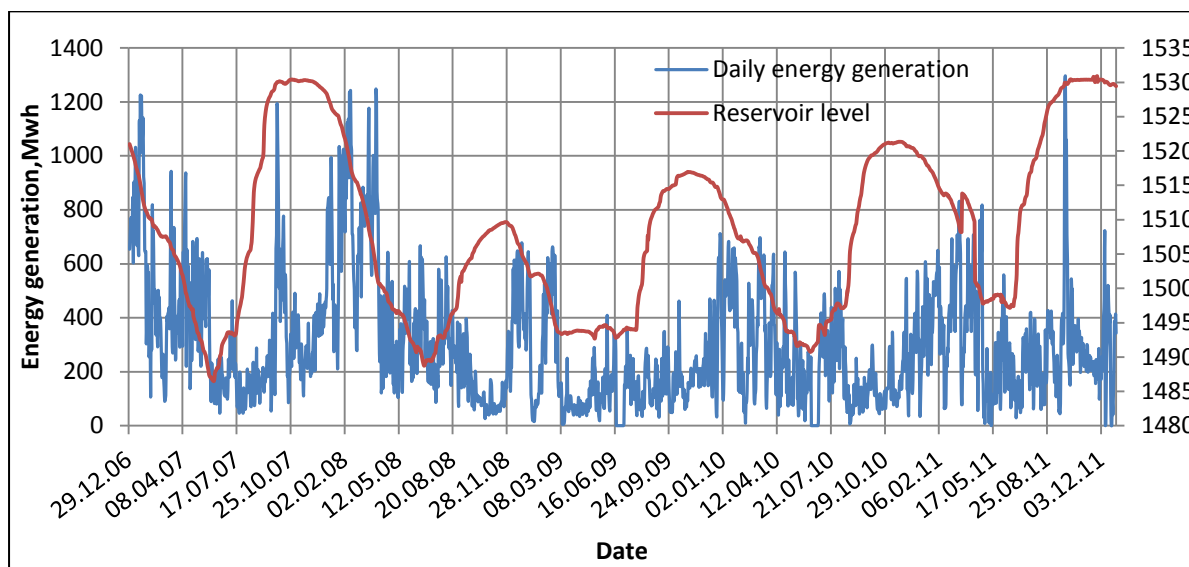


Figure 6-7: Daily reservoir level and energy generation from Kulekhani I project

The reservoir capacity curve for Kulekhani reservoir produced by Shrestha (2012) as shown in Figure 6-8 is used to determine the reservoir volume with respect to reservoir level.

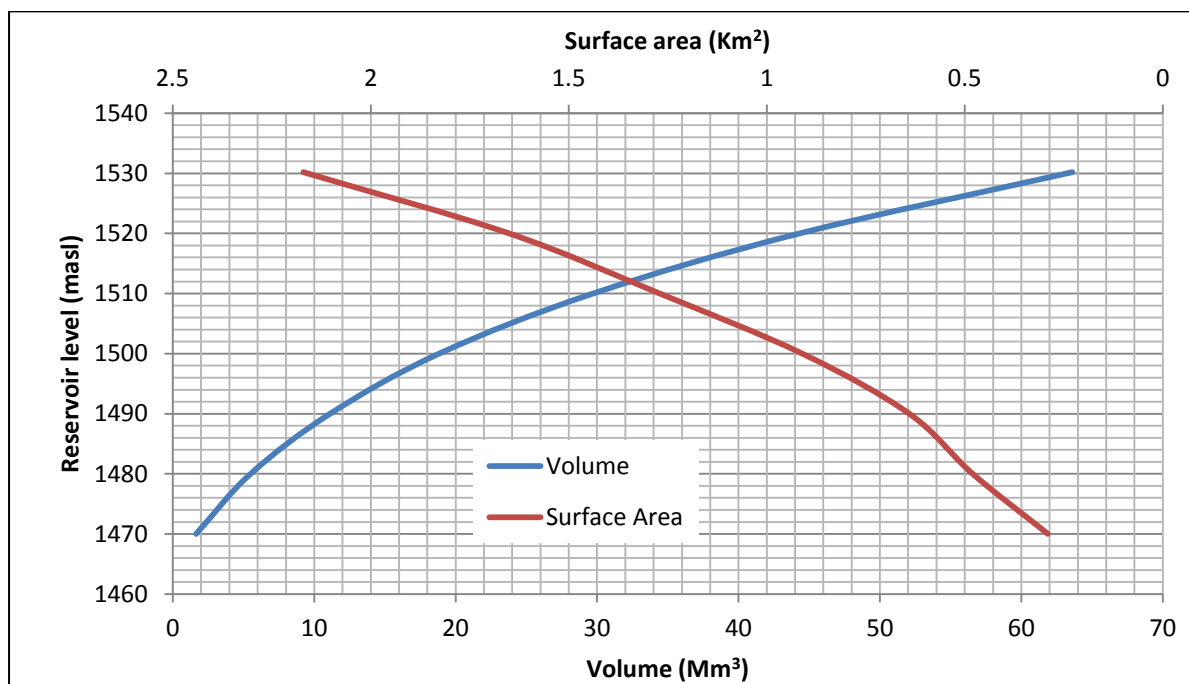


Figure 6-8: Reservoir capacity curve of Kulekhani reservoir (Shrestha, 2012)

Table 6-2: Surface area and reservoir volume (Shrestha, 2012)

Elevation (masl)	Area (km <sup>2</sup> )	Volume (Mm <sup>3</sup> )
1470	0.29	1.64
1480	0.48	5.49
1490	0.64	11.11
1500	0.91	18.82
1510	1.27	29.7
1520	1.65	44.3
1530.2	2.17	63.6

The calculation process described by Shrestha (2012) on his doctoral thesis is followed step by step as below:

1. Reservoir volumes are obtained from the reservoir capacity curve Figure 6-8 according to the reservoir level. Water volume to the reservoir at time t is calculated as :

$$\Delta V_{r(t)} = V_{rt} - V_{r(t-1)}$$

Where,

$\Delta V_{r(t)}$  : Change in volume at time t, m<sup>3</sup>

$V_{rt}$  : Volume of reservoir at time t, m<sup>3</sup>

$V_{r(t-1)}$  : Volume of reservoir at time t-1, m<sup>3</sup>

2. Water volume used for energy generation is calculated as :

$$V_{G(t)} = P_{G(t)} \times 1000 / \text{EEK}$$

Where,

$V_{G(t)}$  : Water volume used for generation, m<sup>3</sup>

$P_{G(t)}$  : Generation, MW

EEK: Energy equivalent, kWh/m<sup>3</sup>

3. Then total inflow to the reservoir is calculated as:

$$Q_{(t)} = \frac{V_{G(t)} + \Delta P_{r(t)}}{24 \times 60 \times 60}$$

The calculated inflow is presented in Figure 6-9.

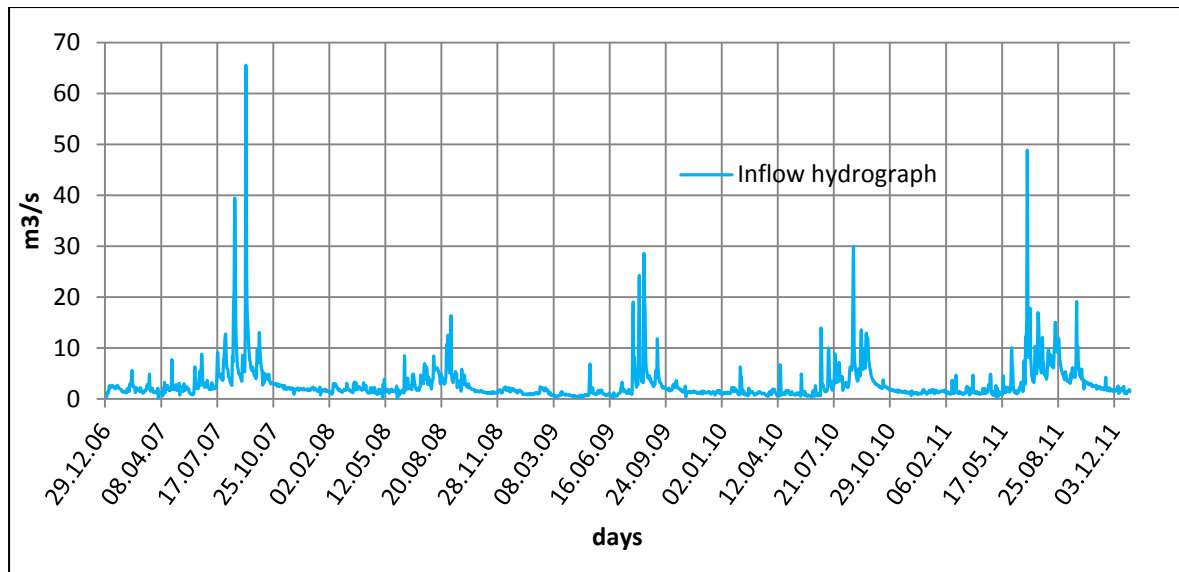


Figure 6-9: Daily inflow to Kulekhani reservoir

The evaporation from reservoir is also considered in inflow calculation. The potential evapotranspiration computed in section 6.3.3 by Thornthwaite method is used to calculate the inflow to the reservoir. The inflow calculation process takes the following principle.

$$I_{(t)} = O_{(t)} + \frac{\Delta s}{t} + ET_{(t)}$$

Where,

$I_{(t)}$ : Inflow to the reservoir,  $m^3/s$

$O_{(t)}$ : Outflow from the reservoir,  $m^3/s$

$\Delta s$ : Change in storage,  $m^3$  at time  $t$

$ET_{(t)}$ : Evaporation from the reservoir

### 6.3.5 Area –Elevation Curve

The Area-Elevation curve often called as hypsometric curve, for Kulekhani catchment is computed with the SRTM 90m DEM data downloaded from the Consortium for Spatial Information (CGIAR-CSI). The ‘R’ program is used to calculate the hypsometric curve for Kulekhani reservoir. The R-script is shown in Appendix C and result from the R is presented below in Table 6-3.

Table 6-3: Area-Elevation curve for Kulekhani catchment

% Area greater than	0	10	20	30	40	50	60	70	80	90	100
Elevation,masl	2579	2265	2150	2066	1983	1910	1857	1795	1742	1690	1533

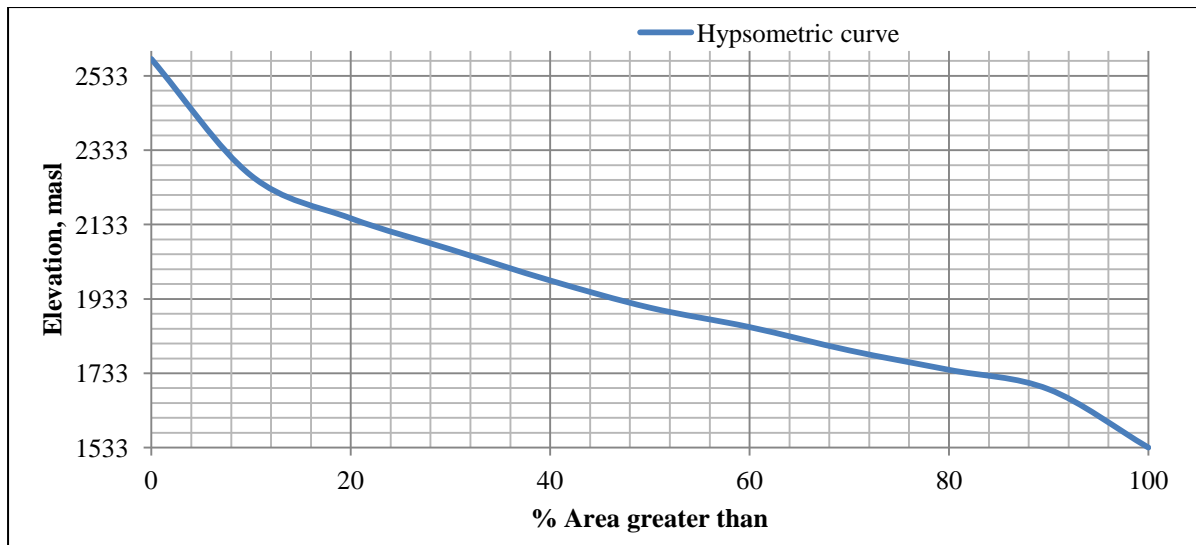


Figure 6-10: Hypsometric curve for Kulekhani catchment

### 6.4 MODEL CALIBRATION

Model calibration refers to the process of determining the set of free parameters in the model that gives the best possible correspondence between observed and simulated runoff for a catchment. A general method for model calibration process is shown in Figure 6-11.

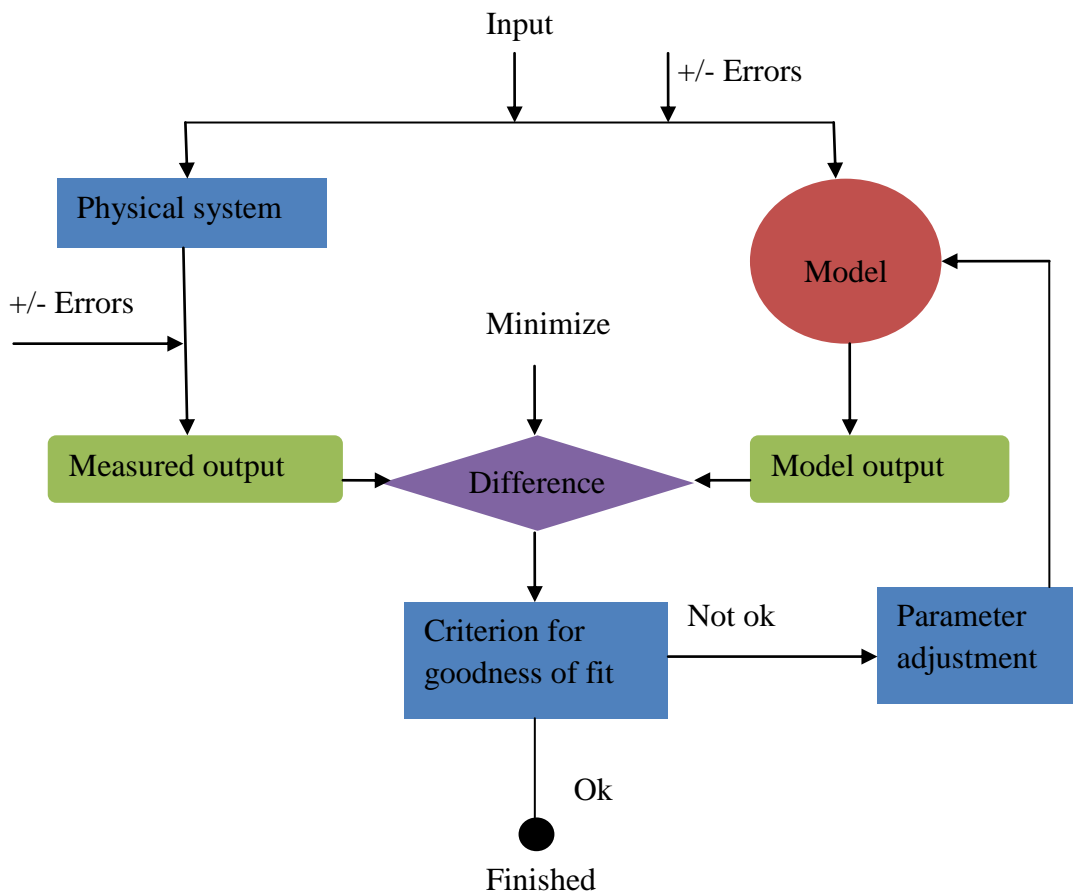


Figure 6-11: Model calibration process (Killingtveit and Sælthun, 1995)

The goodness of fit is evaluated by a function built using the Nash-Sutcliffe efficiency ( $R^2$ ).

$$R^2 = \frac{\sum(Q_o - \bar{Q}_o)^2 - \sum(Q_s - \bar{Q}_o)^2}{(Q_o - \bar{Q}_o)^2}$$

Where,  $Q_o$  = Observed runoff,  $\bar{Q}_o$  = Average runoff,  $Q_s$  = Simulated runoff

The observed runoff timeseries computed by indirect method as described in section 6.3.4 is only available for the period 2007-2011 due to unavailability of daily energy generation and reservoir level data for other years. Thus the model calibration is carried out based on the data for the period of whole 5 years (2007-2011). Excel based HBV model is used to perform the model calibration, validation, update and forecast. The Model calibration is done with the parameters described as below:

### 6.4.1 Confined Parameters

The confined parameters used in the HBV model are shown in tabular form as in Table 6-4.

Table 6-4: Main parameters for the Kulekhani catchment

MAIN PARAMETERS FOR THE CATCHMENT:									
Area		126.00	km**2						
Lake precentage		0.00	%						
Catchment name:		Kulekhani							
Zone #	Area-elevation distribution:				Catchment type		Glacier model parameters		
	% of total area				Forest	Mountain	Zone	% Glaciers	
1	10%	<	1690	m.a.s.l	1	0	1690	m.a.s.l	0.00
2	20%	<	1742	m.a.s.l	1	0	1742	m.a.s.l	0.00
3	30%	<	1795	m.a.s.l	1	0	1795	m.a.s.l	0.00
4	40%	<	1857	m.a.s.l	1	0	1857	m.a.s.l	0.00
5	50%	<	1910	m.a.s.l	1	0	1910	m.a.s.l	0.00
6	60%	<	1983	m.a.s.l	1	0	1983	m.a.s.l	0.00
7	70%	<	2066	m.a.s.l	1	0	2066	m.a.s.l	0.00
8	80%	<	2150	m.a.s.l	1	0	2150	m.a.s.l	0.00
9	90%	<	2265	m.a.s.l	1	0	2265	m.a.s.l	0.00
10	100%	<	2579	m.a.s.l	1	0	2579	m.a.s.l	0.00
					Melt increase in		Glaciers		
					mountain	1.00	Meltincrease	1.00	
					CX-mount.	3.0	Snowdistribution	0.5	

Table 6-5: Elevation for Markhu station

ELEVATION FOR HYD-MET STATIONS:		
Temp. station 1:	1530	m.a.s.l
Precip. station 1:	1530	m.a.s.l

The elevation of the meteorological station (Markhu station) is 1530 masl. Since Markhu station does not record the temperature data, the temperature data recorded in another station was transformed to this station by using temperature lapse rate as described in section 2.2.2.

#### 6.4.2 Model Initial States

It is important that model calibration is performed with some model initial states value to reduce the discrepancy between observed and simulated runoff at the start period. The initial states of model which has given the best possible correspondence between observed and simulated runoff in the initial period are shown in Table 6-6.

Table 6-6: Model states at start

<b>MODEL STATES AT START:</b>					
Elevation-zone	Snow pack (mm)		Free water content		
			%	mm	
1690 m.a.s.l	0.00	mm	10.00	0.0	
1742 m.a.s.l	0.00	mm	10.00	0.0	
1795 m.a.s.l	0.00	mm	10.00	0.0	
1857 m.a.s.l	0.00	mm	10.00	0.0	
1910 m.a.s.l	0.00	mm	10.00	0.0	
1983 m.a.s.l	0.00	mm	10.00	0.0	
2066 m.a.s.l	0.00	mm	10.00	0.0	
2150 m.a.s.l	0.00	mm	10.00	0.0	
2265 m.a.s.l	0.00	mm	10.00	0.0	
2579 m.a.s.l	0.00	mm	10.00	0.0	
Mean values	0.0	mm	0.0	0.0	
Soil water storage	200.00	mm	Maximum:	300	
Upper zone storage	4.00	mm	Treshold:	40	
Lower zone storage	200.00	mm			
Runoff, computed:	1.85	m**3/sec (at start)			
Runoff, observed:	0.51	m**3/sec (at start)			

The values of initial storages are chosen in such a way that the computed runoff matches the observed runoff up to some period after the start point. So it is not attempted to match exactly the computed and observed runoff only at the start point. However, this attempt still could not maintain good correspondence between computed flow and observed flow at the start period, a warm up period of first 2 weeks is set and model performance is evaluated for the period other than first 2 weeks.

#### 6.4.3 Free Parameters

The model simulation for the Kulekhani catchment is carried out by trying large number of free parameter combinations to produce the good correspondence between observed and simulated runoff. The value of each parameter as suggested by Killingtveit and Sælthun (1995) as shown in Table 6-7 are tried in calibration process. The free parameters which have produced possible best result as  $R^2=0.76$  are also presented in the Table 6-7.

Table 6-7: Free parameters in the HBV model (Killingtveit and Sælthun, 1995) and calibrated value

Recommended value					Observed value	Observed value matches Recommended value?
Name	Meaning	Value range	Default value	Units		
Tx	Thresholt temperature Rain/Snow	-1.0-2.0	1.0	°C	-1.0	Yes
Ts	Thresholt temperature Snowmelts	-1.0-2.0	0.0	°C	-1.0	Yes
Cx	Degree-day-factor	3.0-2.0	4.0	mm/°C *Day	3.0	Yes
CFR	Re-freezing efficiency in snow	0.0-0.01	0.005			
PKORR	Precipitation correction - Rainfall	1.05-1.2	1.05		1.0	No
SKORR	Precipitation correction - snowfall	1.15-1.5	1.2		1.15	Yes
TTGRAD	Temperature lapse rate for clear days	-0.6--1.0	-1.0	°C/100 m	-1.0	Yes
TVGRAD	Temperature lapse rate during precipitation	-0.4--0.6	-0.4	°C/100 m	-0.5	Yes
PGRAD	Precipitatin lapse rate	1.0-1.10	1.05		1.0	Yes
FC	Field capacity in soil moisture zone	75-300	150	mm	300.0	Yes
LP	Thresholt value for potET in soil moisture	70%-100%	100	% of FC	250.0	Yes
$\beta$	Parameter in soil moisture routine	1.0-4.0	2.0		1.0	Yes
UZL	Threshold level for quick runoff in upper zone	10-40	20	mm	40.0	Yes
KUZ1	Recession constant in upper zone	0.1-0.5	0.3	1/day	0.34	Yes
KUZ	Recession constant in upper zone	0.05-0.15	0.1	1/day	0.12	Yes
PERC	Percolation from upper to lower zone	0.5-1.0	0.6	mm/day	3.62	No
KLZ	Recession constant in lower zone	0.005-0.002	0.001	1/day	0.006	Yes

In addition to the attempt to get highest  $R^2$  value, high attention is also given to reduce the error in water balance throughout the calibration period. It is also considered that the parameter logic ( $KLZ < KUZ1 < KUZ2$ ) is well maintained.

The snow parameters are insensitive since Kulekhani catchment does not have snow. The percolation from upper to lower zone (PERC) and precipitation correction –Rainfall (PKORR) for the Kulekhani catchment are found to be out of recommended range. The soil moisture storage obtained during model calibration is shown in Figure 6-12.

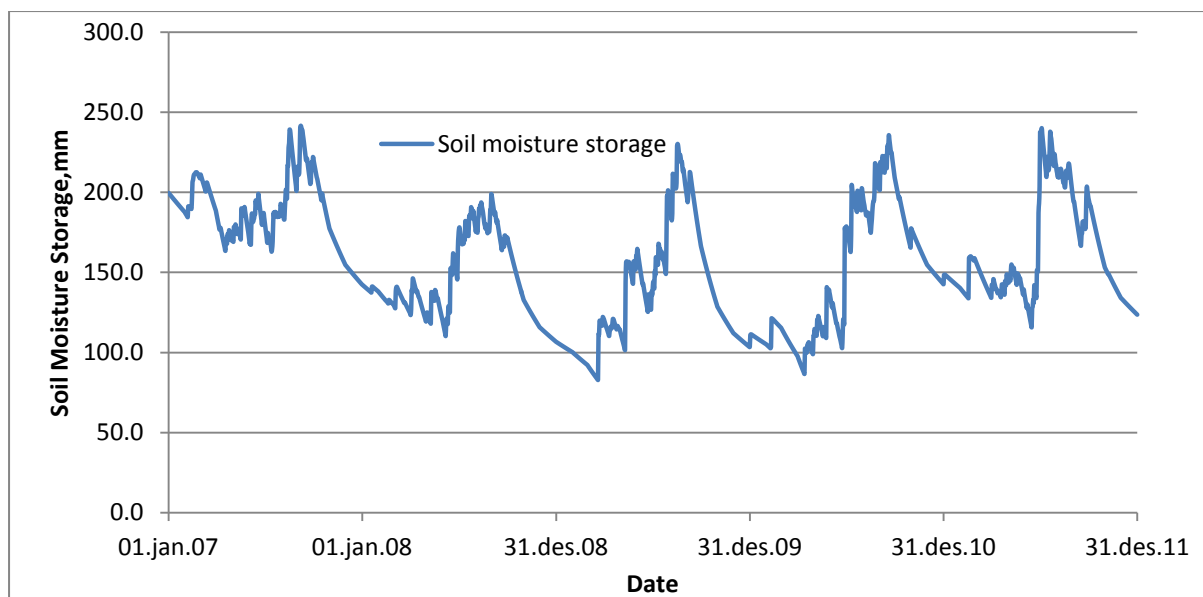


Figure 6-12: Soil moisture storage for Kulekhani catchment

The timeseries plot of observed and simulated runoff and water volume are shown in Figure 6-13.

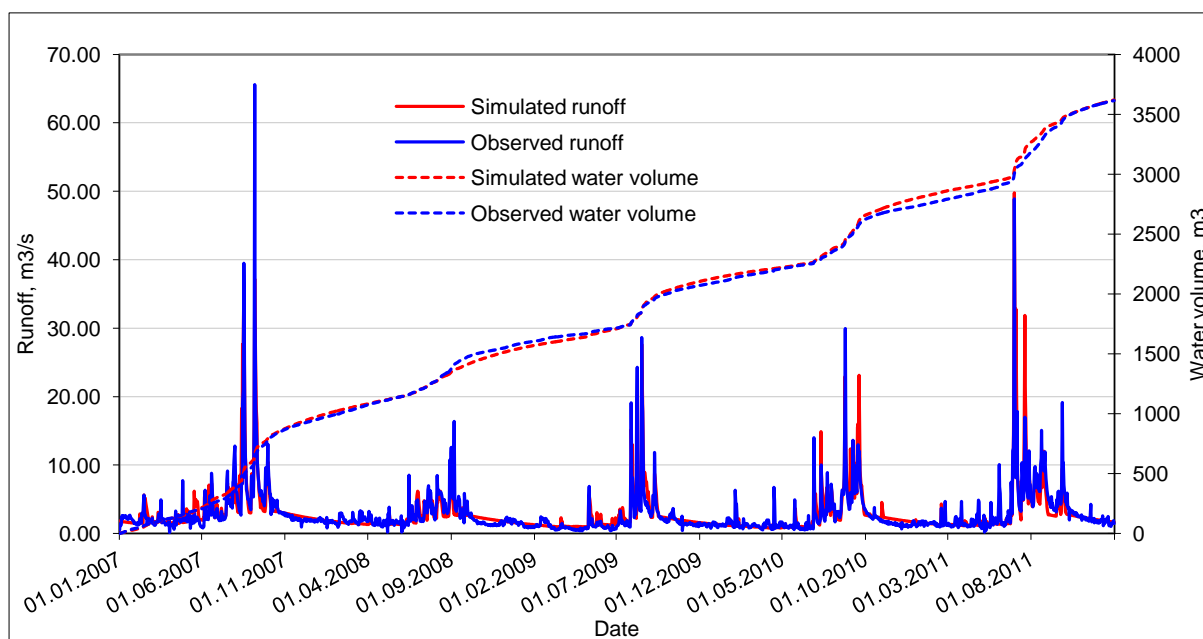


Figure 6-13: Observed and simulated runoff for Kulekhani catchment 2007-2011

It is seen that the variability of flow over time is well maintained and the simulated water volume follows the observed water volume quite closely.

### 6.5 MODEL VALIDATION

A calibration should normally be performed for at least five complete years of observations, and supplemented with additional five years for model validation. This ideal situation does not always exist (Killingtveit and Sælthun, 1995). This case is particularly true for the Kulekhani case. Only 5 years observed runoff timeseries is available due to limited records of

daily energy generation and daily reservoir level of reservoir. The whole period of 5 years is used for model calibration to achieve variability in simulated runoff over time as much as possible so model validation is not done due to lack of other remaining independent period.

## 6.6 DISCUSSION AND CONCLUSIONS

The low value of  $R^2 = 0.76$  is characterized by the uncertainty in computed runoff timeseries. Since there is no gauge station recording runoff from the Kulekhani catchment, the inflow to the reservoir was calculated as described in section 6.3.4 by indirect method. A closer look on the computed inflow e.g. for January month is made to examine the error associated with computed inflow.

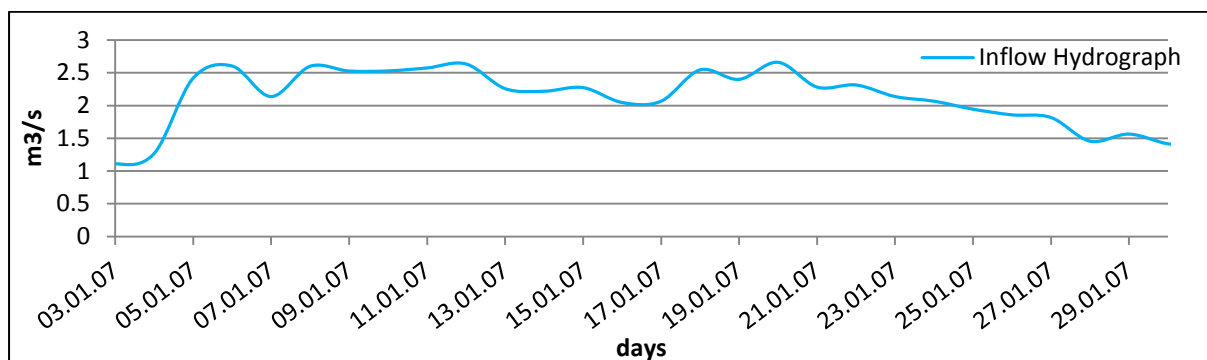


Figure 6-14: Inflow to the Kulekhani reservoir for January month

The precipitation gauge station records ‘no precipitation’ for the month of January but the computed inflow for the same month shows the variability in inflow within the month as shown in Figure 6-14. The ups and downs in inflow are not expected as there is no precipitation at all. Both recorded reservoir level and turbine efficiency could have error. Such type of error and uncertainty in computed inflow could have led to low  $R^2$  value. This example demonstrates the particular problem in working with ungauged catchment.

It also must be noted that the low value of  $R^2$  is also due to the unavailability of long observational timeseries. There are 18 parameters to be adjusted through calibration process that simply emphasizes the need of long data series to get the better result. It is also worthwhile mentioning the fact that the calibration of small catchment is really a challenging job as the catchment response to the rainfall is too fast so the inflow peak cannot be reproduced by the HBV model run with daily timestep which highlights the need of calibration of the model with finer timestep, for example, in hourly basis.

In this context, it is particularly noticed that there are good possibilities for improvements of HBV response for the Kulekhani catchment if the calibration is performed with direct measured inflow for sufficiently long period.



---

## 7 SHORT TERM INFLOW FORECASTING AND RESERVOIR OPERATION

### 7.1 INTRODUCTION

Runoff forecasting is a challenging job, since it requires true representation of physical processes which are very complex in nature thus are far from being considered as adequately described by a system of the corresponding equations (Pisarenko et al., 1993). Runoff forecasting is the process of computing runoff for the forecast period with the given input of precipitation and temperature forecasts. Short term runoff forecast includes the forecast for the time span of several hours to several days in advance. A reliable runoff forecast is necessary for the large number of hydrological applications, for example, reservoir operation, flood warnings, recreation and water quality, etc. Certainly, the reliability of operative runoff forecast depends on the quality of the existing meteorological forecasts, and on the memory of the system, i.e., how strongly the runoff in the forecast period depends on the initial states of the system (Killingtveit and Sælthun, 1995).

Short term inflow forecast can be performed only with some compulsory preparations beforehand. It requires a calibrated hydrological model (e.g. HBV in this context), meteorological data (precipitation, temperature) up till today, inflow data for model updating up till today, meteorological forecasts (precipitation, temperature) for coming days. Then model updating is carried out which is in turn followed by inflow forecast simulation (Rinde, 2012).

For the demonstration purpose it is planned to perform the inflow forecasting for the coming seven days as Global Forecast System (GFS) model outputs (precipitation, temperature) are available only for seven days with finer temporal resolution. Inflow forecasting is carried out on 8 successive days to illustrate the runoff forecast variability over time, with each day having capacity to forecast for coming seven days.

### 7.2 MODEL UPDATING

Model updating is the first crucial step in forecast simulation process. Before the forecast is run, it is very important that correct 'start' condition is established. Model updating is done with the model parameters which are determined through model calibration process as described in section 6.4.

Due to practical difficulties in acquiring real time hydro-meteorological data of Kulekhani catchment from Trondheim, a historical period is chosen to carry out the inflow forecast. It is assumed that we are in 31<sup>th</sup> July, 2009 and the seven days long forecast with daily timestep is run at each successive day from 01<sup>st</sup> – 08<sup>th</sup> August, 2009. To run the first model forecast at 01<sup>st</sup> August, 2009, model updating is done by adjusting model inputs (precipitation, temperature) and model state variables for the past 7 days till model output for that period matches the observed runoff. Model updating for other successive days is done in the same way with adjustment in past 7 days. As we move ahead, the output for the last day is only to be adjusted. The update for past 6 days remains same as it is already updated when the model is run on previous day. Table 7-1 clearly shows the model updating process for each

consecutive model run. The date with the yellow highlight is the model run and other dates are model update period for respective model run.

Table 7-1: Correction in model input and state variables for each consecutive model run

Day nr .	Update data for Input (Prec and Temp) or for States (Upper and Lower Zone)				Day nr .	Update data for Input (Prec and Temp) or for States (Upper and Lower Zone)			
	Precipitation mm	Air. Temp Deg. C	Upper zone mm	Lower zone mm		Precipitation mm	Air. Temp Deg. C	Upper zone mm	Lower zone mm
	Sum mm	Sum ( ° C)	Sum mm	Sum mm		Sum mm	Sum ( ° C)	Sum mm	Sum mm
	19	0	-16	-100		19	0	-18	-32
25. j ul				-75	26. j ul			12	
26. j ul			12		27. j ul	31		-13	-10
27. j ul	31		-13	-10	28. j ul	-5		-12	
28. j ul	-5		-12		29. j ul	-2			
29. j ul	-2				30. j ul	-5		-3	-15
30. j ul	-5		-3	-15	31. j ul			-2	-7
31. j ul					01. aug				
01. aug					02. aug				
	19	0	-30	-45		-12	0	-17	-45
27. j ul	31		-13	-10	28. j ul	-5		-12	
28. j ul	-5		-12		29. j ul	-2			
29. j ul	-2				30. j ul	-5		-3	-15
30. j ul	-5		-3	-15	31. j ul			-2	-7
31. j ul			-2	-7	01. aug				-13
01. aug				-13	02. aug				-10
02. aug					03. aug				
03. aug					04. aug				
	13	0	1	-45		15	0	-5	-39
29. j ul	-2				30. j ul	-5		-3	-15
30. j ul	-5		-3	-15	31. j ul			-2	-7
31. j ul			-2	-7	01. aug				-13
01. aug				-13	02. aug				-10
02. aug				-10	03. aug			6	
03. aug			6		04. aug	20		-6	6
04. aug	20				05. aug				
05. aug					06. aug				
	49	0	8	-24		78	0	10	-17
31. j ul			-2	-7	01. aug				-13
01. aug				-13	02. aug				-10
02. aug				-10	03. aug			6	
03. aug			6		04. aug	20		-6	6
04. aug	20		-6	6	05. aug			10	
05. aug			10		06. aug	29			
06. aug	29				07. aug	29			
07. aug					08. aug				

Excel based HBV model with updating and forecasting interface developed by prof. Ånund Killingtveit at NTNU is used for model updating process. The model is capable of doing model update up to 7 past days and forecast simulation for 8 coming days. Figure 7-1 shows the model updating results for the first two consecutive model run as an example.

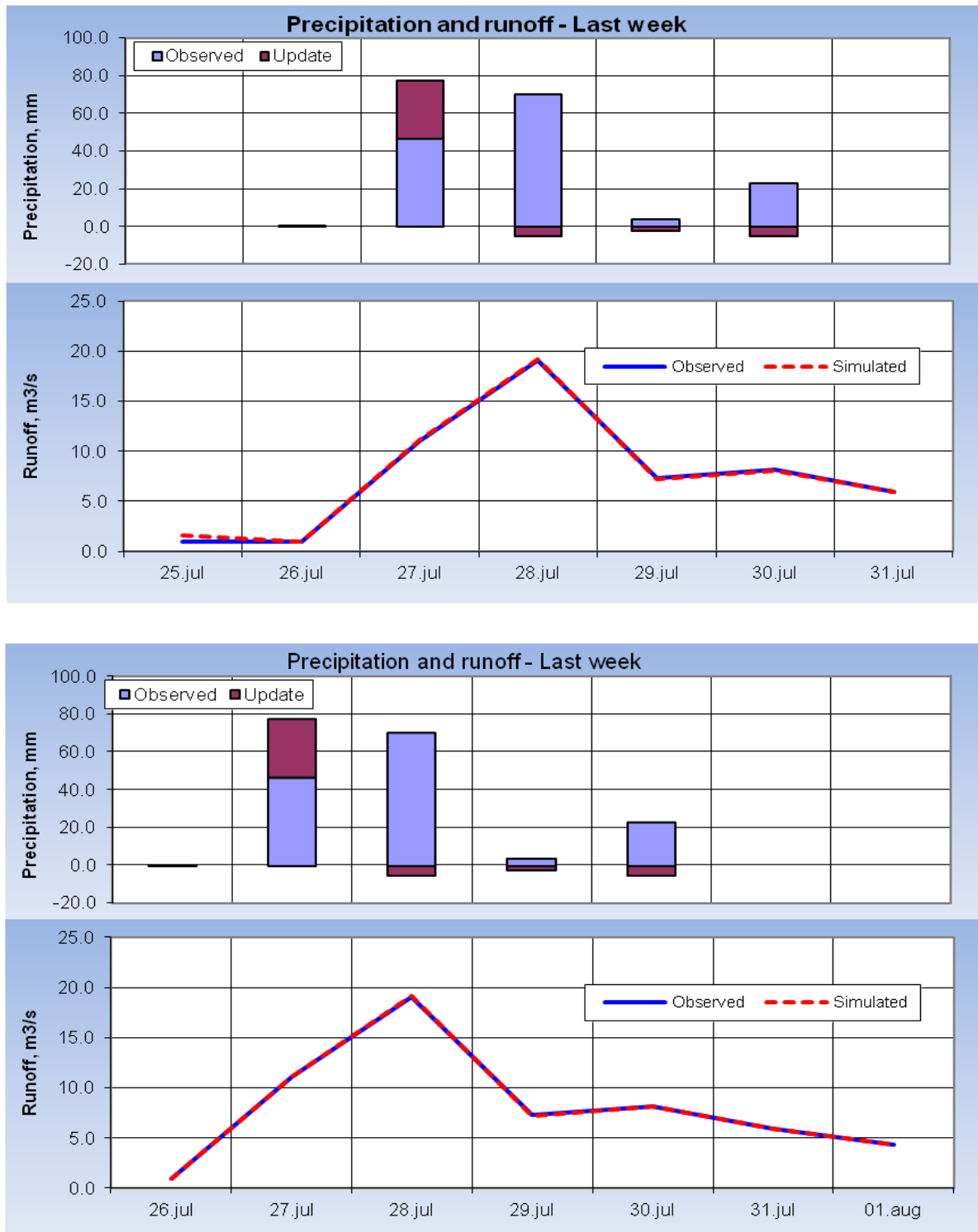


Figure 7-1: Model update results for first two consecutive model run

The above figure shows the model update for past seven days when model is ready to run at 01 August, 2009 and 02 August, 2009 respectively.

### 7.3 FORECAST SIMULATION

The updated HBV model is run at eight consecutive days on meteorological forecasts made on respective day. The meteorological forecasts (precipitation, temperature) are subjected to bias correction before they are used in forecast simulation. Statistical bias correction factor derived in section 5.2.2 is applied to the weather forecasts. The Table 7-2 shows the seven days precipitation forecasts made on each successive day from 01 August, 2009 to 08 August, 2009. These values are obtained after bias correction to the GFS model outputs.

Table 7-2: Precipitation forecasts made on different date

Forecast made on	Precipitation forecast in mm for the date													
	01.aug	02.aug	03.aug	04.aug	05.aug	06.aug	07.aug	08.aug	09.aug	10.aug	11.aug	12.aug	13.aug	14.aug
01.aug.09	9.8	8.0	11.6	8.6	21.3	46.8	34.8							
02.aug.09		14.4	2.5	15.5	0.0	18.7	40.3	28.5						
03.aug.09			7.5	19.9	3.4	3.2	3.6	2.2	1.6					
04.aug.09				15.6	17.5	14.0	50.8	12.8	2.8	1.3				
05.aug.09					23.6	23.7	39.8	0.8	0.5	0.0	0.0			
06.aug.09						59.8	1.9	3.4	0.0	0.0	0.0	3.6		
07.aug.09							6.9	11.4	0.0	0.0	0.0	0.0	0.0	
08.aug.09								1.4	5.4	0.0	0.2	9.9	0.6	11.0
Actual Precip	0	0	1.2	0.1	0.1	0.1	17.5	73	0.1	0.1	14	1.3	2.3	9

Table 7-3: Temperature forecasts made on different date

Forecast made on	Temperature forecast in °C for the date (after lapse rate correction)													
	01.aug	02.aug	03.aug	04.aug	05.aug	06.aug	07.aug	08.aug	09.aug	10.aug	11.aug	12.aug	13.aug	14.aug
01.aug.09	21.7	21.9	21.9	22.2	21.9	18.9	18.2							
02.aug.09		22.1	21.8	22.3	21.6	20.7	18.2	19.2						
03.aug.09			22.3	22.3	21.8	20.4	20.9	22.0	21.3					
04.aug.09				22.6	22.3	21.1	19.4	20.1	19.6	20.4				
05.aug.09					22.0	19.7	18.5	21.8	21.6	22.0	22.0			
06.aug.09						19.4	19.4	22.1	22.0	22.1	22.6	22.4		
07.aug.09							21.3	22.1	21.7	23.2	22.5	21.3	21.6	
08.aug.09								21.6	21.7	22.3	21.7	22.2	19.4	20.8
Actual Temp	22.4	23.6	23.9	22.9	23.9	21.8	21.6	23.3	22.4	22.7	23.4	22.9	22.3	21.7

The first forecast simulation is run at 01<sup>st</sup> Aug, 2009 on meteorological forecasts (first row data in Table 7-2 and Table 7-3) that is made from 01<sup>st</sup> Aug, 2009 for coming seven days. Similarly, the model is again run at second day but with the meteorological forecasts that are made from second day for coming seven days. Same process is repeated for eight successive

days with seven days forecasts that are made from each day. Table 7-4 shows the runoff forecasts made from eight successive days.

Table 7-4: Inflow forecasts made on different date

Forecast made on	Inflow forecast in m <sup>3</sup> /s for the date													
	01.aug	02.aug	03.aug	04.aug	05.aug	06.aug	07.aug	08.aug	09.aug	10.aug	11.aug	12.aug	13.aug	14.aug
01.aug.09	5.8	5.6	5.8	5.6	7.0	17.5	22.8							
02.aug.09		5.0	4.2	5.0	3.9	5.1	10.3	15.5						
03.aug.09			3.1	4.5	3.9	3.3	2.8	2.2	1.6					
04.aug.09				3.3	4.4	5.0	13.9	12.2	7.8	6.5				
05.aug.09					6.5	8.6	17.9	10.6	7.1	5.7	4.6			
06.aug.09						10.6	7.3	6.3	5.1	4.0	3.0	2.6		
07.aug.09							6.5	6.6	5.3	4.2	3.2	2.3	1.5	
08.aug.09								10.5	7.7	6.3	5.1	5.2	4.1	4.5
Actual flow (m <sup>3</sup> /s)	4.3	3.2	2.3	4.9	2.8	7.0	17.4	24.3	7.4	4.6	4.4	3.5	3.3	3.5

These forecasted inflows are used in existing reservoir model to estimate the capability of plant to meet the energy demand and reservoir level in relation to inflow forecast up to seven days in advance.

## 7.4 RESERVOIR OPERATION

### 7.4.1 Introduction

Reservoir operation is one of the important applications of inflow forecasting as it calculates optimal production profile based on the probable future inflow and price variations. Having known short term inflow and price level of energy, it is possible to decide whether reservoir water is to be stored for the future production or to be used by today to get the optimum benefit from the project. The strategy of the reservoir operation is to reduce the spill amount by saving some spaces in reservoir to capture the coming floods and to maintain the long term strategy of the reservoir within the short term operation, i.e. to reserve some water for the dry period.

### 7.4.2 Reservoir Operation In The Case of Kulekhani Reservoir

In contrast to the common reservoir operation strategies, Kulekhani reservoir offers only limited application of inflow forecast. The real fact of energy system in Nepal is that there are no energy price variations and long term reservoir operation strategy. It has been reported that spilling from the Kulekhani reservoir has not occurred for many years. Kulekhani project is put in to the operation when the energy demand is not covered from run-of- the river and daily peaking hydropower connected in INPS (Integrated Nepalese Hydropower System). When the energy demand is too high, Kulekhani project will be insufficient to meet the increased energy demand and in consequence, loadshedding occurs. It is the real fact that loadshedding in Nepal has occurred not only because of the limited water in the Kulekhani reservoir but also because of the limited capacity of the turbines of the Kulekhani project.

This situation is well understood when the evidence shows the loadshedding even in monsoon season.

### 7.4.3 Existing Reservoir Operation Model for Kulekhani Reservoir

Incorporating all the facts associated with energy planning in the Nepalese context Shrestha (2012) has developed a tailor-made model for Kulekhani reservoir operation. The working principle of the model is shown in Figure 7-3.

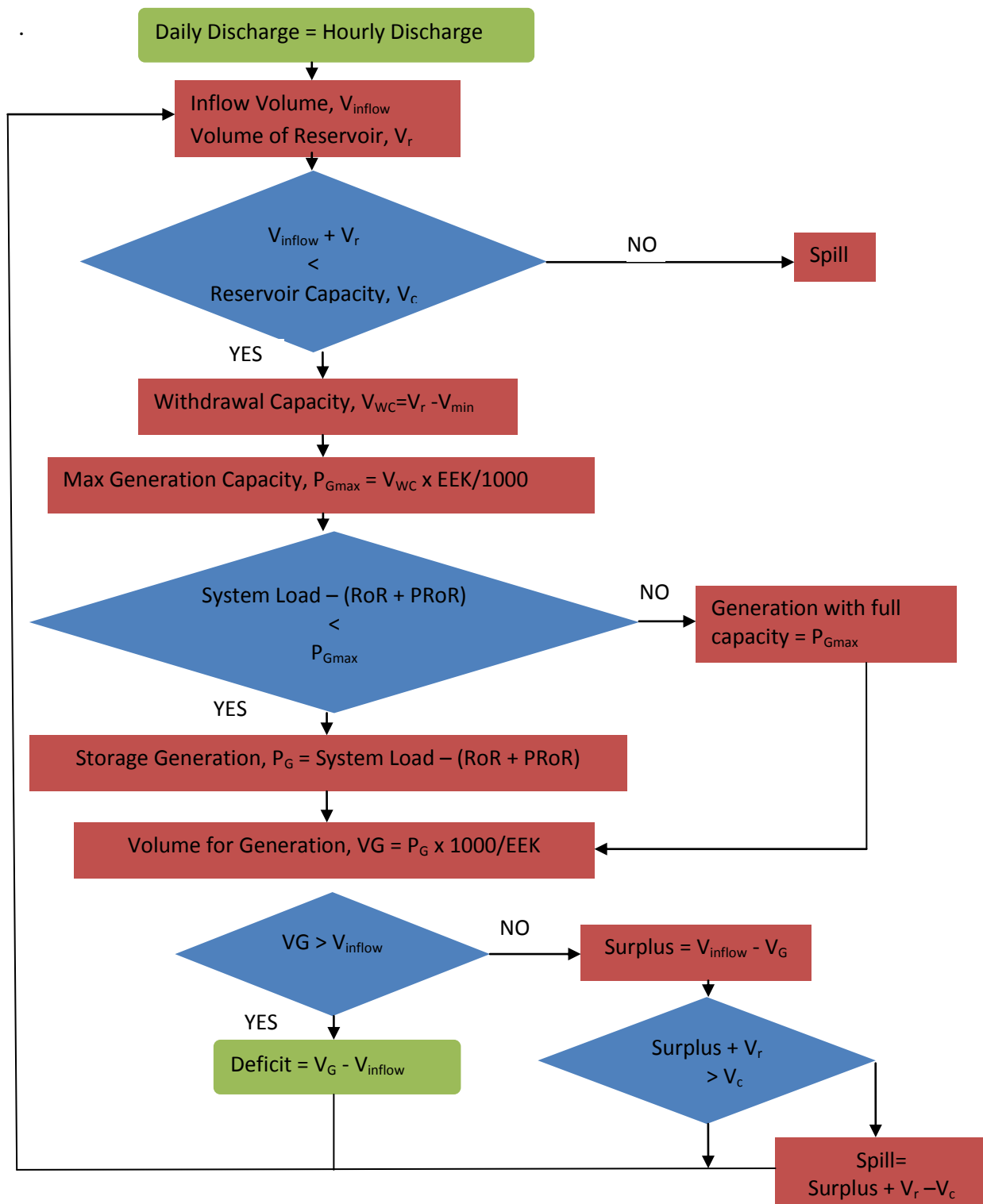


Figure 7-3: Working principle of Kulekhani reservoir operation model (Shrestha, 2012)

This model was used to estimate the reservoir levels, capacity to produce the energy to meet the energy demand that is not covered from other hydropower system and extent of loadshedding if any for historical period of July, 2006 - July, 2007 but it can also be used for future period with inflow and load forecasts.

The model calculates the reservoir volume at time step  $t$  according to the inflow and reservoir volume at time step  $t-1$ . Maximum withdrawal capacity will be checked with respect to minimum reservoir level. The corresponding maximum generation capacity is calculated with energy equivalent method. The calculated maximum capacity is compared with the demand to the Kulekhani project and the water volume required for generation from Kulekhani project is calculated. Finally net available water volume in the reservoir is calculated and reservoir level is computed as a function of reservoir volume. If the system demand load is beyond the capacity of turbines then the result will be the loadshedding.

The model incorporates the energy generated from the Kulekhani II project too as it is cascade with Kulekhani I. Both plants run simultaneously with the same volume of water so it is worthwhile to include energy generation from Kulekhani II project in to the calculation.

The load demand for the forecast period to the Kulekhani project is assumed to be as of historical demand for the same date in 2006 year which is shown in Figure 7-4.

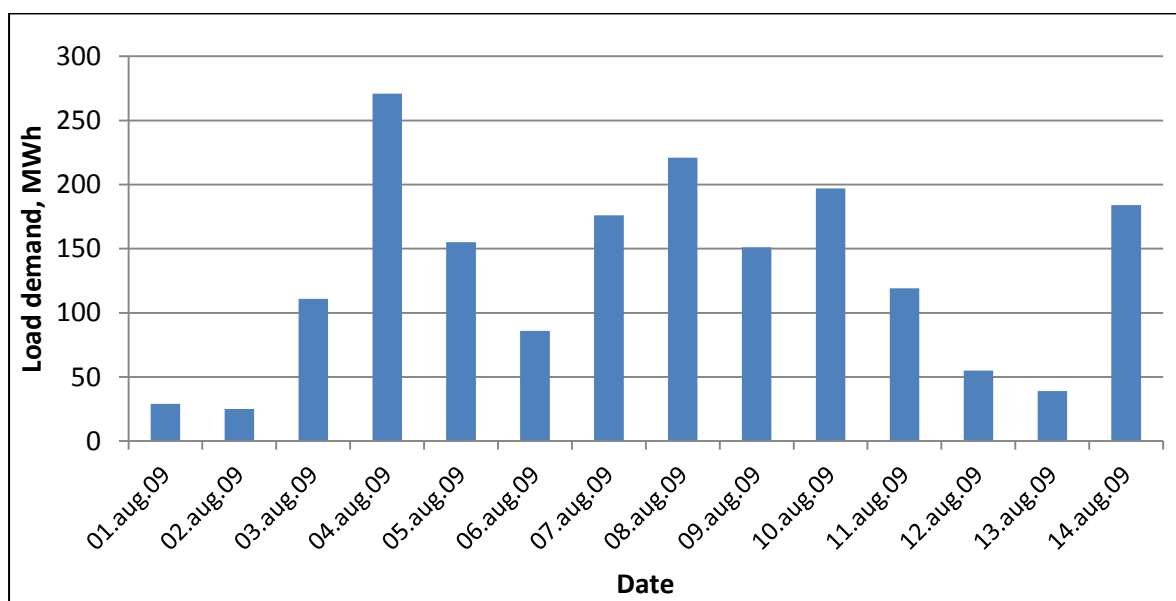


Figure 7-4: Daily load demand to Kulekhani plant

With the given energy demand to the Kulekhani plant, the model predicts in advance whether the plant can produce sufficient energy to meet the energy demand or creates loadshedding up to seven days in relation to inflow forecast. The reservoir level is also computed for each day within forecast period.

### 7.4.4 Results

For the demonstration purpose the model was run at each successive day from 01August, 2009 to 08 August, 2009 based on the inflow forecasts made on each day for 7 days in advance. Table 7-5 shows the probable extent of loadshedding during forecast period with respective model run.

Table 7-5: Loadshedding forecast made on different date

Forecast made on	Loadshedding (Mwh) forecast for the date													
	01.aug	02.aug	03.aug	04.aug	05.aug	06.aug	07.aug	08.aug	09.aug	10.aug	11.aug	12.aug	13.aug	14.aug
01.aug.09				23.9										
02.aug.09				23.9				8.8						
03.aug.09				23.9				8.8						
04.aug.09				23.9				8.8						
05.aug.09								8.8		6.5				
06.aug.09								8.8		6.5				
07.aug.09								8.8		6.5				
08.aug.09								8.8		6.5				0.8

The model also predicts reservoir level for the coming seven days with each model run from 01-08 August, 2009. The reservoir level in turn governs the reservoir operation strategy since it has to follow the predefined reservoir guide curve. But, in the case of Kulekhani reservoir, there is no predefined reservoir operation strategy as the plant is run when the national energy demand is not met by other projects.

Table 7-6: Reservoir level forecast made on different date

Forecast made on	Reservoir level (masl) forecast for the date													
	01.aug	02.aug	03.aug	04.aug	05.aug	06.aug	07.aug	08.aug	09.aug	10.aug	11.aug	12.aug	13.aug	14.aug
01.aug.09	1499.7	1500.2	1500.6	1501.0	1501.4	1502.8	1504.5							
02.aug.09		1500.0	1500.3	1500.6	1500.8	1501.2	1501.9	1503.0						
03.aug.09			1500.0	1500.3	1500.5	1500.7	1500.9	1500.9	1501.0					
04.aug.09				1500.1	1500.4	1500.7	1501.7	1502.6	1503.2	1503.6				
05.aug.09					1500.7	1501.3	1502.7	1503.4	1503.9	1504.3	1504.6			
06.aug.09						1501.3	1501.7	1502.1	1502.5	1502.7	1502.9	1503.1		
07.aug.09							1501.4	1501.8	1502.2	1502.4	1502.6	1502.8	1502.9	
08.aug.09								1503.0	1503.5	1504.0	1504.3	1504.7	1505.0	1505.3
Actual water level	1499.5	1499.7	1499.9	1500.3	1500.4	1501.0	1502.3	1504.1	1504.7	1505.0	1505.2	1505.3	1505.3	1505.4

## 7.5 DISCUSSION ON UNCERTAINTY IN SHORT TERM INFLOW FORECASTING

Large degree of uncertainty is observed in inflow forecasting. The uncertainty in inflow forecasting is the result of the uncertainty in meteorological forecasts (precipitation and temperature) and in computed observed runoff. Table 7-2 and Table 7-3 show that there is a

large disagreement between meteorological forecasts and observed values which have made the inflow forecast very uncertain. The error variability in inflow forecast over the time does not show any systematic pattern. In some cases, the inflow forecast made for a particular day on 7 days in advance shows the better result than the forecast made for the same day on one day before. But this is not valid for all cases. Figure 7-5 shows the inflow forecast made on different date and error variability over time.

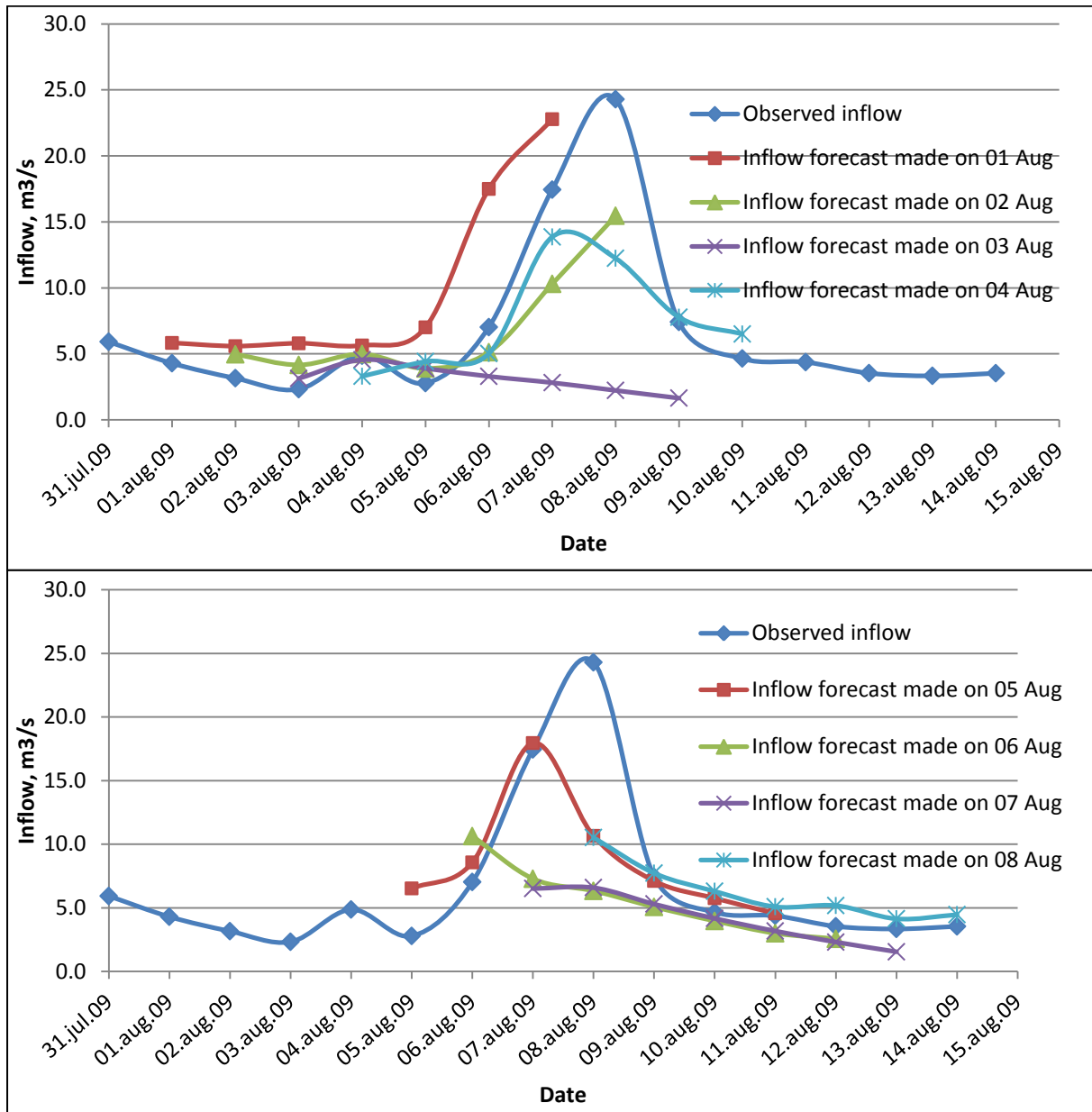


Figure 7-5: Uncertainty in short term inflow forecasting

The uncertainty associated with inflow forecast ultimately led to the uncertainty in reservoir operation. Figure 7-6 shows the reservoir level forecast and error variability over the time.

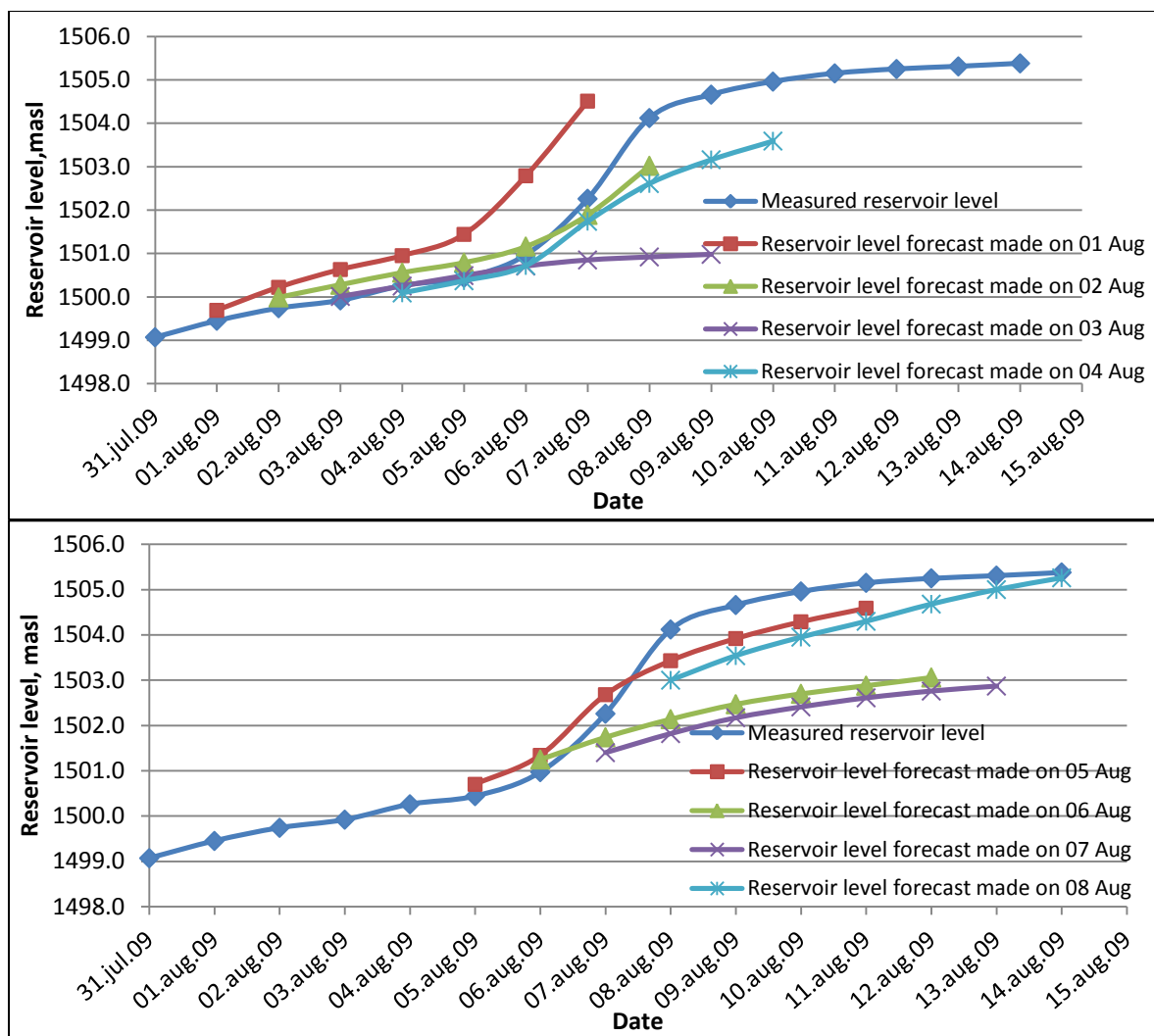


Figure 7-6: Uncertainty in reservoir level forecast and error variability

Because of the uncertainty in inflow forecasting, the reservoir operation model is unable to forecast the reservoir level precisely.

### 7.6 CONCLUSION AND RECOMMENDATION

The uncertainty in inflow forecasting and reservoir operation has come from uncertainty in meteorological forecasts (precipitation and temperature) and model calibration due to uncertainty in estimated observed runoff. Thus, without having a good meteorological forecast system and reliable model calibration, it is almost impossible to get the reliable inflow forecasts and reservoir operation. The result can be improved by working with reliable operational meteorological forecast system that is run with finer spatial resolution.

The reservoir operation model which is used here for demonstration purpose was developed by considering the existing situation of Kulekhani reservoir. In future, if the different prices for energy are set according to time of energy consumption and real time energy demand on INPS grid are included in the model, this reservoir operation model will get the high attention in optimizing the reservoir operation to full extent.

## 8 FLOOD WARNING SYSTEM

### 8.1 INTRODUCTION

The world is changing. In this changing world our environment is continuously facing the increasing challenge of flooding due to climate change and other conditions such as land use change and rapid urbanization. Floods usually impose negative impacts in the economy, society and environment. The negative impacts of the flooding comprise of (Australian Government, 2009):

- Direct damage to residential, commercial, educational, recreational, cultural and industrial buildings
- Damage to infrastructure
- Damage to stock, equipment and facilities
- Indirect losses due to disruption of economic activity, both in areas which are inundated and areas which are isolated
- Stress and anxiety in those affected by flooding
- Injury and death
- Polluted water supplies and
- Damage to wildlife habitats

The United Nations Educational, Scientific and Cultural Organization (UNESCO) World Water Assessment Programme ([http://webworld.unesco.org/water/wwap/facts\\_figures/managing\\_risks.shtml](http://webworld.unesco.org/water/wwap/facts_figures/managing_risks.shtml)) provides a clear statement of the problem. Figure 8-1 shows the significance of flooding in the context of all water-based natural hazards.

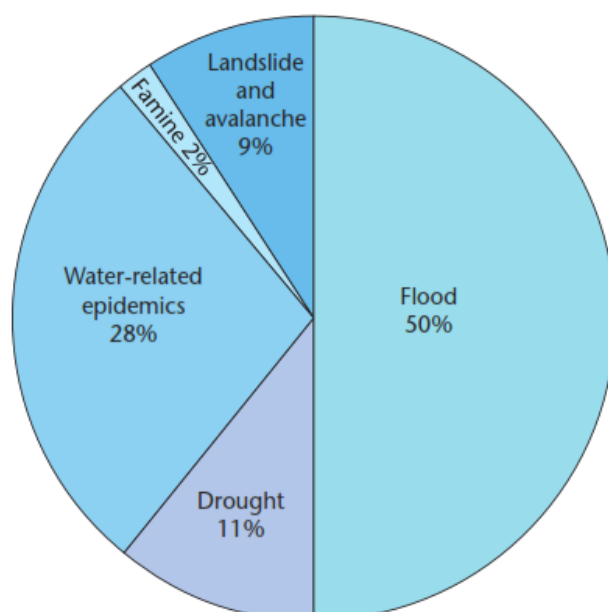


Figure 8-1: Type of water-related natural disasters, 1990-2001 (Source: UNESCO)

UNESCO reports the fact that floods account for 15% of all deaths related to natural disasters. For example, between 1987 and 1997, 44% of all flood disasters affected Asia,

claiming 228,000 lives (roughly 93 per cent of all flood-related deaths worldwide). Economic losses for this region totaled US\$ 136 billion.

Floods are inevitable events and are always criticized for its negative impacts on anywhere. The risks from flooding can never be completely eliminated but the harm caused by floods can be greatly reduced or mitigated by effective flood warning systems. Flood warning is the provision of advance warning of conditions that are likely to cause flooding to property and a potential risk to life. The main purpose of flood warning is to save life and property by allowing people, support and emergency services time to prepare for flooding.

## 8.2 WARNING TIME AND LEVEL OF ACCURACY

People who are at risk of floods need to know as accurately as possible the magnitude of flood with enough time in advance to protect themselves and their properties. The longer time is allocated, the better it is to take the necessary preparation but the time available for warning depends on the rate at which streams respond to rainfall. A small urban creek may respond within minutes, producing flash flooding, while floods generated from the large catchments may take several hours to reach some downstream communities.

Generally, Prediction of flood in advance is always associated with large degree of uncertainty. High accuracy in flood prediction can be achieved only in the later stage of its development when information on observed rainfall becomes available. Therefore it is a common practice that less accurate prediction are also accepted in order to provide the sufficient warning time. Thus there is a trade-off between prediction accuracy and warning time. The Figure 8-2 illustrates an example of the trade-off between the warning time which can be provided and the level of accuracy which can be achieved for the case of flash flood warning.

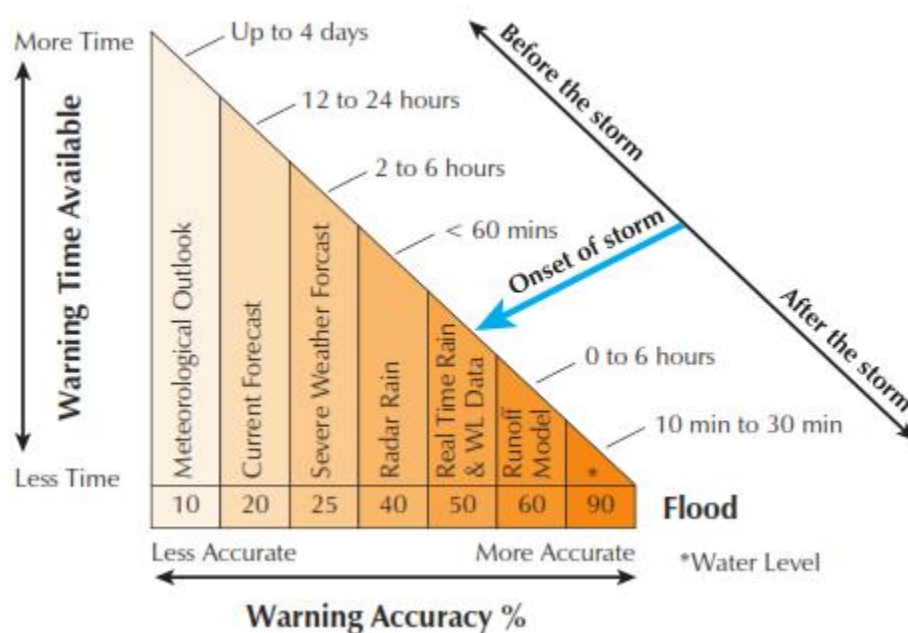


Figure 8-2: The trade-off between warning time and warning accuracy for flash flood situations (Wright, 2001)

Meteorological forecasts can be used to extend the lead time for flood forecasts. However, because forecasts of rainfall for specific locations and timing are not fully accurate, flood forecasts based on rainfall forecasts are often subject to significant uncertainty.

### 8.3 WARNING LIMITS

The rise in water level during flooding situation determines the area of flood encroachment and vulnerability of the society to the flooding. So it is important that a detail survey is carried out throughout the flood prone areas to assess the effects of flooding at different heights. This survey should include the identification of low lying area, existing situation of road, bridge and other infrastructure likely to be hit by flood, valuation of agricultural lands, damage to the livestock and other properties such as buildings, stores etc. A quantitative assessment of flooding disaster is more site specific and requires a lot of works to be done beforehand to define the warning limits. So, it is a common practice that warnings limits are linked with some predefined return period of flood. The Norwegian system of flood warnings is discussed in this report. A similar system is proposed to set up in Kulekhani catchment. The maximum floods for different re occurrence intervals calculated by different methods are presented in the Table 8-1 below:

Table 8-1: Maximum flood in the Kulekhani river (NIPPON KOEI Co. Ltd., 1983)

Return Period Year	Peak flood m <sup>3</sup> /s			
	By Gumbel's	by Hazen's	by Iwai's	by log pearson type III
5	345	314	387	335
10	451	405	398	455
20	553	494	517	550
50	685	610	688	701
100	783	696	830	794
200	882	782	984	880
1000	1110	977	1391	1100
10000	1435	1234	2113	1400

According to nve ([www.nve.no](http://www.nve.no)), when the flow in the river exceeds the flow with re occurrence interval of 5 years then the flow is considered as flood and the flow which exceeds 50 years return period flow is the major flood.

The flood warning limits are defined based on the re occurrence frequency of the predicted stream flow. Different kind of warning messages will be issued based on the magnitude of the floods in the Kulekhani river as discussed below:



**Notification of flooding:** This notification will be delivered when the flow in the river is expected to exceed the flow with a re-occurrence interval of 5 years. The corresponding flow in Kulekhani river with 5 years return period is 345m<sup>3</sup>/s according to Gumbel's method.



**Notification of major flooding:** This notification will be issued when the expected flow in the river exceeds the flow with 50 years return period. The corresponding flow with 50 years return period is  $685\text{m}^3/\text{s}$  according to Gumbel's method.

The inflow forecast made for demonstration purpose as discussed in section 7.3 are very smaller as compared to the 5 years and 50 years return period flood. For an example, the inflow forecast made on 01 August, 2009 for coming 7 days is shown on the Figure 8-3 to analyze it in terms of flood and major flood.

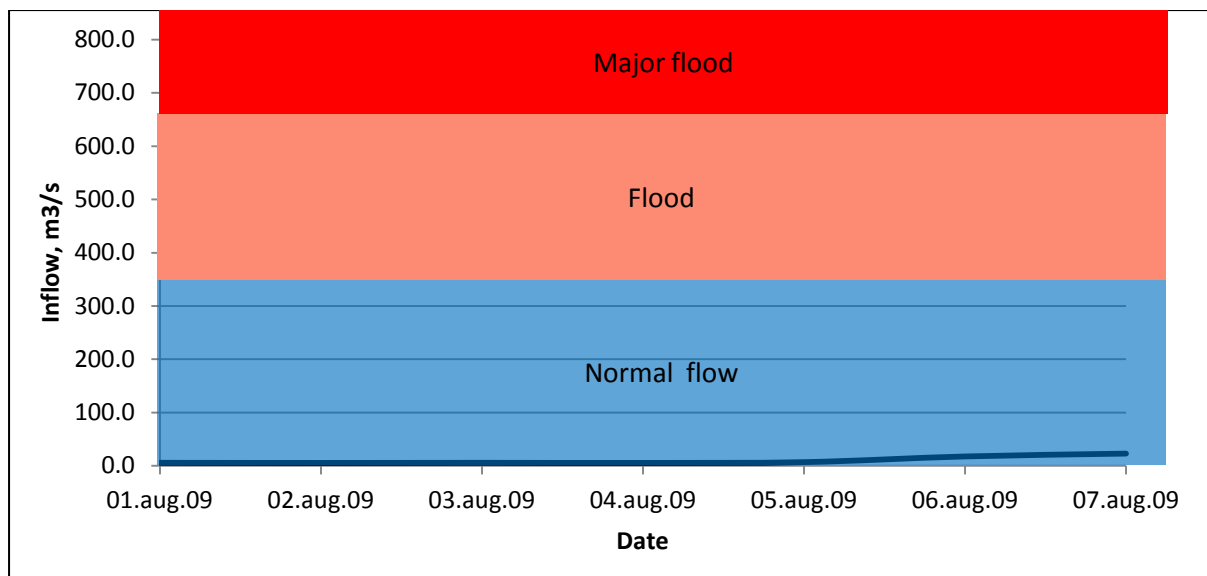


Figure 8-3: Inflow forecast made on 01 August, 2009 and flood warning limits

A flood warning is not necessarily a warning of the flood damage. Some areas could be very vulnerable to damage with 5 years return period flow while some areas are safe even with 50 years return period of flow. So the warning messages are only meant to inform the people about the probable situation of flooding in specified areas. People are expected to respond to the floods according to the vulnerability of their area to the flooding of specified return period.

#### 8.4 OPERATIONAL FLOOD WARNING SYSTEM

The purpose of a flood warning system is to empower individuals and communities to respond to floods appropriately in order to reduce the risk of death, injury, property loss and damage. Thus, a successful warning system not only needs to address the technical issues that would make it possible to issue an accurate warning with sufficient lead time, but it also should ensure these warnings are translated to actions that would lead to a reduction of flood damage (Herath et al., n.d.).

A flood warning system is made up of a number of components which must be integrated if the system is to operate effectively. Figure 8-4 shows the components of effective operational flood warning system. These components are interdependent and linked to each other.

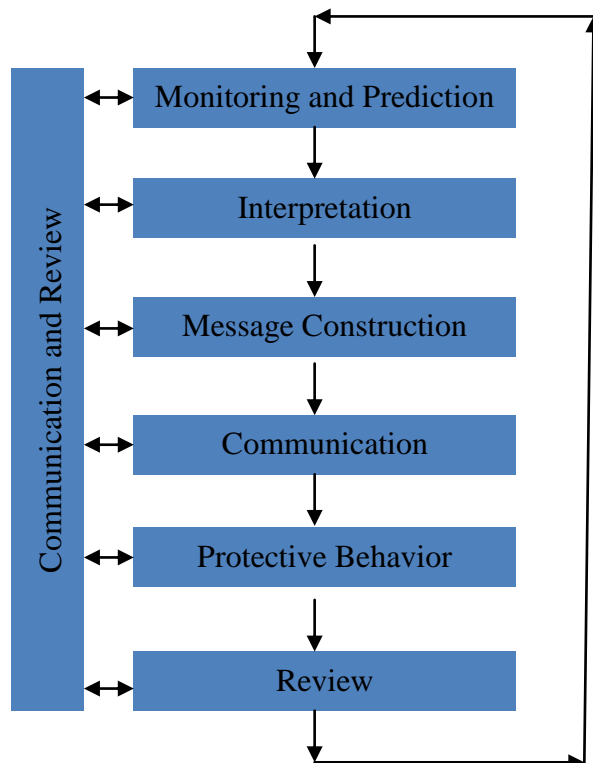


Figure 8-4: Components of operational flood warning system (Australian Government, 2009)

An effective operational flood warning system can be defined as having six components:

- Monitoring and prediction: Detecting environmental conditions that lead to flooding, and predicting river levels during the flood.
- Interpretation: Identifying in advance the impacts of the predicted flood levels on communities at risk.
- Message construction: Devising the content of the message which will warn people of impending flooding.
- Communication: Disseminating warning information in a timely fashion to people and organizations likely to be affected by the flood.
- Protective behavior: Generating appropriate and timely actions and behaviors from the agencies involved and from the threatened community, and
- Review: Examining the various aspects of the system with a view to improving its performance.

## 8.5 FLOOD PREPAREDNESS

A comprehensive preparedness program as described by (World Meteorological Organization, 2011) is proposed to be followed during flooding situation. Followings are the necessary preparation plan with respect to different level of flood.



**Flood watch:** Flooding of low-lying land and roads is expected. Be aware, be prepared, and watch out!

- Watch water levels
- Stay tuned to local radio or TV
- Make sure you have what you need to put your flood plan into action
- Alert your neighbors, particularly the elderly
- Check pets and livestock
- Reconsider travel plans



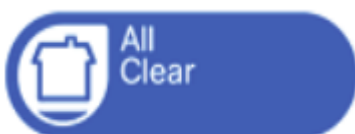
**Flood Warning:** Flooding of homes and business is expected. Act now!

- Move pets, vehicles, food, valuables and other items to safety
- Put sandbags or flood boards in place
- Prepare to turn off gas and electricity
- Be prepared to evacuate your home
- Protect yourself, your family and others that need your help



**Severe flood warning:** Severe flooding is expected. There is extreme danger to life and property. Act now!

- Be prepared to lose power supplies-gas, electricity, water, telephone
- Try to keep calm, and to reassure others, especially children
- Co-operate with emergency services and local authorities
- People may be evacuated



**All clear:** Flood watches or Warnings are no longer in force for this area.

- Flood water levels receding

- Check all is safe to return
- Seek advice

## **8.6 CONCLUSION**

Floods are inevitable disasters but manageable to great extent. The negative impacts of the flooding can be easily reduced through an effective warning system. An effective flood warning system should show the ability to enable individuals and communities to respond appropriately to a major flood threat to reduce the risk of death, injury and property loss, however, effectiveness of warnings system are linked with available lead time. The more lead time is given, the better the opportunity to prepare and activate responses and relief actions. By using meteorological forecasts, it is possible to extend the lead time to several days but they are associated with large degree of uncertainties.



---

## 9 CONCLUSION AND RECOMMENDATION

### 9.1 CONCLUSION

However each chapter is already equipped with necessary discussions and conclusion, the main conclusion is presented in a sequential order as below:

The main objectives of this study were to establish the inflow forecasting system to the Kulekhani reservoir, to link the forecasted inflow into the reservoir operation model to see the response of reservoir for a given load in relation to inflow forecast and to present an example of flood warning system.

All the observed meteorological data were collected from the Department of Hydrology and Meteorology (DHM), Nepal. The consistency and quality of observed meteorological data were evaluated through the systematic quality check procedures. Double mass curve has been a very useful tool to detect the inconsistency and error in recorded data for two stations: Daman and Thankot so those data were discarded from the initial stage. Meteorological forecast data used in this study are the outputs of the Global Forecast System (GFS) model which is run by National Weather Service (NWS) in U.S.A. Downscaling of GFS model data was not done because the spatial resolution of the model is on Regional Circulation Model (RCM) level since the model is run on approximately 50 km x 50 km spatial resolution.

While comparing model outputs with corresponding observed values, large disagreements between their values was observed. These disagreements were the result of the inability of the GFS model to resolve the local terrain impacts of the study area. The GFS model with coarser spatial resolution was unable to produce accurate forecasts in catchment scale. Thus the meteorological forecasts were subjected to bias correction. Two advanced techniques: empirical adjustment method and statistical bias correction methods were applied to the model output. The empirical method was not useful in bias correction of precipitation forecast so statistical method was applied further but the bias correction of modeled temperatures was done successfully with empirical adjustment method.

The HBV model was calibrated based on the observed meteorological data with a daily time step. The inflow to the reservoir was computed by indirect method based on the daily energy production and reservoir level. The goodness of fit was evaluated in model calibration by Nash efficiency ( $R^2$ ). The best value of Nash efficiency ( $R^2$ ) was observed to be 0.76. The low value of  $R^2$  was characterized by the uncertainty in observed runoff and recorded precipitation.

Model validation was carried out by adjusting precipitation and temperature values and model states for the last 7 days. Then inflow forecast simulation was performed on eight consecutive days. The variation in inflow forecast between the same days made from different date was due to uncertainty in meteorological forecasts and in HBV model calibration.

The forecasted inflow was used in reservoir operation model to examine whether the reservoir can meet the demand or not for 7 coming days in advance and to see how reservoir

level fluctuates in relation to inflow forecasts and energy demands. The reliability of the reservoir operation was also affected by the uncertainty associated in inflow forecasts.

The forecasted inflow was not only used in reservoir operation model but also analyzed in terms of probable flooding along the water course. Norwegian system of defining warning limits was adopted in the Kulekhani case also. An effective operational warning system was proposed to reduce damages caused by flooding. The use of meteorological forecasts can extend the lead time in flood warning system thus reduces the loss of lives by allowing the sufficient time to protect people during flooding.

In conclusion, Inflow forecasting is a very useful tool in energy optimization, effective reservoir operation and also in establishing effective flood warning system. The uncertainty of observed runoff used in model calibration and uncertainty of meteorological forecasts used in forecast simulation were the sources of uncertainty in inflow forecasting which in turn has led to uncertainty in reservoir operation and flood warning system. So to get the good result in subsequent application of inflow forecast, it is very important to work with good quality of runoff data and reliable meteorological forecasts which is run with finer spatial resolution.

## **9.2 RECOMMENDATION FOR FUTURE RESEARCH**

This study can be considered as a pilot work in inflow forecasting, reservoir operation and flood warning system for Nepal since no similar studies were carried out previously by using output from forecast model.

The results in the HBV model calibration can be improved by using directly measured runoff in the future so it is recommended to set up the gauge station in the Kulekhani river to record the runoff.

The potential evaporation data also play greater role in the HBV model calibration so the accuracy in forecast simulation can be further improved with the use of observed potential evaporation values.

The output from the GFS model with spatial resolution of approximately 50 km x 50 km was used in this study so the uncertainty in the inflow forecast can be greatly reduced when the meteorological forecast model are available with finer spatial resolutions.

---

## REFERENCES

- AUSTRALIAN GOVERNMENT 2009. Flood Warnings. *Australian Emergency Manuals Series*. Attorney-General's Department, Australia.
- BERGSTROM, S. 1976. *Development and application of a conceptual runoff model for Scandinavian catchments*, Norrköping.
- DINGMAN, S. L. 1994. *Physical hydrology*, Prentice Hall Englewood Cliffs, NJ.
- EHRET, U., ZEHE, E., WULFMEYER, V., WARRACH-SAGI, K. & LIEBERT, J. 2012. HESS Opinions" Should we apply bias correction to global and regional climate model data?". *Hydrology and Earth System Sciences*, 16, 3391.
- ENGEN-SKAUGEN, T. 2007. Refinement of dynamically downscaled precipitation and temperature scenarios. *Climatic Change*, 84, 365-382.
- HERATH, S., JHA, R. & DUTTA, D. n.d. Assessing lead time in flood forecasting for better emergency response.
- HOUGHTON, D. D. 1985. *Handbook of applied meteorology*, New York.
- KILLINGTVEIT, Å. & SÆLTHUN, N. R. 1995. *Hydrology*, NTNU, Norwegian Institute of Technology, Division of Hydraulic Engineering.
- LYNCH, P. 2006. *The emergence of numerical weather prediction: Richardson's dream*, Cambridge University Press.
- MARAUN, D. 2012. Nonstationarities of regional climate model biases in European seasonal mean temperature and precipitation sums. *Geophysical Research Letters*, 39.
- MORIASI, D., ARNOLD, J., VAN LIEW, M., BINGNER, R., HARMEL, R. & VEITH, T. 2007. Model evaluation guidelines for systematic quantification of accuracy in watershed simulations. *Transactions of the ASABE*, 50, 885-900.
- NIPPON KOEI CO. LTD. 1983. Project completion report. Kulekhani Hydroelectric project, HMG of Nepal, Kulekhani Hydroelectric Development Board, Kathmandu.
- PAN, H.-L. & MAHRT, L. 1987. Interaction between soil hydrology and boundary-layer development. *Boundary-Layer Meteorology*, 38, 185-202.
- PIANI, C., HAERTER, J. & COPPOLA, E. 2010. Statistical bias correction for daily precipitation in regional climate models over Europe. *Theoretical and Applied Climatology*, 99, 187-192.
- PISARENKO, V., LYUBUSHIN, A., CANU, S., KANEVSKY, M., SAVELIEVA, E., DEMIANOV, V., BOLGOV, M., RUKAVISHNIKOVA, T. & ZALIAPIN, I. 1993. STATISTICAL METHODS FOR RIVER'S RUNOFF FORECAST. *International Institute of Earthquake Prediction and Mathematical Geophysyc, Moscu*.

PONCE, V. M. 1989. *Engineering hydrology: Principles and practices*, Prentice Hall Englewood Cliffs.

RINDE, T. 2012. *Hydrological Modelling*, Lecture/Class notes, Norwegian university of science and technology(NTNU).

SANGROULA, D. 2005. *Sedimentation and Sustainability of Kulekhani Reservoir. A Himalayan case*. Thesis for the Degree of Doctor Engineer, NTNU, Norway.

SHRESTHA, H. S. 2012. *Sedimentation and sediment handling in Himalayan reservoirs*. Norwegian University of Science and Technology.

WORLD METEOROLOGICAL ORGANIZATION 2011. *Manual on Flood Forecasting and Warning*. Switzerland.

WRIGHT, C. J. 2001. *Flash Flooding in an Urban Environment: Causes, Effects, Potential Damages and Possible Remedies, with Particular Reference to Keswick Creek in the Inner Suburbs of Adelaide*, University of Adelaide, Department of Civil and Environmental Engineering.

XU, C. Y. & SINGH, V. 2001. Evaluation and generalization of temperature-based methods for calculating evaporation. *Hydrological processes*, 15, 305-319.

**APPENDICES**

Appendix A: Preparation of forecasted temperature time series in 'R'

Appendix B: Calculation of monthly value of potential evapotranspiration by Thornthwaite method in 'R'

Appendix C: Generation of hypsometric curve for Kulekhani catchment in 'R'



## Appendix A

### 1. Preparation of forecasted temperature time series in 'R'

```

library(raster)

#subset the files read only 0000 hour files
fl = list.files()
dfa = data.frame(fl,1:length(fl),stringsAsFactors = FALSE)
hr <- substr(dfa[,1], 28,31)
dfa2<- cbind(dfa,hr,stringsAsFactors = FALSE)
dfa3 = subset(dfa2, dfa2[,3]=="0000")
fl1 <- dfa3[,1] #fl1 is temp and pcp file with 00hr model run

#segregating temp
dfa4=data.frame(fl1,1:length(fl1),stringsAsFactors = FALSE)
hr1=substr(dfa4[,1],38,40)
hr1
dfa5=cbind(dfa4,hr1,stringsAsFactors = FALSE)
dfa6=subset(dfa5,dfa5[,3]=="2mt"|dfa5[,3]=="mtm")
dfa6 # dfa6 is temperature file
dir.create("Temperature")# Makes new folder "temp_2007"
file.copy(dfa6[,1],"Temperature")# Copy temperature files to
folder"Temperature2007"

# Converting UTM to Geographic system as historical data are in UTM
rs1=raster("F:\\catchm.asc")
ext=extent(304700,323200,3051200,3063800) # extent of window
rs1=crop(rs1,ext) # reduce the size of catchment raster
pr1=projectRaster(rs1,crs="+proj=longlat +datum=WGS84 +ellps=WGS84
+towgs84=0,0,0")# Projection from UTM to Geographic System
plot(pr1)
result <- matrix(ncol=2,nrow=length(d1),NA)# Creates matrix with no data
"NA"

# subsetting file name based on day
dfa60=fl_new
fln60 <- substr(dfa60,19,26) #
Extracts character from length 19-26
dfa61=data.frame(dfa60,fln60,stringsAsFactors = FALSE) # Creates dataframe
with files and string(character)
d1=seq(as.Date("2007-01-01"),as.Date("2007-12-31"),1) # Produces all
dates in a year
d1_1=sub("-", "",d1) # Replace "-"
d1_1=sub("-", "",d1_1) # Replace "-"

# For daily mean temperature
j=1 # j is total count of iteration from the beginning.
for (k in 1:length(d1)){ # Length(d1) is number of days in a year
if (dfa61[j,2]==d1_1[k]){ # Checks if each day file is available. If
yes, enters in to the loop
df_fl=subset(dfa61,dfa61[,2]==d1_1[k]) # Subsets files based on
date (for ex, 8 files of 20070101)
stk=t1
# Base layer to add other layers, creates new layer when 'i' loop is terminated
for (i in 1:length(df_fl[,1])){ # Length(df_fl[,1]) is numbers of file
for each same date
x1=raster(df_fl[i,1]) # Reads new raster files
t1 = crop(x1,pr1) # Crops value by pr1 cathment
stk = stack(stk,t1) # Makes stack with previous layer(s)

```

---

```
    }
    stk <- dropLayer(stk, 1) # Removes first layer from latest created stack
    fln <- paste("temp_",df_fl[1,2], sep="") # Write file names for daily data
    wr <- cellStats(stk,"mean") # Evaluate mean of each layers in a stack
    wr1=mean(wr) # Evaluate mean of each layer mean
    result[k,1] <- fln # Replace matrix value with new value
    result[k,2] <- round(wr1,2) # Replace matrix value with new value
    j=j+i # Counts total number of iterations from the begining
  } else {

    result[k,1] = 999 # If day file is not available
    result[k,2] = 999 # If day file is not available
    j=j+1 # Jumps to next day
  }
# Ends if statement
}
# Ends 'k' loop
write.csv(result,"Temp2012") # Writes the temperature timeseries in .csv format
```

**Appendix B**

2. Calculation of monthly value of potential evapotranspiration by Thornthwaite method in 'R'

```
install.packages("SPEI")
library(SPEI)
Ret=read.table("Thornthwaite.csv",FALSE,sep=";")
asm=as.matrix(Ret)
thr= thornthwaite(asm,27.5)
write.csv(thr,"Potevt.csv")
```



**Appendix C**

## 3. Generation of hypsometric curve for Kulekhani catchment in 'R'

```
hp=raster("F:\\ArcGIS\\maskinR.asc")
hp=as(hp,"SpatialGridDataFrame")
jpeg('rplot.jpg')

hypsometric(hp,main="Hypsometric Curve",
            xlab="Relative Area above Elevation, (a/A)",
            ylab="Relative Elevation, (h/H)", col="blue")
```